

AD-A148 289

UTILIZATION OF NUMERICAL OPTIMIZATION TECHNIQUES IN THE 1/2
DESIGN OF ROBUST... (U) NAVAL POSTGRADUATE SCHOOL
MONTEREY CA V C GORDON SEP 84

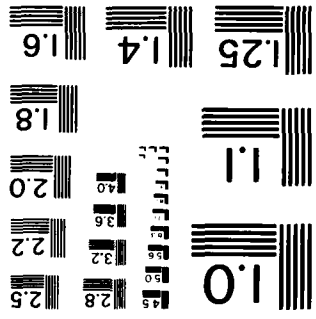
UNCLASSIFIED

F/G 12/1

NL

The table consists of 10 columns and 10 rows. The top row contains 10 blacked-out cells. The second row contains 10 blacked-out cells. The third row contains 10 blacked-out cells. The fourth row contains 10 blacked-out cells. The fifth row contains 10 blacked-out cells. The sixth row contains 10 blacked-out cells. The seventh row contains 10 blacked-out cells. The eighth row contains 10 blacked-out cells. The ninth row contains 10 blacked-out cells. The tenth row contains 10 blacked-out cells.

MICROCOPY RESOLUTION TEST CHART
NATIONAL BUREAU OF STANDARDS - 1963 - A



2

NAVAL POSTGRADUATE SCHOOL

Monterey, California

AD-A148 289



DEC 4 1984
A

THESIS

UTILIZATION OF NUMERICAL OPTIMIZATION
TECHNIQUES IN THE DESIGN OF ROBUST
MULTI-INPUT MULTI-OUTPUT CONTROL SYSTEMS

by

Vernon Curtis Gordon

September 1984

Thesis Advisor:

D. J. Collins

DTIC FILE COPY

Approved for public release; distribution unlimited.

84 12 03 020

UNCLASSIFIED

SECURITY CLASSIFICATION OF THIS PAGE (When Data Entered)

REPORT DOCUMENTATION PAGE		READ INSTRUCTIONS BEFORE COMPLETING FORM
1. REPORT NUMBER	2. GOVT ACCESSION NO. AD-A148 289	3. RECIPIENT'S CATALOG NUMBER
4. TITLE (and Subtitle) Utilization of Numerical Optimization Techniques in the Design of Robust Multi-Input, Multi-Output Control Systems		5. TYPE OF REPORT & PERIOD COVERED Doctor of Philosophy September 1984
7. AUTHOR(s) Vernon Curtis Gordon		6. PERFORMING ORG. REPORT NUMBER
9. PERFORMING ORGANIZATION NAME AND ADDRESS Naval Postgraduate School Monterey, California 93943		8. CONTRACT OR GRANT NUMBER(s)
11. CONTROLLING OFFICE NAME AND ADDRESS Naval Postgraduate School Monterey, California 93943		10. PROGRAM ELEMENT, PROJECT, TASK AREA & WORK UNIT NUMBERS
14. MONITORING AGENCY NAME & ADDRESS (if different from Controlling Office)		12. REPORT DATE September 1984
		13. NUMBER OF PAGES 175
		15. SECURITY CLASS. (of this report) Unclassified
		15a. DECLASSIFICATION/DOWNGRADING SCHEDULE
16. DISTRIBUTION STATEMENT (of this Report) Approved for public release; distribution unlimited.		
17. DISTRIBUTION STATEMENT (of the abstract entered in Block 20, if different from Report)		
18. SUPPLEMENTARY NOTES		
19. KEY WORDS (Continue on reverse side if necessary and identify by block number) Multi-input Multi-output Control, Robustness, Modern Control, Multivariable Systems.		
20. ABSTRACT (Continue on reverse side if necessary and identify by block number) A direct design method for solving the problem of robustness to cross-coupling perturbations in multivariable control systems is presented. The method uses numerical optimization procedures to manipulate the system feedback gains as direct design variables. The manipulation is accomplished in a manner that produces desired performance by pole placement and robustness by modification of the minimum singular values of the system return difference matrix.		

DD FORM 1473
1 JAN 73

EDITION OF 1 NOV 65 IS OBSOLETE
S N 0102-LF-014-560

UNCLASSIFIED

1 SECURITY CLASSIFICATION OF THIS PAGE (When Data Entered)

Channels affected by cross-coupling perturbation may be recognized by the character of their transfer function plot. The mechanism used by the pole placement and robustness routine in obtaining a robust design is evident from the gain changes associated with the transfer function diagram and the zero shifts shown on pole-zero plots. The pole placement and robustness routine uses gain equalization and zero assignment to modify the characteristics of the system in the areas of low singular values, producing a robust design.

A modification of the pole placement and robustness routine that may be applied to the design of robust observers is also presented. Using feedback and filter gains as direct design variables a practical design procedure for robustness recovery in observer based systems is obtained.



SEARCHED
SERIALIZED
INDEXED
FILED
A-1

Approved for public release; distribution unlimited.

Utilization of Numerical Optimization Techniques
in the Design of
Robust Multi-input Multi-output Control Systems

by

Vernon C. Gordon
Commander, United States Navy
B.A.E., Auburn University, 1968
M.S.A.E., Naval Postgraduate School, 1970

Submitted in partial fulfillment of the
requirements for the degree of

DOCTOR OF PHILOSOPHY

from the

NAVAL POSTGRADUATE SCHOOL
September 1984

Author: Vernon C Gordon

APPROVED BY:

Max F. Platzer
M. F. Platzer
Professor of Aeronautics

Robert D. Strum
R. D. Strum
Professor of Electrical
Engineering

Daniel J. Collins
D. J. Collins
Professor of Aeronautics
Thesis Supervisor

T. H. Gawain
T. H. Gawain
Professor of Aeronautics

G. E. Latta
G. E. Latta
Professor of Mathematics

Approved by: Max F. Platzer
Chairman, Department of Aeronautics

Approved by: David A. Schrad
David A. Schrad, Academic Dean

ABSTRACT

A direct design method for solving the problem of robustness to cross-coupling perturbations in multivariable control systems is presented. The method uses numerical optimization procedures to manipulate the system feedback gains as direct design variables. The manipulation is accomplished in a manner that produces desired performance by pole placement and robustness by modification of the minimum singular values of the system return difference matrix.

Channels affected by cross-coupling perturbation may be recognized by the character of their transfer function plot. The mechanism used by the pole placement and robustness routine in obtaining a robust design is evident from the gain changes associated with the transfer function diagram and the zero shifts shown on pole-zero plots. The pole placement and robustness routine uses gain equalization and zero assignment to modify the characteristics of the system in the areas of low singular values, producing a robust design.

A modification of the pole placement and robustness routine that may be applied to the design of robust observers is also presented. Using feedback and filter gains as direct design variables a practical design procedure for robustness recovery in observer based systems is obtained.

TABLE OF CONTENTS

I.	INTRODUCTION	12
II.	SINGLE-INPUT SINGLE-OUTPUT SYSTEMS	14
III.	MULTIVARIABLE SYSTEMS	26
IV.	OPTIMIZATION	33
V.	OPTIMIZATION DESIGN PROCEDURE	52
VI.	INTRODUCTORY PROBLEM	60
VII.	A HELICOPTER STABILITY PROBLEM	82
VIII.	SIMPLE OBSERVER	113
IX.	ROBUST OBSERVER DESIGN	124
X.	CONCLUSIONS	130
	LIST OF REFERENCES	173
	INITIAL DISTRIBUTION LIST	175

LIST OF TABLES

1.	Comparative Results Simple Problem	77
2.	CH-46 Helicopter Parameter Definitions	84
3.	Design One Pole Placement	92
4.	Helicopter Problem Feedback Gains	104
5.	Observer Parameter Data	116

LIST OF FIGURES

2.1	Basic Gain and Phase Margin Determination Model	15
2.2	Classical Bode Plot	16
2.3	Nyquist Plot of Stable System	17
2.4	Additively Perturbed System	18
2.5	Additive Nyquist Plot	19
2.6	Nyquist for Inequality Additive Condition	20
2.7	Multiplicative System	21
2.8	Nyquist Plot for Multiplicative System	22
2.9	Typical Equivalent Feedback System	23
2.10	Polar Plot of an Optimal System	24
3.1	Nyquist D Contour	28
3.2	Basic Multi-input, Multi-output System	29
3.3	Additive Perturbation	30
3.4	Multiplicative Perturbation	32
4.1	Design Space for Example Problem	34
4.2	Design Space for Column Problem	36
4.3	Illustrative Example for Iteration	38
4.4	Plot of Various Points With Zero Gradient	40
4.5	Constrained Optimization Example	42
4.6	Organization of ADS Program	44
4.7	Golden Section Diagram	45
4.8	Steepest Descent Algorithm	48
4.9	Fletcher-Reeves Conjugate Direction Algorithm	49
5.1	Universal Gain and Phase Singular Value Plot	55
5.2	Observer Implementation	58
6.1	Basic Multi-input Multi-output System	61

6.2	Multivariable Nyquist for $2s+3/(s+1)^2$	62
6.3	Minimum Singular Value Plot, Example Problem	64
6.4	Nyquist Diagram of $1/s+1$	65
6.5	Perturbed System	66
6.6	Singular Value Plot for Simple Problem	67
6.7	Closed-loop Poles for Pole Placement Only Case	68
6.8	Singular Value Plot Case Three	70
6.9	Open-loop Transfer Function 2-1 for Baseline	72
6.10	Transfer Function 2-1 Optimized(3 Var)	73
6.11	Transfer Function 1-1 Baseline	74
6.12	Transfer Function 1-1 Optimized (3 variables)	75
6.13	Closed-loop Pole-Zero Plot Case 3	76
6.14	Pole-Zero Plot Simple Problem (4 Variables)	79
6.15	System Block Diagram	80
7.1	Feedback Control Structure	85
7.2	System Diagram	86
7.3	Alphatech Design Singular Value Plots	88
7.4	Design One Perturbation Input	89
7.5	Design Two Perturbation Input	90
7.6	Transfer Function $\delta_B - \delta_B$ Design One, Nonoptimized	93
7.7	Transfer Function $\delta_B - \delta_B$ Design One , Optimized	94
7.8	Transfer Function $\delta_C - \delta_B$ Design One, Nonoptimized	96
7.9	Transfer Function $\delta_C - \delta_B$ Design One, Optimized	97
7.10	Pole-Zero Plots for Design 1	98
7.11	Pole-Zero Plcts for Design 1 (cont.)	99
7.12	Pole-Zero Plots for Design 1 (cont.)	100
7.13	Pole-Zero Plots for Design 1 (cont.)	101

7.14	The δ_B to v Frequency Response, Nonopt. . . .	102
7.15	The δ_B to v Frequency Response, Optimized . .	103
7.16	Transfer Function $\delta_c - \delta_B$ Design 1 Case2, Nonopt.	105
7.17	Transfer Function $\delta_c - \delta_B$ Design 1 Case 2, Opt .	106
7.18	Transfer Function $\delta_c - \delta_B$ Design Two, Nonopt. .	108
7.19	Transfer Function $\delta_c - \delta_B$ Design Two, Optimized	109
7.20	Singular Value Plot Design Two	110
7.21	Time Response Design Two	111
8.1	Simple Observer	113
8.2	Nyquist Plot	115
8.3	Nyquist Plot for Robustness Recovery	117
8.4	Singular Values of Observer System	118
8.5	Singular Value Comparison Plot	120
8.6	Nyquist for Computed Robustness Recovery . . .	121
8.7	Time Response Plot for Simple Observer	122
9.1	Observer Based Controller	125
9.2	Singular Value Plot of Observer Results . . .	126
9.3	Time Response for Observer System	127

ACKNOWLEDGEMENTS

For over fifteen years the United States Navy has allowed me to make practical application of the science of flight as a Naval Flight Officer and as a flight test project officer. I wish to express my appreciation to the Navy and the citizens of the United States for the opportunity to further expand my knowledge of aviation by pursuing this degree.

I would also like to express a sincere thank you to the Doctoral Committee of professors Platzner, Gawain, Latta, Strum and Collins for their support in these efforts. Of course special thanks must go to Professor D.J. Collins for heading the committee and having worked so long and hard with me on two theses. Without his support this effort would never have been completed.

Thanks are also expressed to Professor G.N. Vanderplaats for allowing me to use the Automated Design Synthesis code. His help in integrating the code into the pole placement and robustness design program and the insight into the power of numerical optimization that he provided were extremely beneficial to the outcome of this thesis.

The Naval Postgraduate School Library staff and Roger Martin are appreciated tremendously for providing excellent service. No request for reference material was ever too difficult for them to handle. The W.R. Church Computer Center is acknowledged for their support in the computational processing for this thesis. I would also like to acknowledge the work of CDR Al Diel and LTs Cliff Cooksey, John Boden and Mike Iaptas for the work done to provide an excellent control system analysis package at the Naval Postgraduate School. Their efforts made the analysis of data from the pole placement and robustness routine much easier.

I would also like to thank my wife, Janice, and children, Bradley and Melissa. As anyone knows who has undertaken an effort of this magnitude without their love and support this would have been impossible. They have "gone it alone" quite often so that this paper could be completed.

Above all thanks to Him who started it all.

I. INTRODUCTION

With the rising interest in multivariable control theory brought on by increasingly complex systems the need has arisen to develop design methods that will allow the designer to specify system performance while at the same time ensuring relatively high stability margins or robustness. In the single-input single-output (SISO) case the designer has had the tools to do these tradeoffs in the form of Nyquist, Bode and root locus plots. In the multi-input multi-output (MIMO) case the classical methods are not totally appropriate.

With the increased interest in MIMO systems numerous methods of design have been employed to obtain suitable system performance and robustness with varying degrees of success. One primary method of design is to keep the plant as decoupled as possible throughout the design so that each individual element may be controlled independently and designed essentially as a single loop system. Rosenbrock [Ref. 1] has developed a procedure where the multiloop system is modified into a system that has diagonal elements that are much larger than any off-diagonal elements. This diagonally dominant system is then in a form where conventional Nyquist type techniques can be employed in the analysis. A third common MIMO design method is that of the Linear Quadratic (LQ) method. This method uses a quadratic cost functional and optimization principles to allow the designer to design for various performance levels by adjusting the matrix weighting terms used in the cost function. The major difficulty with all of the above methods is that they are not necessarily robust. This is especially true for cross-coupling terms between loops.

The primary achievement of this thesis has been the incorporation of the time domain pole placement design procedure with a method of using return difference matrix singular values to improve the robustness of the design. The technique, which utilizes a modern optimization routine, can significantly assist the designer in obtaining robustness in the face of cross-coupling perturbations. It has also been shown that the cross-coupling perturbation problem can be detected by using classical open-loop Bode diagrams as well as modern control analysis. The pole placement and robustness design routine developed for this thesis has been used on several problems discussed in recent literature. In these studies the pole placement and robustness design code has proven capable of meeting the desired goals of pole placement and robustness and also brought to light some interesting aspects of the cross-coupling perturbation problem. A slightly modified pole placement and robustness routine has proven effective in the design of robust observers.

The remainder of the thesis will present background material on SISO systems in Chapter Two and on MIMO systems in Chapter Three. Optimization will be discussed in Chapter Four along with a discussion of the Automated Design Synthesis (ADS) program used as the optimizer routine for the pole placement and robustness design procedure developed in this thesis. The thesis methodology will be discussed and outlined in Chapter Five. This will be followed by chapters discussing results from selected problems. Conclusions will be presented in the final chapter.

II. SINGLE-INPUT SINGLE-OUTPUT SYSTEMS

The purpose of this thesis research has been to develop a method of obtaining a robust multivariable control system design. A brief review of the concept of robustness and stability in the framework of a conventional SISO system will be done before pursuing the concepts in a more complicated fashion in the following chapters. A simple interpretation of robustness is the ability of the system to tolerate design perturbations. These perturbations could be in the form of actuator failures, plant parameter uncertainty, unmodeled dynamics or nonlinear terms, or any one of many other perturbations to the nominal design of the system.

The primary reason for feedback systems is the control of uncertainty within the system. By appropriate use of feedback, properties that would lead to an unstable system may be controlled. When stability and robustness aspects are considered for a SISO system, frequency domain design concepts, using either Nyquist or Bode plots, are normally used. Robustness in SISO systems is formulated naturally by the concept of gain and phase margins, both of which are readily available on the Nyquist or Bode diagram.

In figure 2.1 a nominal feedback system can be seen with a perturbation element $\alpha(s)$ placed in series with the nominal system. When $\alpha=1$ the system is nominal and stable. To determine the positive phase margin of the system the value of $\alpha(s) = \alpha(j\omega) = e^{j\psi}$ will be changed by varying ψ until the system just becomes unstable. This value of ψ will then be the system phase margin. The negative phase margin can be computed in the same way. To find the gain margin the magnitude value of α is increased until the system just

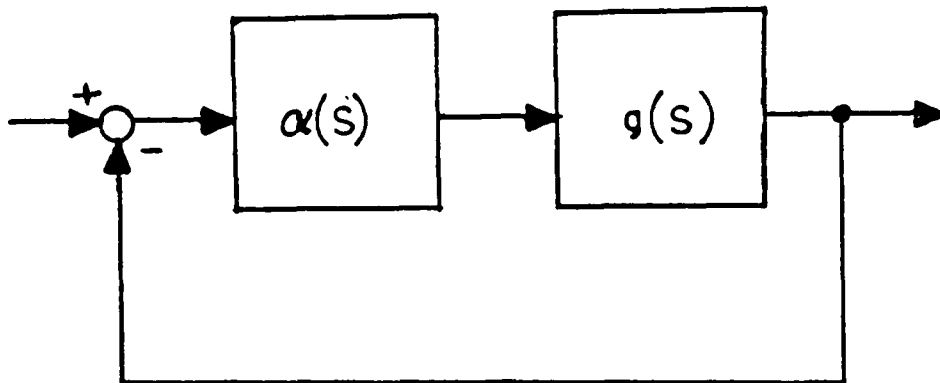


Figure 2.1 Basic Gain and Phase Margin Determination Model.

becomes unstable. This is the upward gain margin. A similar lower margin is also defined.

These gain and phase margins may not be adequate measures of robustness [Ref. 2] because they do not account for simultaneous variation in both gain and phase. Therefore, while large individual gain or phase changes may not destabilize the system, small simultaneous changes in gain and phase may destabilize the system. This is not a major difficulty in classical SISO techniques because the effect can be easily detected.

Gain and phase margin can be defined in terms of the open-loop frequency domain plots in either the Bode or Nyquist format. Figure 2.2 depicts a classical Bode plot showing gain and phase margin determination from the plot. The Nyquist plot may also be used to obtain this information. Nyquist criterion states that if the open-loop transfer function $G(s)H(s)$ has n poles in the right half plane and the limit of $G(s)H(s) = \text{constant}$ as $s \rightarrow \infty$ then for a

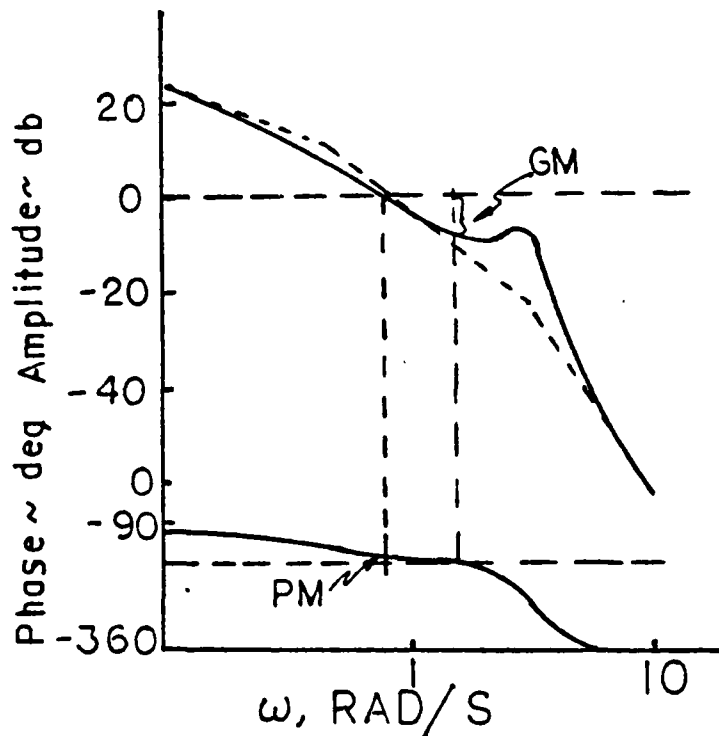


Figure 2.2 Classical Bode Plot.

stable system the locus of $G(s)H(s)$ will encircle the $-1+j0$ point n times in the counterclockwise direction as s varies along the Nyquist contour. If there are no poles in the right half s plane then the locus will not encircle the $-1 + j0$ point. The diagram in figure 2.3 illustrates a nominally stable system. The gain and phase margin may be determined directly from the diagram.

Any change in the loop transfer function, provided the order of $G(s)H(s)$ does not change, that changes the number of times the locus of $G(s)H(s)$ encircles the $(-1,0)$ point in the Nyquist plot causes the system to become unstable. This leads to the conclusion that the minimum distance of the

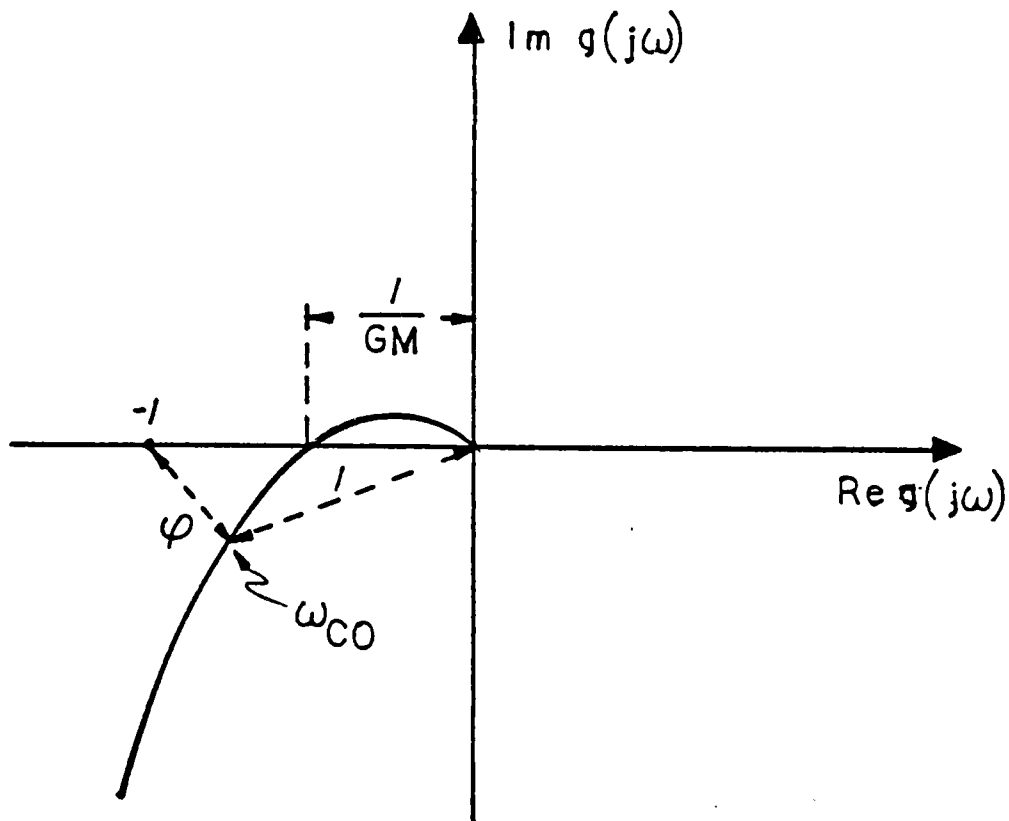


Figure 2.3 Nyquist Plot of Stable System.

locus of $G(s)H(s)$ to the $(-1,0)$ point is a measure of the system stability. This distance concept carries over directly to the MIMC system as will be shown in the next chapter. Examples of a multiplicative perturbation and an additive perturbation illustrate this idea. Figure 2.4 is an additively perturbed system. Figure 2.5 shows the Nyquist plot for this system. Assuming that the plant is itself stable and the perturbations are also stable the diagram may then be used to determine how near the system is to instability for the given perturbation.

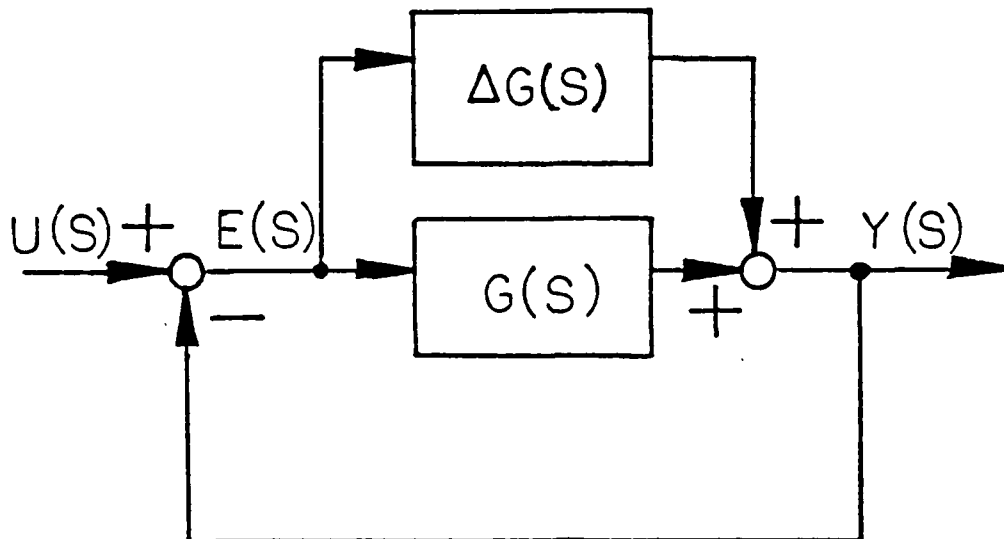


Figure 2.4 Additively Perturbed System.

Since the system is stable the $(-1,0)$ point is encircled the correct number of times by the nominal plant. If the locus of $g(j\omega)$ in the diagram is warped until it passes beyond the $(-1,0)$ point then clearly the number of encirclements of this point will change and the system will become unstable, assuming the order of the plant is not changed by the perturbation. To keep the locus of points from moving beyond the $(-1,0)$ point equation 2.1 must hold.

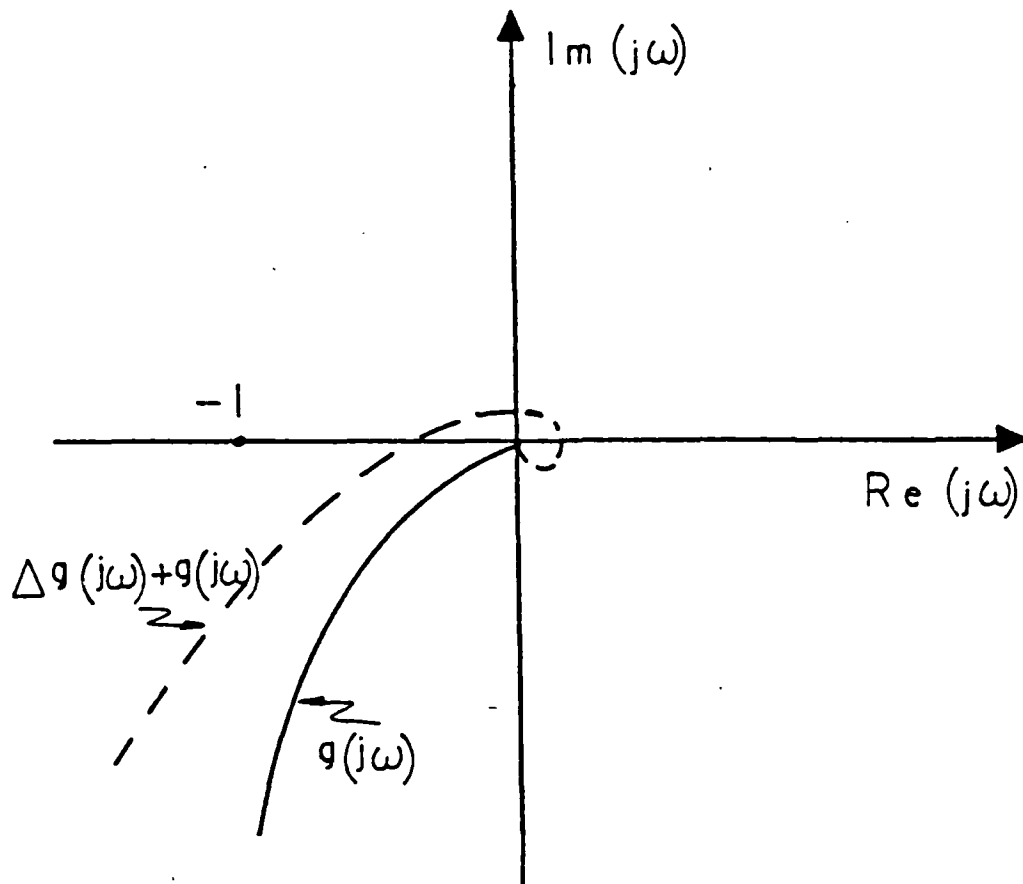


Figure 2.5 Additive Nyquist Plot.

$$|\Delta g(j\omega)| < |1 + g(j\omega)| \quad (2.1)$$

This condition is illustrated in figure 2.6. The right-hand side of equation 2.1 is just the magnitude of the return difference transfer function of the nominal system. The multiplicative case is depicted in figure 2.7 with its associated Nyquist plot in figure 2.8. The requirement for stability is similar to the additive case and may be stated in equation 2.2

$$|\Delta g(j\omega)| < |1 + (g(j\omega))^{-1}| \quad (2.2)$$

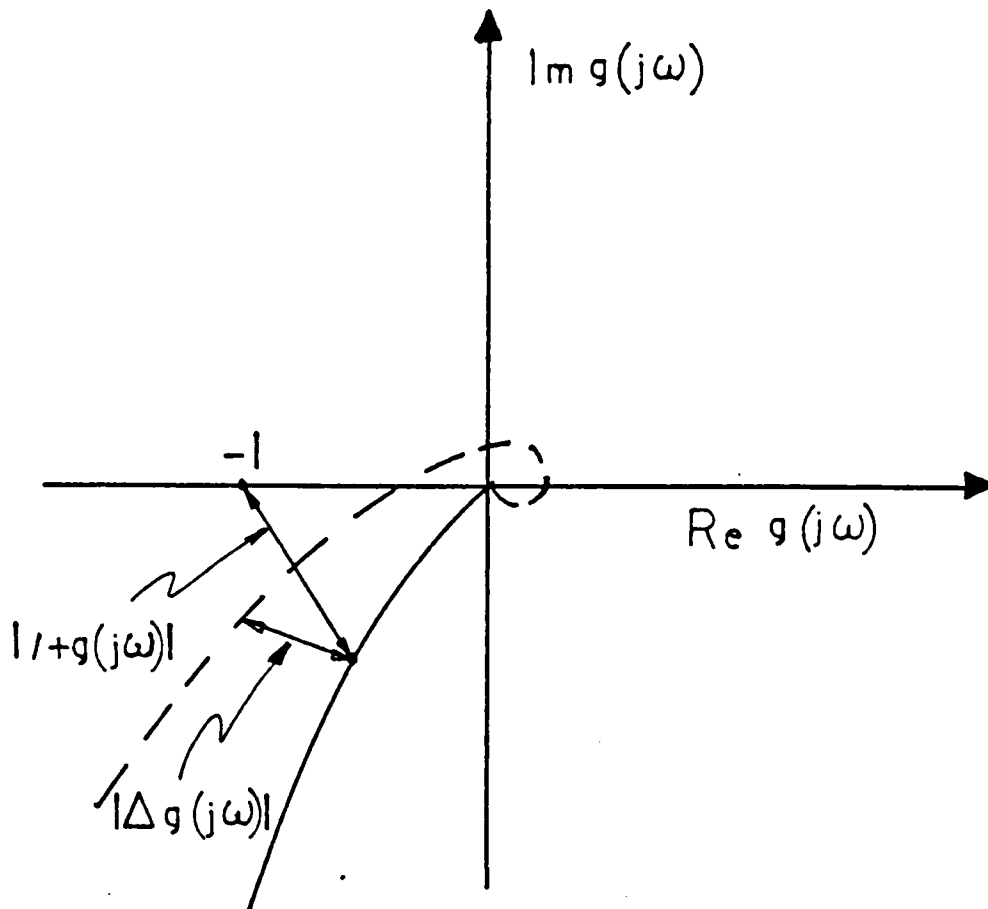


Figure 2.6 Nyquist for Inequality Additive Condition.

The above arguments will be applied again in Chapter 3 to develop multivariable stability and robustness properties.

The linear quadratic design has been the primary method employed in modern control design practice. In this method an optimal state feedback control law is developed to find a set of feedback gains that optimizes a chosen performance index. The performance index for the steady-state case is given in equation 2.3

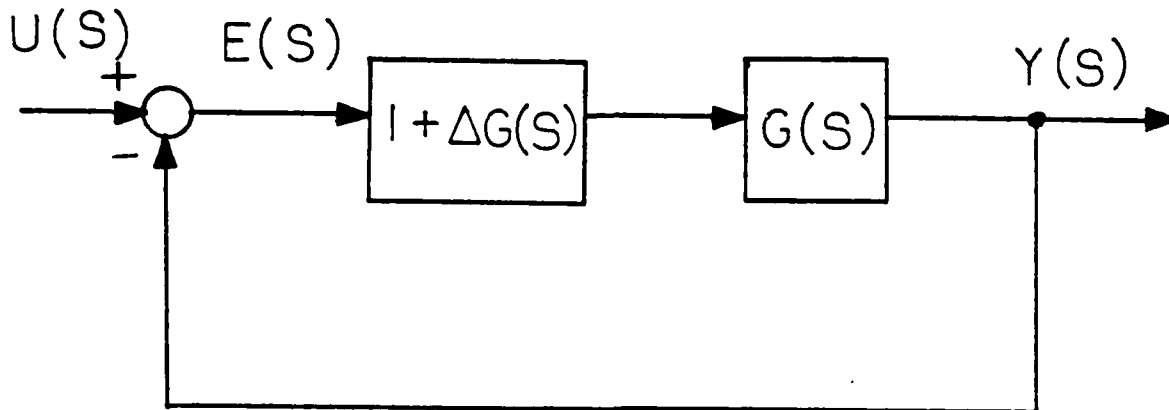


Figure 2.7 Multiplicative System.

$$PI = \int (\underline{x}'\underline{Q} \underline{x} + \underline{u}'\underline{R} \underline{u}) dt \quad (2.3)$$

where the $\underline{x}'\underline{x}$ term and the $\underline{u}'\underline{u}$ term form quadratics. The \underline{Q} and \underline{R} matrices are chosen by the designer to provide the best compromise between the minimum error of the system and the minimum energy needed to control the system. The LQ method is based on the use of closed-loop state variable feedback for the control of the system. In the MIMO problem LQ methods have been used extensively because of their guaranteed stability margins with diagonal weighting matrices. For diagonal weighting matrices the LQ method yields a guaranteed phase margin of 60 degrees and -6 db to infinite gain margin.

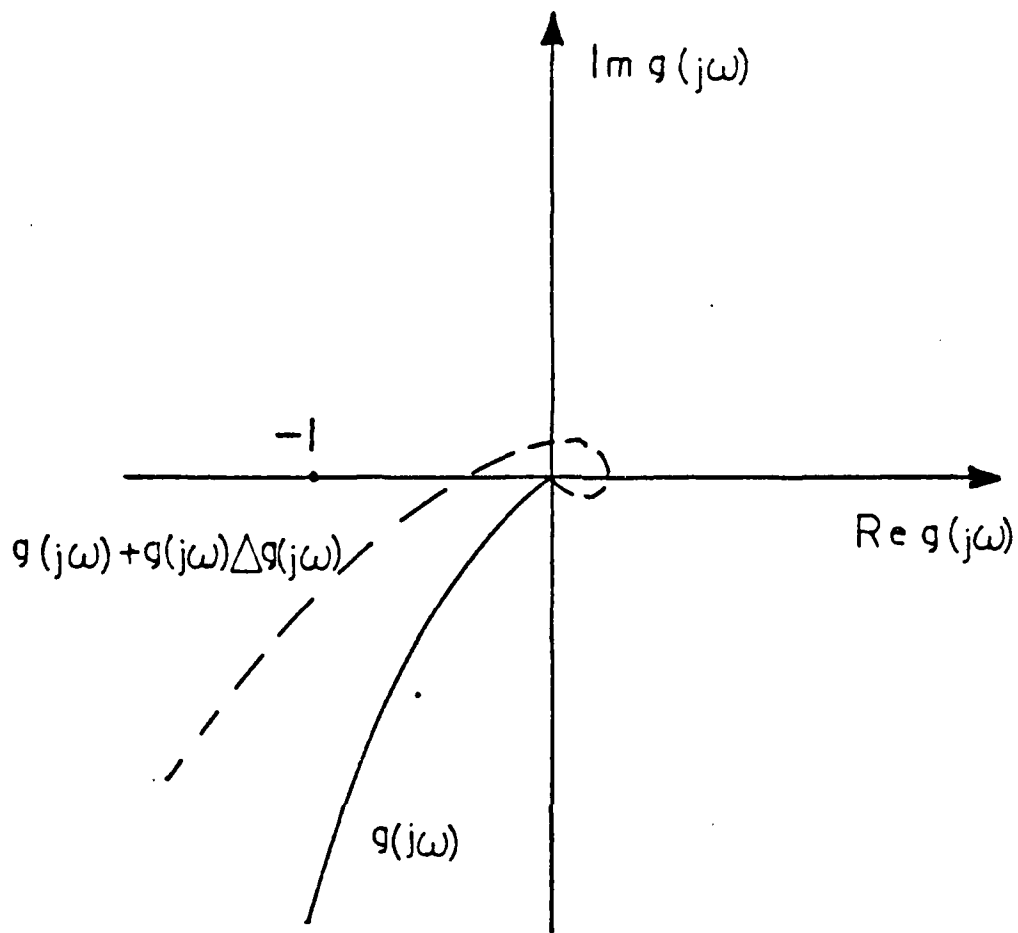


Figure 2.8 Nyquist Plot for Multiplicative System.

For SISO linear quadratic optimal regulators these stability margins can be developed from inequality 2.4 [Ref. 3]

$$|1 + f'(j\omega I - a)^{-1}b| \geq 1 \quad (2.4)$$

Writing the Kalman equation as 2.5

$$|1 + f'(sI-a)^{-1}b|^2 = 1 + (1/\rho) |G_K(s)|^2 \quad (2.5)$$

one has further

$$|1 + G(s)H(s)|^2 = 1 + (1/\rho) |G_K(s)|^2 \quad (2.6)$$

and for all $s=j\omega$ and $0 \leq \omega < \infty$ the function $(1/\rho)G_K(s)$ is greater than zero, therefore the Kalman inequality is shown to be 2.7.

$$|1 + G(s)H(s)| > 1 \quad (2.7)$$

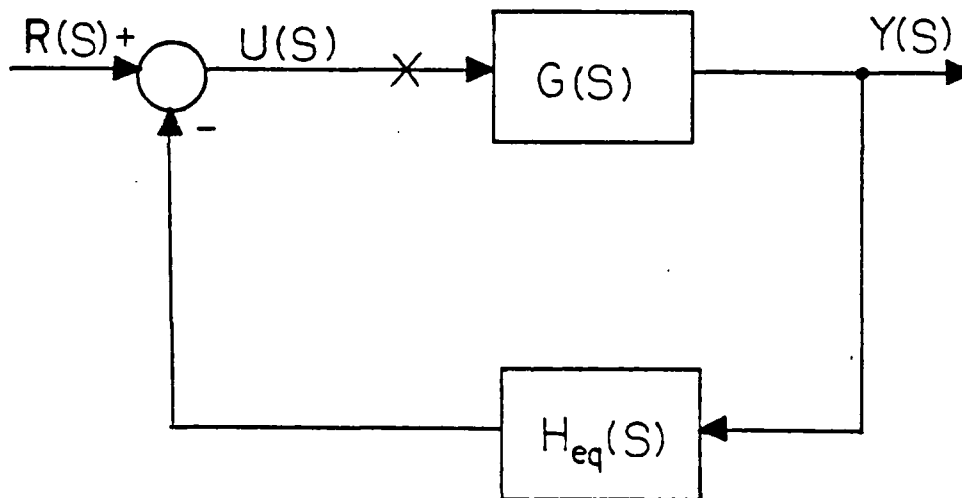


Figure 2.9 Typical Equivalent Feedback System.

The graphical interpretation of this result is that the polar plot of $G(s)H(s)$ must remain outside the unit circle centered at the $-1 + j0$ point for all frequencies. Figure

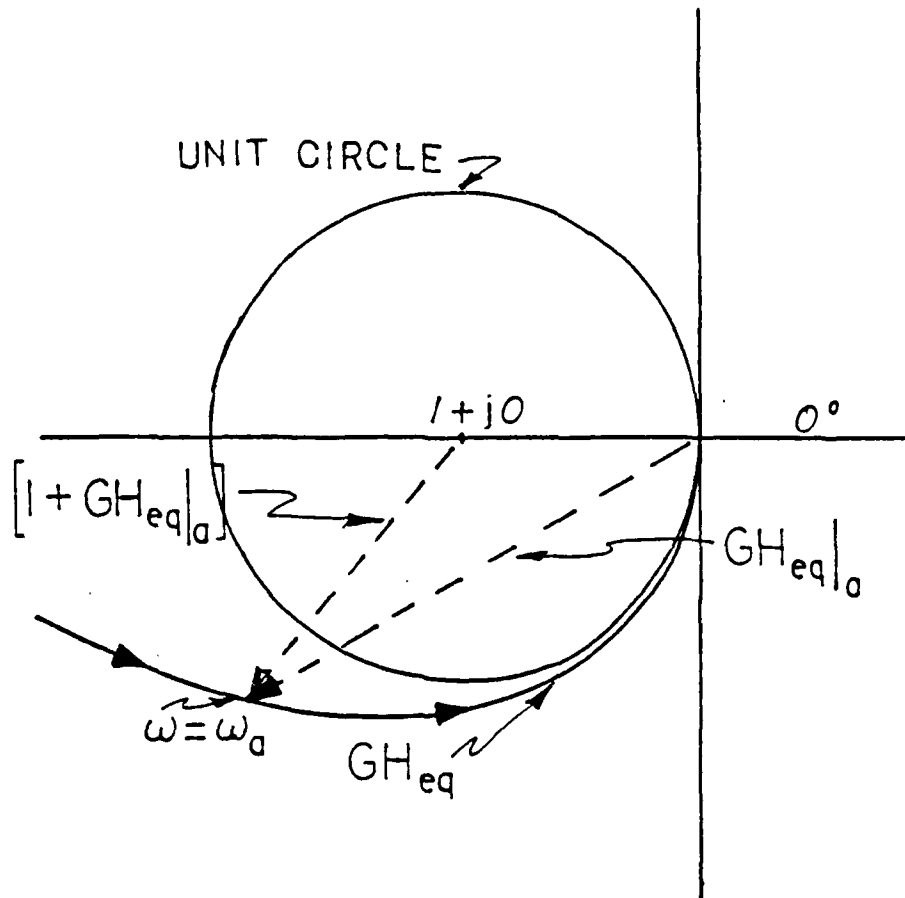


Figure 2.10 Polar Plot of an Optimal System.

2.10 shows such a polar plot. Since the optimal regulator with the loop broken at the input to the plant (denoted by the x in figure 2.9) does not penetrate the unit disk about $-1 + j0$ this means that the single input regulator will have

a phase margin of at least 60 degrees and a gain margin tolerance of fifty percent gain reduction and infinite upward margin. Further discussion of this property may be found in Anderson and Moore [Ref. 4]. With this basic review of the concepts of stability and robustness in the classical SISO system complete, the next chapter will extend some of these basic concepts to the MIMO system.

III. MULTIVARIABLE SYSTEMS

Linear quadratic design has performed relatively well in aircraft control concepts because of the ability to formulate the system state equation and to quantify acceptable performance indices for the system. Industrial applications for LQ theory have been less successful and have led British researchers to look into forms of decoupled design methods. One of the primary methods used in multivariable design is to make the system totally decoupled. This method allows each loop to be designed as a separate entity by classical means. One of the primary difficulties with this method is the problem of finding a compensator which will totally decouple the system. The method also suffers from the effects of cross-coupled perturbation terms. A method that does not totally decouple the system but makes the design problem simpler by designing a compensator that only causes the diagonal terms of the transfer matrix to be dominant over all off-diagonal terms has also been developed, [Ref. 5]. Classical frequency domain techniques are then used to design each loop of the system. The major difficulty with this and other single loop design techniques is their failure to account for cross-coupling perturbation terms that may interact between the loops. The individual loops may be highly robust in these designs but the overall system robustness may be low because of the loop interaction not accounted for in the design. This is the precise area that the singular value analysis has proven so beneficial in design. Singular value concepts may be applied to conventionally designed systems to assess their robustness. For instance, if a system is designed by LQ methods the designer may then formulate the transfer function of the system and

assess the singular values of the return difference matrix of the system. If the minimum singular value is found to be low at some critical frequencies the designer can then modify the \underline{Q} and/or \underline{R} matrices chosen in the LQ performance index and recalculate the design. In this iterative fashion a robust design would be developed.

A generalization of the SISO Nyquist theory discussed in the previous chapter has been made for the MIMO problem. This generalization leads directly to the singular value concept. The generalization is expressed in the form of the multivariable Nyquist theorem which requires that a closed loop stable system have the same number of counterclockwise encirclements of the origin by the locus of the $\det(\underline{I} + \underline{G}(j\omega))$ as the number of open loop poles that are unstable. This theorem is formally stated as;

Let $N[f(s)]$ denote the number of clockwise encirclements of $(-1, 0)$ by the locus of $f(s)$ as s traverses the contour D of figure 3.1 in a clockwise sense. The closed-loop system will be stable if and only if for all R sufficiently large

$$N[f(s)] = -P$$

where

$$f(s) = -1 + \det[\underline{I} + \underline{G}(s)] = \varphi_{o_L}(s) / \varphi_{p_L}(s) - 1 \text{ and}$$

$P =$ the number of closed right-half plane zeros of $\varphi_{o_L}(s)$.

The application of the Nyquist theorem comes through the fact that a multivariable system will not be robust to modelling errors if the return difference matrix, $\underline{I} + \underline{G}$, is nearly singular for some frequency. If $\underline{I} + \underline{G}$ is nearly singular a small change in \underline{G} may make $\underline{I} + \underline{G}$ exactly singular. This causes the $\det(\underline{I} + \underline{G})$ to become zero and the Nyquist encirclement count to change indicating an unstable system. It is possible for very small changes in $\underline{I} + \underline{G}$ to produce large changes in the determinant of $\underline{I} + \underline{G}$. The matrix

$\underline{I} + \underline{G}$

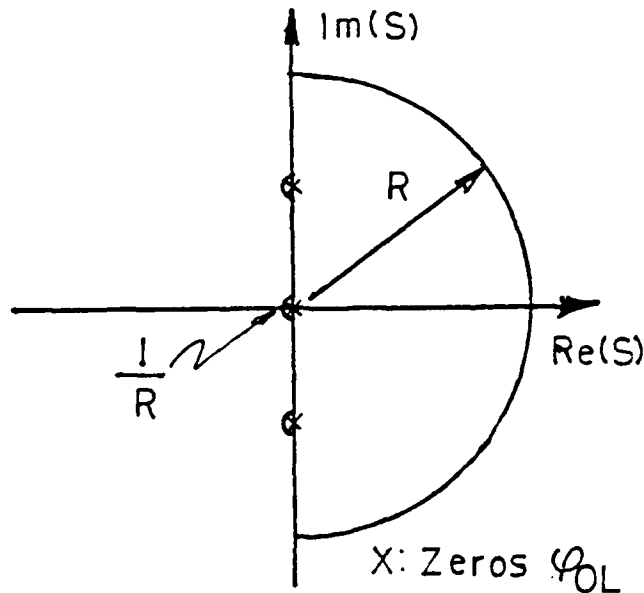


Figure 3.1 Nyquist D Contour.

$$\begin{bmatrix} 10/s+a & 9.99/s+a \\ 10/s+a & 10/s+a \end{bmatrix}$$

has determinant $0.1/(s+a)^2$. If the element p_2 , is changed by only one percent to $9.9/s+a$ the determinant becomes $1.1/(s+a)^2$ which is a significant change in the determinant value. Therefore, it is evident that $\det(\underline{I} + \underline{G})$ is not an accurate measure of how near the return difference is to singularity. Researchers, in the field of controls [Ref. 6], [Ref. 7], [Ref. 8], [Ref. 9] have used singular value analysis to determine how near the return difference matrix is to singularity.

Since the number of encirclements of the Nyquist diagram changes as $f(s)$ passes through the -1 point or when $\det(\underline{I} + \underline{G})$ is zero it is important to find how near the return difference matrix $\underline{I} + \underline{G}$ is to being singular. This nearness to singularity can be interpreted as closeness of the matrix \underline{G}

to the critical point, -1. A quantity which can be used to express the nearness to singularity of the matrix is the minimum matrix singular value denoted by $\underline{\sigma}$. Given a matrix A the singular value may be expressed by equation 3.1

$$\underline{\sigma}(A) = \min_i (\lambda_i (A^H A))^{1/2} \quad (3.1)$$

where $\lambda_i (A^H A)$ is the eigenvalue of the complex conjugate transpose of A times A . A basic MIMO linear system is

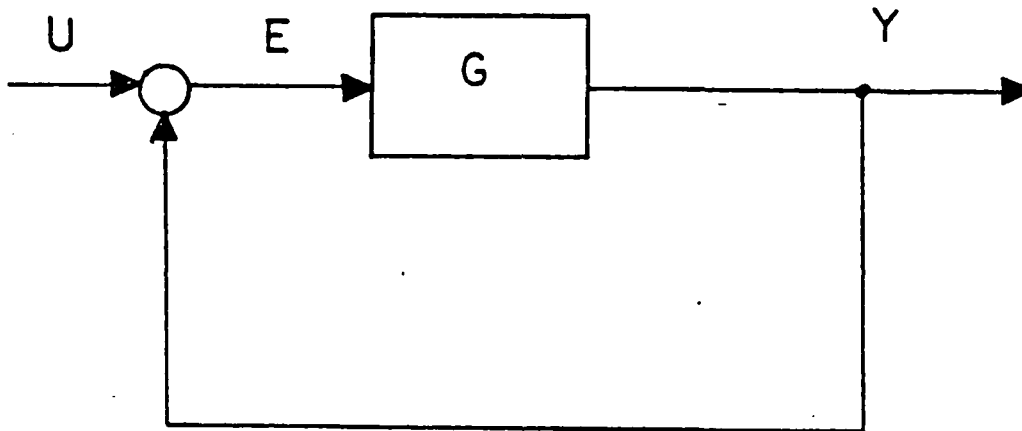


Figure 3.2 Basic Multi-input, Multi-output System.

depicted in figure 3.2. An additive perturbation to the plant is shown in figure 3.3. If the plant is stable before the perturbation is added to the system the Nyquist theorem will be satisfied and the locus of GH will not encircle the -1,0 critical point. When the perturbation is added to the system as long as the Nyquist locus is not forced to

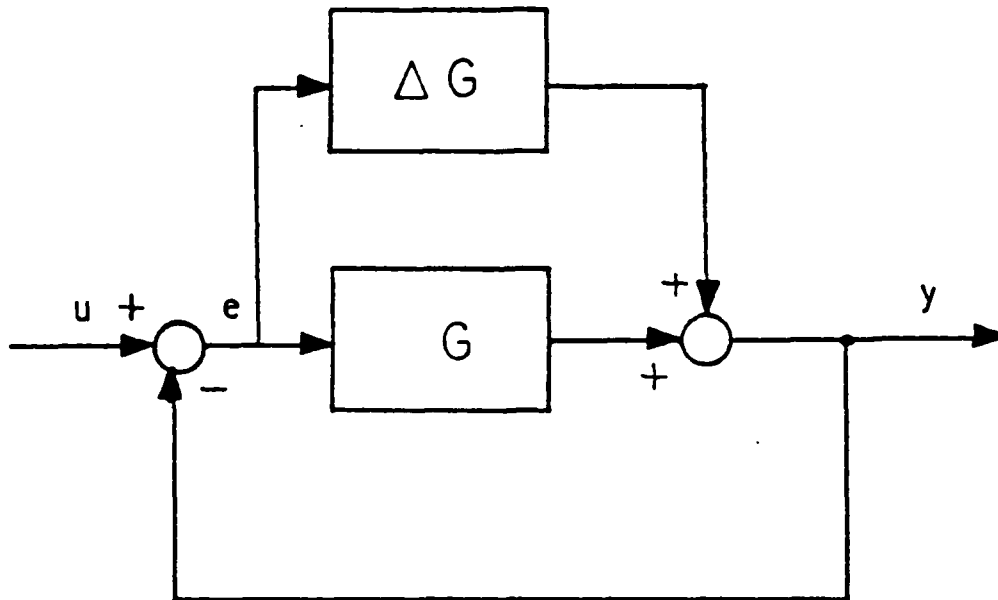


Figure 3.3 Additive Perturbation.

encircle the -1 point the system will remain stable. A sufficient condition, recalling the SISO discussion in chapter 2, for the perturbed Nyquist plot not to change encirclements is that the norm of the perturbation ΔG remain less than the norm of the return difference matrix as expressed in equation 3.2.

$$\| \Delta G(j\omega) \| < 1 / \| (I + G)^{-1} \| \quad (3.2)$$

$\omega \geq 0$ This condition will guarantee that the locus of the $\det(I + G)$ does not pass through the -1 point. If the l_2 or Euclidean norm is assumed for this condition the equation

3.2 may be expressed in terms of singular values as equation 3.3.

$$\bar{\sigma}(\Delta G) \leq \underline{\sigma}(I + G) \quad (3.3)$$

This result states that as long as the maximum singular value of the perturbation matrix ΔG is below the minimum norm value of the return difference matrix the system will remain stable. The problem of guaranteeing robustness becomes that of finding the largest norm of the perturbation quantity, the largest singular value, for which the smallest norm or singular value of the return difference matrix will remain non singular.

The multiplicative form for a system such as figure 3.4 gives the similar norm equation in 3.4

$$\|\Delta G(j\omega)\| < 1 / \|(I + (G)^{-1})^{-1}\| \quad (3.4)$$

$\omega \geq 0$. which may be expressed as;

$$\bar{\sigma}(\Delta G) \leq \underline{\sigma}(I + G^{-1}) \quad (3.5)$$

Singular value decomposition software is readily available to determine how near the matrix $I+G$ or $I+ (G)^{-1}$ is to singularity.

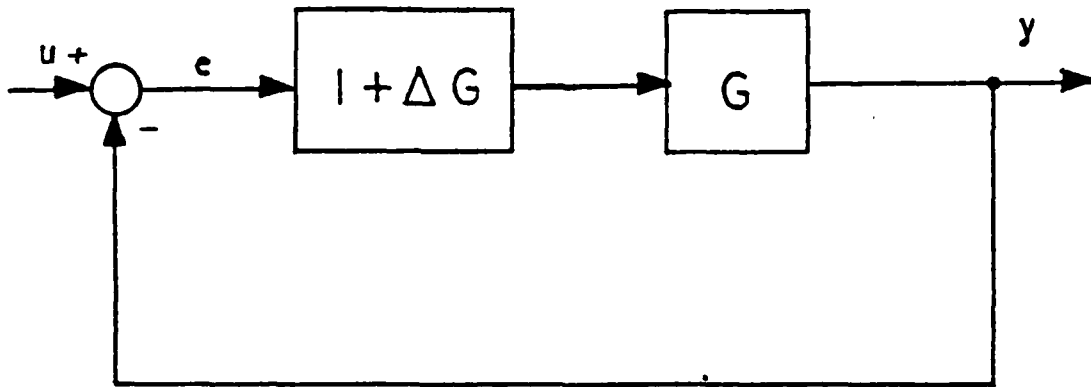


Figure 3.4 Multiplicative Perturbation.

IV. OPTIMIZATION

The purpose of this chapter will be to briefly describe several of the currently employed optimization techniques and the Automated Design Synthesis (ADS) program, [Ref. 10], which employs these techniques. In general, optimization implies finding the "best" possible solution to a problem. In actuality the best solution found by an optimization technique might really only be a "better" solution to the problem. The purpose of ADS and other optimization routines is to allow a rational search to be conducted to find the best possible design. The techniques of numerical optimization are used to logically vary the various parameters that affect the design until a good solution is found.

As an example of an unconstrained optimization problem consider the following problem developed in [Ref. 11]. The problem is to minimize the function

$$F(\underline{x}) = 10x_1^4 - 20x_1^2x_2 + 10x_2^2 + x_1^2 - 2x_1 + 5 \quad (4.1)$$

$F(\underline{x})$ is often called the objective function, the cost function or the penalty function. Since there are no conditions imposed on the design variables, x_1 , and x_2 , and no additional limits imposed on the overall design, the problem is considered to be one of unconstrained minimization. Figure 4.1 represents this problem in the design space. From the figure it appears the optimum is near the point 1,1. Calculus may be applied to determine the optimum exactly. Taking the derivatives

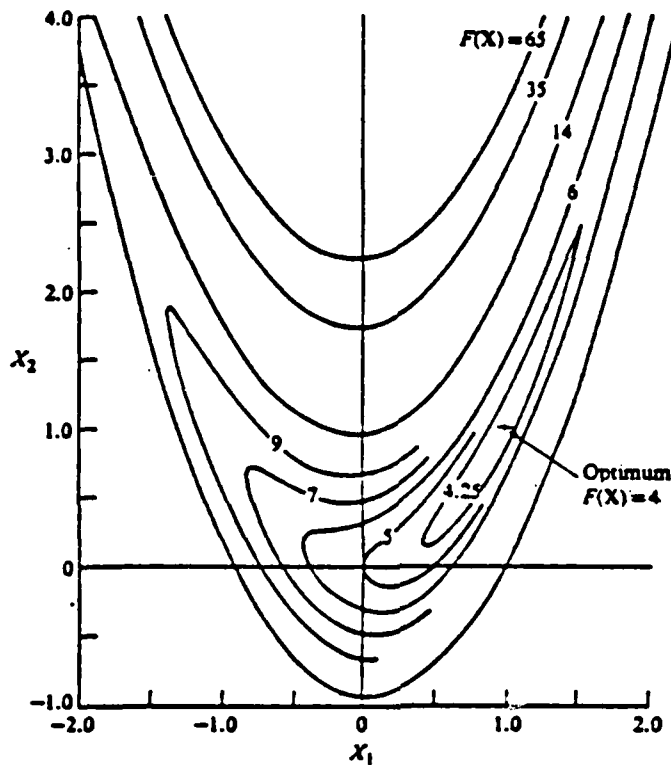


Figure 4.1 Design Space for Example Problem.

$$\frac{\partial F(\underline{x})}{\partial x_1} = 40x_1^3 - 40x_1x_2 + 2x_2 - 2 = 0 \quad (4.2)$$

$$\frac{\partial F(\underline{x})}{\partial x_2} = -20x_1^2 + 20x_2 = 0 \quad (4.3)$$

and then solving the set of equations it is found that $x_1 = 1.0$ and $x_2 = 1.0$.

If design conditions are imposed on the problem then the optimization becomes one of constrained function minimization. In other words, while the minimum of a function is still sought, this minimum must exist within the limits

imposed by the design conditions or constraints. The minimum of an unconstrained function will not necessarily be the same minimum for a constrained function.

As another example, also from [Ref. 11], a design is sought which gives the minimum weight of a particular column. This weight is expressed as:

$$W = \rho Ah = \rho \pi D h \quad (4.4)$$

where ρ is the unit weight of the material and A the cross sectional area. The stress in the column is given by:

$$\sigma = P/A = P/\pi D t \quad (4.5)$$

without going into detail the design will be constrained by the allowable stress on the structure. Other constraints, Euler buckling and shell buckling, are also of interest to the designer of this column. The design problem is then stated as:

$$\text{minimize } W = \rho \pi D t h \quad (4.6)$$

for the constraints

$$g(1) = \sigma / \bar{\sigma} - 1 \leq 0 \quad (4.7)$$

$$g(2) = \sigma / \sigma_D - 1 \leq 0 \quad (4.8)$$

$$g(3) = \sigma / \sigma_S - 1 \leq 0 \quad (4.9)$$

with $D \geq 10e-06$ and $t \geq 10e-06$.

$$g(4) = t - D \leq 0$$

(4.10)

$\bar{\sigma}$, σ_b , σ_s refer to the allowable design stress, Euler buckling stress and the shell buckling stress respectively.

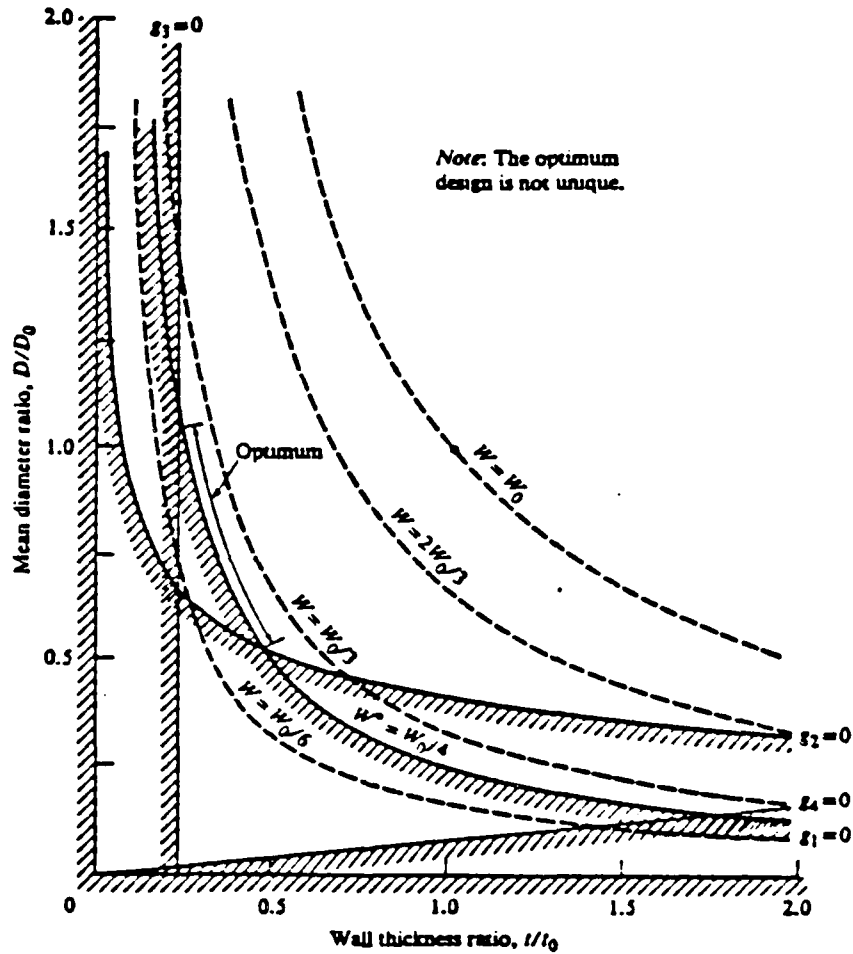


Figure 4.2 Design Space for Column Problem.

Figure 4.2 is a design space diagram for this problem. It is noted from the figure 4.2 that the optimum is not unique and can be any value along the arc noted as optimum in the figure.

The general optimization problem is then written as:

$$\text{minimize } F(\underline{x}) \qquad \text{objective} \qquad (4.11)$$

$$\text{subject to } g_j(\underline{x}) \leq 0 \quad j=1, m \text{ inequality constraint} \quad (4.12)$$

$$h_k(\underline{x}) = 0 \quad k=1, l \text{ equality constraint} \quad (4.13)$$

$$x_i^l \leq x_i \leq x_i^u \quad i=1, n \text{ side constraint} \quad (4.14)$$

where $\underline{x} = \text{col}(x_1, x_2, \dots, x_n)$ is the design variable.

The methods used to solve this problem are usually iterative. After the establishment of an initial set of variables the optimizer will update this initial value until the optimum values are found. Again, borrowing from [Ref. 11], the iterative technique may be demonstrated by a simple example. Figure 4.3 is used to illustrate this problem. Given the initial data set \underline{x}^0 the formula

$$\underline{x}^1 = \underline{x}^0 + \alpha^* \underline{s}^1 \qquad (4.15)$$

can be used to upgrade this estimate of \underline{x} . The vector \underline{s} is the search direction for the iteration and the scalar quantity α is the distance of the move in the \underline{s} direction. Beginning at \underline{x}^0 it is desired to reduce the objective function. The search for values of \underline{x} that reduce the objective function is made in the \underline{s} direction which in this example is the opposite of the gradient of the function at point \underline{x}^0 . The choice of \underline{s} could be arbitrary as long as it reduces the

function. These one dimensional searches are continued until no more reduction in the objective can be found. At this point no further design improvement is possible.

Optimization techniques do not always lead to the absolute optimum when applied to problems of practical interest. The reasons for this could be numerical ill-conditioning of the problem formulation or simply that there are multiple solutions to the problem. Because of these difficulties it may be advisable to choose several different starting points for the optimization process and use engineering judgement as to the design most applicable to the problem under analysis.

Considering the unconstrained case first where the desire is to minimize the function $F(\underline{x})$, it is well known that $F(\underline{x})$ will have a minimum where the gradient of $F(\underline{x})$ is zero. That is:

$$\text{grad}(F(\underline{x}))=0 \quad (4.17)$$

with the $\nabla F(\underline{x})$ defined as:

$$\text{grad}(F(\underline{x})) = (\partial F(\underline{x})/\partial x_1, \dots, \partial F(\underline{x})/\partial x_n)' \quad (4.18)$$

Figure 4.4 shows why this is a necessary condition but does not guarantee a global minimum. The gradient of $F(\underline{x})$ is zero at all four points A, B, C, and D. However, only A and D are minima. A would be the global minimum for the function as defined here. D would be only a relative minimum. To check that the zero gradient corresponds to a minimum the Hessian matrix, i.e. the matrix of second partial derivatives, can be examined for positive definiteness. A positive definite Hessian ensures a relative minimum. The only way to prove a global minimum for the function is to show that the Hessian matrix is positive definite for all design variables x . A test that is seldom possible to perform.

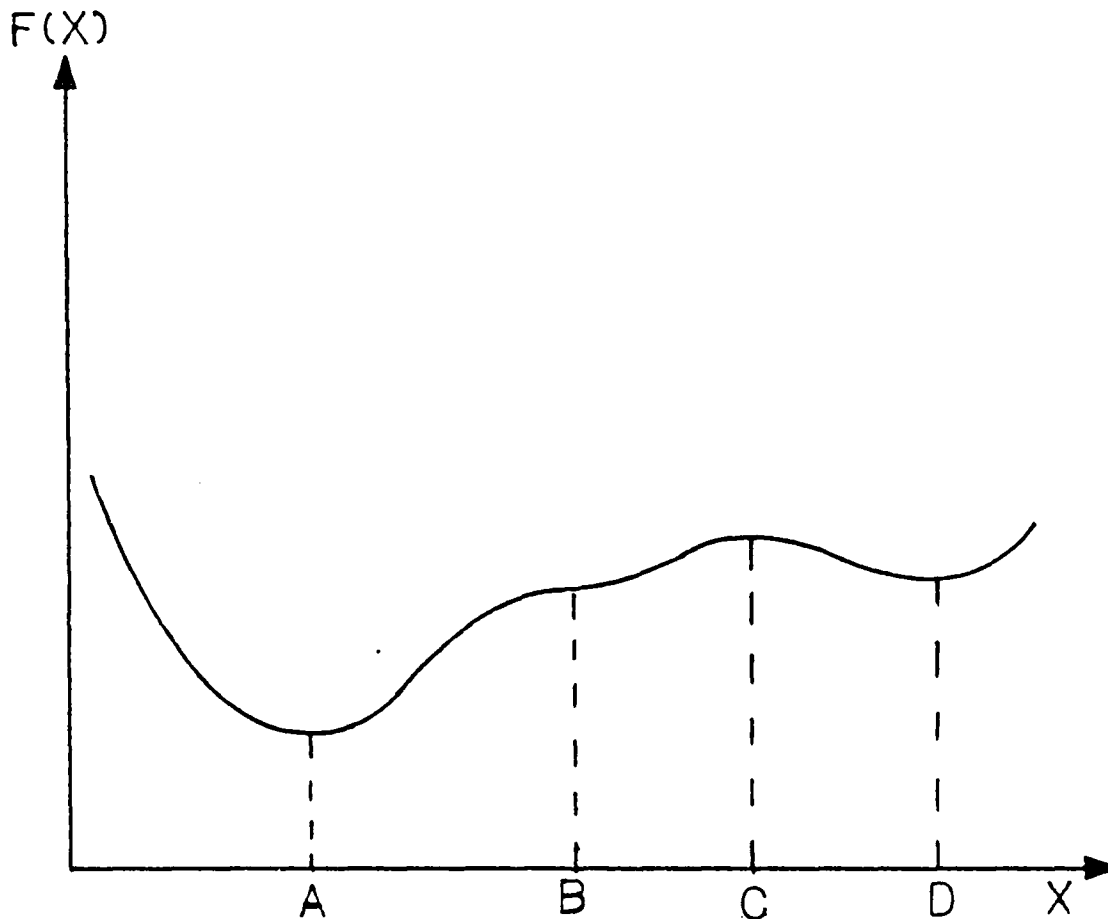


Figure 4.4 Plot of Various Points With Zero Gradient.

If the problem of minimization is a constrained problem the situation is different from that discussed above. The objective function gradient does not have to be zero at the optimum. Figure 4.5 illustrates this case. Using figure 4.5 and assuming a start at point A it is necessary to choose a search direction S which will reduce the objective function while not violating the constraint functions. Any direction that will reduce the objective is said to be useable. This is seen to be the half plane sector below the tangent to $F(x)$ at point A. If a half plane to the right of the tangent to the active constraint at point A is considered then the feasible sector is formed. A combination of the two

conditions gives the useable, feasible sector where the search direction S must be chosen. In mathematical nomenclature the above argument may be stated as:

$$\text{useable direction } \text{grad}(F(\underline{x})) \cdot \underline{S} \leq 0 \quad (4.19)$$

$$\text{feasible direction } \text{grad}(g_j(\underline{x})) \cdot \underline{S} \leq 0 \text{ for all } j \quad (4.20)$$

for which $g_j(\underline{x}) = 0$.

Point B in figure 4.5 shows a point where the gradient of the objective and constraint point in exactly the opposite direction. At a point such as B the only search vector S that meets requirements for useability and feasibility is tangent to the constraint boundary and to a line of constant objective function. This condition is stated as:

$$\text{grad}(F(\underline{x})) + \sum \lambda_j \text{grad}(g_j(\underline{x})) + \sum \lambda_{l+m} \text{grad}(h_k(\underline{x})) = 0 \quad (4.21)$$

where $\lambda_j \geq 0$ and λ_{l+m} -unrestricted.

With this brief background in optimization complete the Automated Design Synthesis (ADS) program will be briefly discussed. More detail on the ADS routine can be found in [Ref. 10]. This code was developed as a follow-on to the successful CONMIN code [Ref. 12] developed by Vanderplaats. It is designed as a black box optimizer which allows the user to choose combinations of one dimensional search, optimization algorithm and optimization strategy. These will be discussed later. For the user with specific requirements the code may be tailored by parameter modification to meet specific requirements. For the work done in this thesis it was assumed the user of the code has no detailed knowledge of optimization and will want to use the code in the

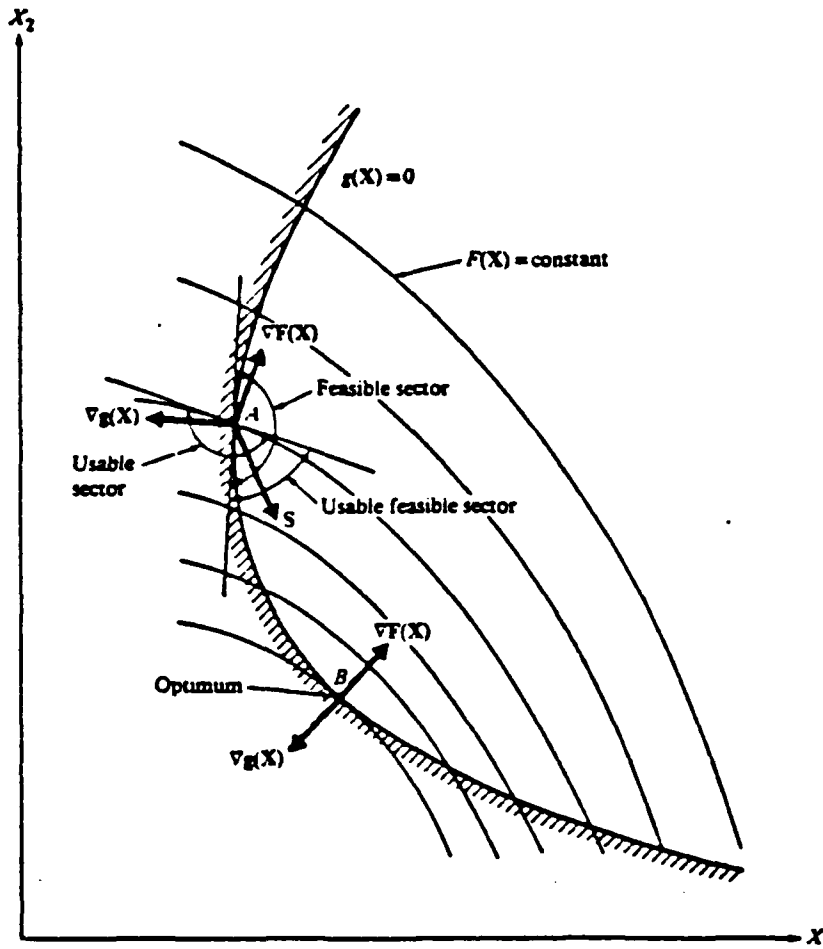


Figure 4.5 Constrained Optimization Example.

simplest form. As such, the ADS calls made from the main program use only default parameters and first forward finite difference gradients. Should analytical gradients be available the user could use them within the code if desired with no difficulty. The calls made by the user to the ADS routines specify several important aspects of the problem solution. The user may call for an optimization strategy to be used in the routine. This is not required and its use

depends on the problem. These strategies are discussed in [Ref. 10]. Two strategies used most often in the analysis done for this thesis have been sequential unconstrained minimization using quadratic exterior penalty function and the augmented Lagrange multiplier (ALM) method. Others available include sequential linear programming and sequential quadratic programming.

The basic optimizer is also chosen by the user from two unconstrained and three constrained optimization algorithms. The unconstrained algorithms are Fletcher-Reeves conjugate directions, Davidon-Fletcher-Powell (DFP) variable metric method and the Broyden-Fletcher-Goldfarb-Shanno (BFGS) variable metric method. The method of feasible directions and robust feasible directions are available for constrained minimization.

The user has available several types of one dimensional searches using Golden Section or polynomial approximation techniques. The ADS code has tailored these one dimensional search algorithms for the unconstrained and constrained cases, allowing the user to make appropriate choices for the type of problem to be solved. Figure 4.6 shows the basic organization of the ADS program.

Since it is not the purpose of this chapter to cover the subject of optimization in detail all the possible routines in ADS will not be discussed. A few of the routines found to work well for the work completed in this thesis will be briefly described, however. There are several methods of optimizing functions of one variable or one dimensional searches. For instance a large number of points, n , could be chosen and the function $F(\underline{x})$ evaluated at each point. The point corresponding to the smallest value of $F(\underline{x})$ could then be considered the optimum value of the one dimensional search. This method is hit and miss and better methods of

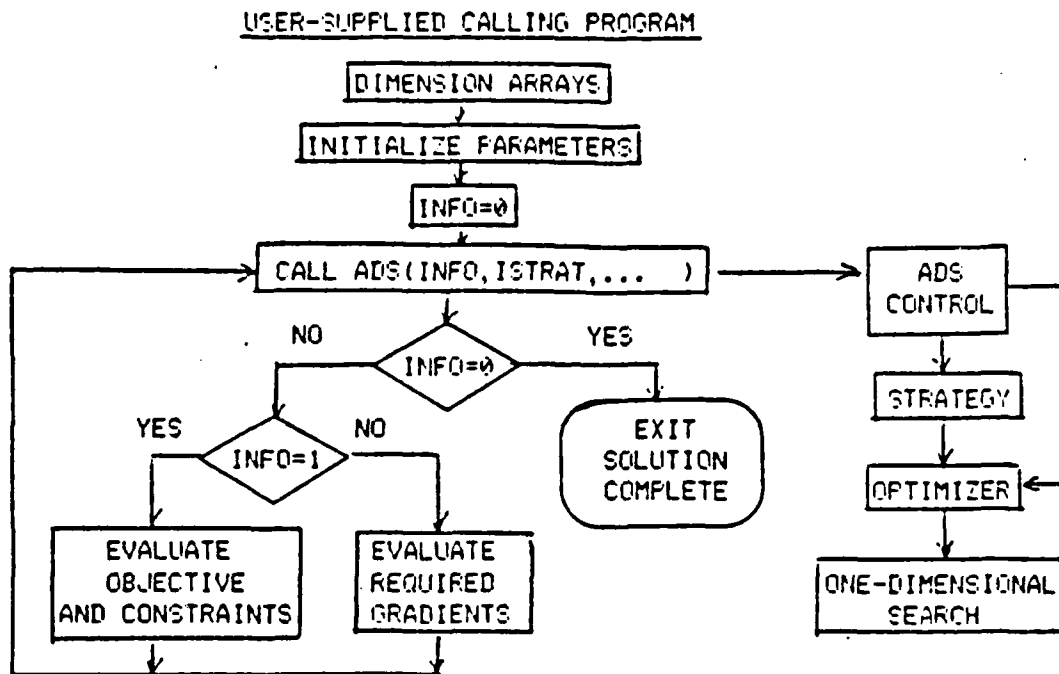


Figure 4.6 Organization of ADS Program.

locating optimum points can be used. The methods used in ADS are Golden Section and polynomial interpolation.

Golden Section search methods are easy to program on the digital computer and do not require continuous derivatives. They have a known convergence rate and are reliable for poorly conditioned problems. The major drawback of the Golden Section routines is the large number of function evaluations require. The Golden Section algorithm is simply illustrated through the use of figure 4.7 Assume that X^0 and X^1 are known to be bounds on the curve's minimum value. Also, the function values of $F(x)$, F^0 and F^1 , are evaluated and known at these points. By picking two intermediate points X^2 and X^3 where $X^2 < X^3$ and evaluating the function

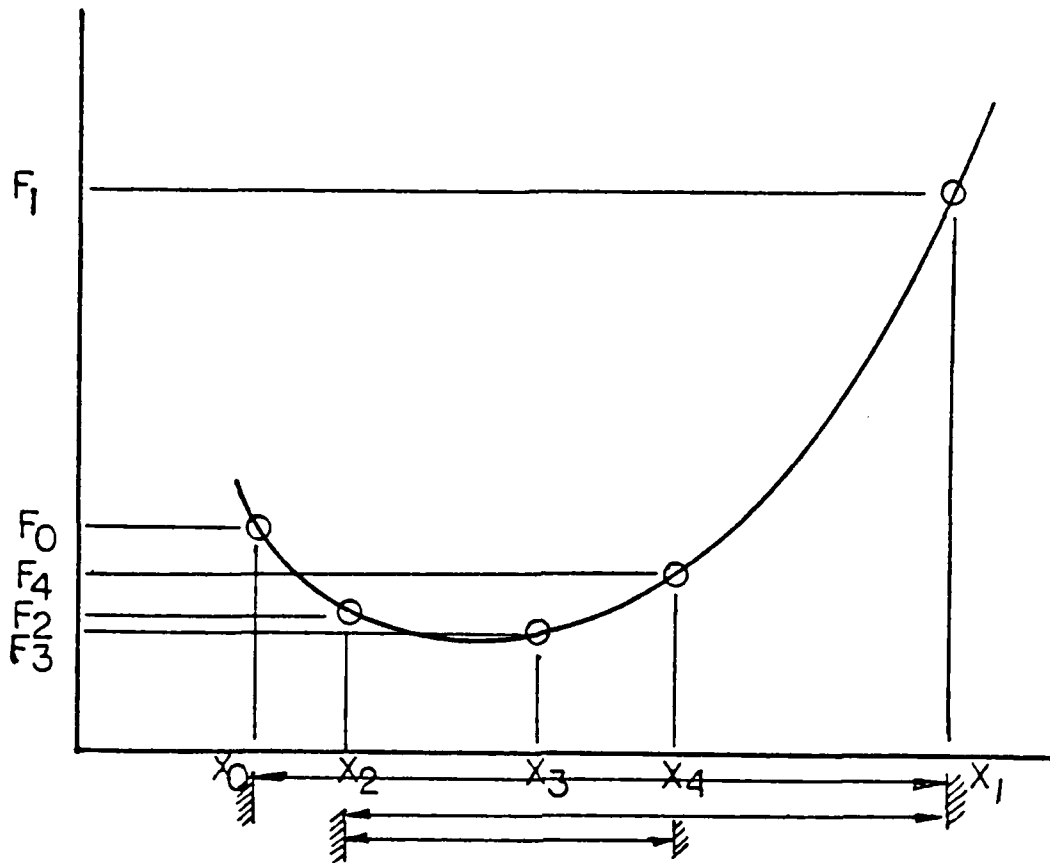


Figure 4.7 Golden Section Diagram.

at these points a bound on the minimum may be modified. Since F_2 for this figure is larger than F_3 the point x_2 forms the new lower bound. The minimum is now between x_2 and x_1 . If the function F_4 at x_4 is determined and shown to be larger than F_3 then x_4 becomes the new upper bound on the minimum. By repeating this procedure the bounds may be narrowed to any desired tolerance. The Golden Section rule is applied to this problem to reduce the bounds in the quickest possible time. By appropriately picking the values of x 's at which each function evaluation is made an efficient algorithm that uses the ratio proportion of the Golden

Section, i.e. $X^2/X^1 = 1.62803$ is developed. By choosing a value τ based on this Golden Section rule where $\tau = 0.38197$ estimates for interior points X^2 and X^3 can be made as:

$$X^2 = (1 - \tau)X^0 + \tau X^1 \quad (4.22)$$

$$X^3 = \tau X^0 + (1 - \tau)X^1 \quad (4.23)$$

As each new bound is found the process repeats until the accepted level of convergence is reached.

The polynomial interpolation method is accomplished by first fitting a polynomial curve to the points about where the minimum is desired and then finding the minimum of the polynomial function. For example if the function $F(X)$ is approximated by a quadratic as:

$$F = a_0 + a_1 X + a_2 X^2 \quad (4.24)$$

Then the value of X , X^* , where F' is zero can be shown to be :

$$X^* = -a_1 / 2a_2 \quad (4.25)$$

If a_2 is positive then F will be minimum. Other degrees of polynomials may be used in similar fashion.

Now that the basic one dimensional search methods have been reviewed the next step is to examine the basic optimization routines. First, the unconstrained case will be reviewed. The optimum X^* is at the point where

$$\text{grad}(F(\underline{X}^*)) = 0 \quad (4.26)$$

Several zero order methods exist for the purpose of finding the minimum value. These include random search, Powell's method and Box's method. Since ADS does not use these methods they will not be discussed.

Automated Design Synthesis makes use of first order methods which will now be discussed. The steepest descent method is best known, but poor in performance. Just as the name implies a search direction is chosen opposite the gradient of the objective function. At iteration 0

$$\underline{s}^0 = -\text{grad}(F(\underline{X}^0)) \quad (4.27)$$

Figure 4.8 shows this algorithm geometrically. Note that the method simply stair steps its way down the "hill" to the valley or minimum. ADS uses the Fletcher-Reeves modification to steepest descent. In this routine a conjugate direction is chosen to improve the speed of the search. Figure 4.9 shows how this method tracks to the solution.

The variable metric methods listed earlier are usually more powerful than Fletcher-Reeves because they store information that allows the algorithm to approximate the inverse of the Hessian matrix or second derivative. For further discussion of these methods see [Ref. 11] or other similar optimization texts.

ADS employs two direct methods for constrained minimization. One method is that of feasible direction and the other is the method of robust feasible direction. Since these two methods were seldom employed within the work presented in this paper they will not be discussed.

The methods chosen to handle the constrained minimization problems formulated in this thesis are referred to as Sequential Unconstrained Minimization Techniques (SUMT).

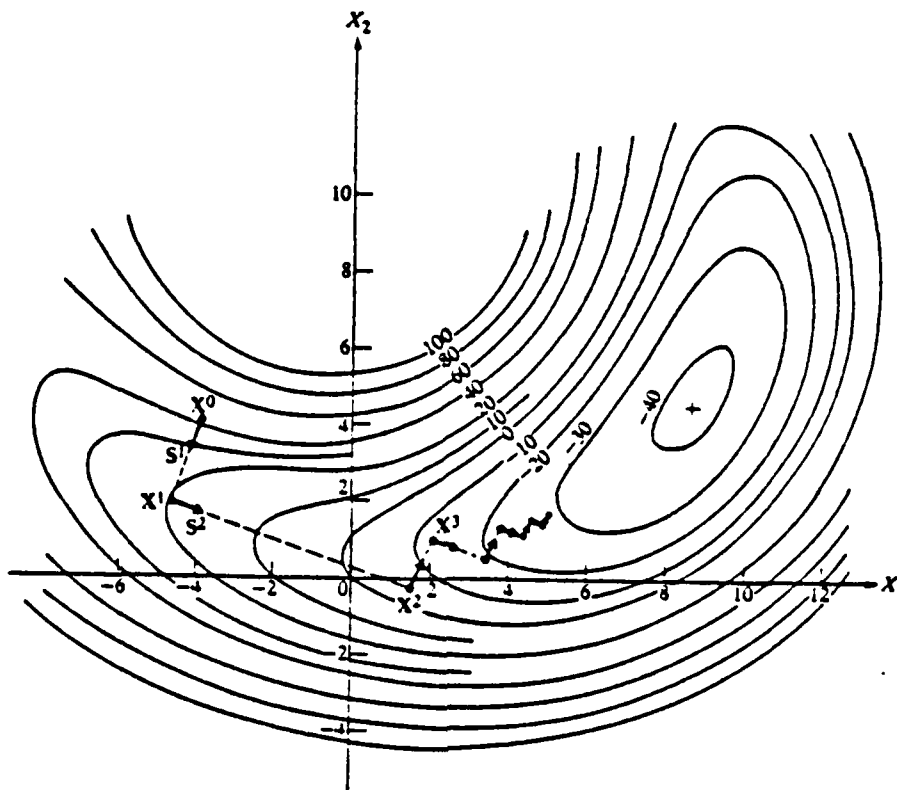


Figure 4.8 Steepest Descent Algorithm.

SUMT methods are methods which formulate the objective function and the constraint functions into an augmented objective function and then solving the problem as if it were an unconstrained optimization task. ADS employs interior and exterior penalty function techniques as well as an Augmented Lagrange Multiplier (ALM) technique.

The exterior penalty function method is incorporated by forming a penalty from the constraint equations. This penalty is of the form :

$$P(\underline{x}) = \sum_{j=1}^m \max(0, g_j(\underline{x}))^2 + \sum_{k=1}^l (h_k(\underline{x}))^2 \quad (4.28)$$

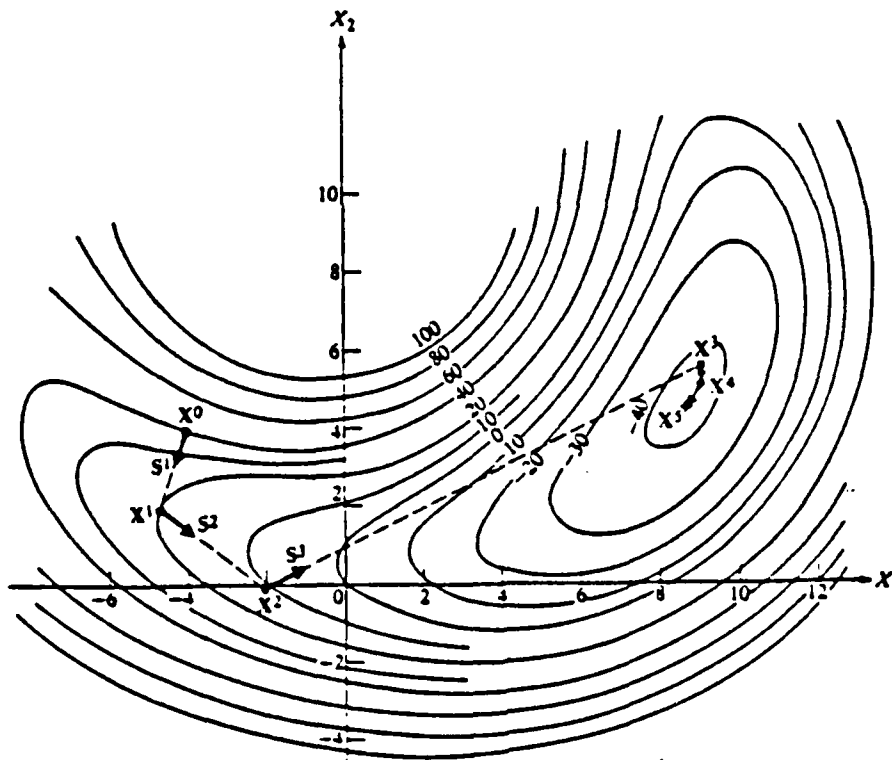


Figure 4.9 Fletcher-Reeves Conjugate Direction Algorithm.

From this equation it is obvious that $P(\underline{x})$ is zero if all the constraints are satisfied. That is, if $g_j(\underline{x}) \leq 0$ and $h_k(\underline{x}) = 0$, then all conditions of the penalty function are satisfied. If an element of the penalty function is violated then the penalty increases as the square of the violated constraint. A pseudo or augmented objective function is formulated where :

$$\Phi(\underline{x}, r_p) = F(\underline{x}) + r_p P(\underline{x}) \quad (4.29)$$

The constant r_p is a weighting factor for the penalty. It is adjusted with ADS as the optimization proceeds to allow the program to systematically converge to an optimum solution.

One disadvantage of this method is that if the optimizer is stopped short of the optimum the design will be in the infeasible region and probably not useful.

Originally developed as a method to solve equality constrained problems the version of ALM in ADS has been modified to work with both equality and inequality constraints. The statement is as follows:

$$\text{minimize } F(\underline{x}) \quad (4.30)$$

$$\text{subject to } h_k(\underline{x}) = 0 \quad k=1, l \quad (4.31)$$

Next a Lagrangian is created such that

$$L(\underline{x}, \lambda) = F(\underline{x}) + \sum_{k=1}^l \lambda_k h_k(\underline{x}) \quad (4.32)$$

Then the equation is augmented with an exterior penalty function such that

$$A(\underline{x}, \lambda, r_p) = F(\underline{x}) + \sum_{k=1}^l (\lambda_k h_k(\underline{x}) + r_p (h_k(\underline{x}))^2) \quad (4.33)$$

The power of this method is that in theory precise constraint matching is possible whereas in the exterior penalty function method it is not. The full details of the method will not be covered here, however, the final form of the objective function will be included:

$$A(\underline{x}, \lambda, r_p) = F(\underline{x}) + \sum_{j=1}^m (\lambda_j \psi_j + r_p \psi_j^2) + \sum_{k=1}^l (\lambda_k h_k(\underline{x}) + r_p (h_k(\underline{x}))^2) \quad (4.34)$$

where $\psi_j = \max(g_j(\underline{x}), -\lambda_j/2r_p)$, and the update formulas for the Lagrange multipliers are:

$$\lambda_j^{p+1} = \lambda_j^p + 2r_p (\max(g_j(x), -\lambda_j/2r_p)) \quad j=1, m \quad (4.35)$$

$$\lambda_{k+m}^{p+1} = \lambda_{k+m}^p + 2r_p h_k(x) \quad k=1, l \quad (4.36)$$

With this brief review of optimization and the ADS program completed the next chapter will discuss the program development for this thesis research.

V. OPTIMIZATION DESIGN PROCEDURE

To accomplish the task of designing a control system with acceptable time domain performance and robustness characteristics in a straight forward manner a numerical optimization technique was chosen as the method of implementation of the design algorithm. Using numerical procedures to adjust selected design variables, in this case the feedback and/or filter gains, a desired level of performance can be achieved. This level of performance is actually a combination of time domain performance and robustness or frequency domain performance. By establishing the criteria for the system performance in terms of an optimization objective and constraint functions a versatile procedure can be developed to set the system feedback gains and affect an acceptable design in terms of performance and robustness. The pole placement and robustness (POPLAR) design procedure uses pole placement to establish a designer selected performance level and then a minimum singular value level to establish the robustness.

The pole placement portion of the procedure will be discussed first. The pole placement technique was chosen because it was relatively easy to implement through a numerical optimization routine. By using this numerical procedure it is also simple to incorporate robustness into the procedure along with the performance requirements. A numerical technique similar to one posed in [Ref. 13] was chosen for the pole placement algorithm. An unconstrained optimization routine from the IBM IMSL library was used for this program. The routine, a Newton method, uses adjustments to the output feedback gains to reduce the size of an objective function. This objective function was expressed as a function of the

pole location of the system and as the objective was reduced the poles were moved toward the desired locations. To provide more versatility in the pole placement algorithm a method that can use constraint functions as well as unconstrained optimization was chosen for this program. The designer may use either objective, constraint or a combination of functions to secure the desired pole locations. As currently implemented in the program the cost or objective portion of the pole placement procedure is constructed as equation 5.1

$$OBJ = \sum_{i=1}^j (\lambda_{R_{D_i}} - \lambda_{R_i})^2 + (\lambda_{I_{D_i}} - \lambda_{I_i})^2 \quad (5.1)$$

where λ_R = real eigenvalue
 λ_I = imaginary eigenvalue
 λ_{R_0} = desired eigenvalue location
 λ_{I_0} = desired eigenvalue location

The constraint formulation is a function that must be kept negative or the constraint is violated. It is written as equation 5.2

$$g(j) = \sqrt{(\lambda_{R_{D_j}} - \lambda_{R_j})^2 + (\lambda_{I_{D_j}} - \lambda_{I_j})^2} - r \quad (5.2)$$

where r is a tolerance circle established as a function of pole placement position. Since the aim of the optimizer is to keep g negative any time the λ function of the constraint is greater than r the constraint will become active, i.e. violated. The optimizer will then attempt to move the constraint to the inactive status by adjusting the design parameters of the system.

Consideration of implementation of the frequency domain or robustness portion of the design procedure begins with the concept of MIMO phase and gain margins. Several useful theorems on singular value analysis of multiloop systems are

presented in [Ref. 8]. One of these theorems relates the matrix singular value of the return difference function to a parameter, α , and further shows that as long as the maximum singular value of the perturbation function ($\underline{I}^{-1} - \underline{I}$) remains less than this α , the system remains stable. The value of α is then related to gain and phase margins of the MIMO system. The relationship developed is given in equations 5.3 and 5.4:

$$\text{gain margin} = \text{GM} = 1/(1+\alpha_0) \quad (5.3)$$

$$\text{phase margin} = \text{PM} = \pm \cos^{-1}(1-\alpha_0^2/2) \quad (5.4)$$

provided that equation 5.5 holds.

$$\sigma(\underline{I}+\underline{G}) \geq \alpha_0 \quad (5.5)$$

for some $\alpha_0 \leq 1$

These phase and gain margins are guaranteed in every loop simultaneously.

Universal gain and phase margin curves, [Ref. 14], based on the minimum singular values of the return difference matrix are developed from equation 5.6.

$$(\underline{I}^{-1}-\underline{I}) = \max \sqrt{(1-1/k_n)^2 + 2/k_n(1-\cos\psi_n)} \quad (5.6)$$

for all n with $k_n > 0$. These curves shown in figure 5.1 allow the designer to pick a singular value that corresponds to a specific gain and phase margin for a given system. In addition to the universal gain and phase plot [Ref. 15] develops an optimizer solution for formulating a robust controller using the CONMIN algorithm [Ref. 12].

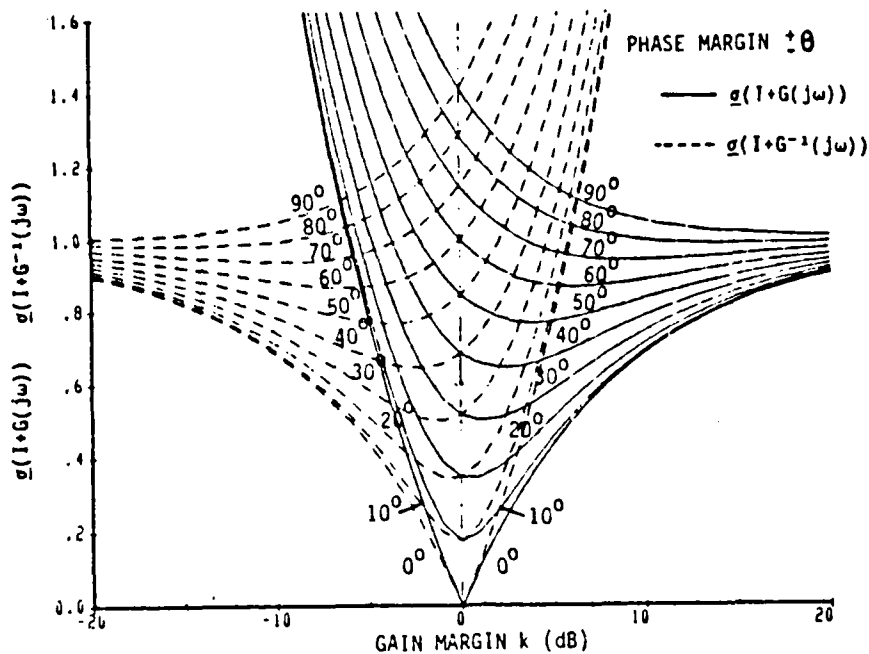


Figure 5.1 Universal Gain and Phase Singular Value Plot.

Since the universal curve in figure 5.1 provides a convenient method of specifying gain and phase margins in terms of singular values the robustness portion of the pole placement and robustness design procedure uses the minimum singular value level of the return difference matrix to determine the robustness. The minimum singular value level is formulated as an objective or constraint function in equation 5.7

$$J = \sum_j (\max(0, (\sigma_j - \sigma_{\text{min}})))^2 \quad (5.7)$$

The optimization procedure may be used to change feedback gains until the minimum singular value is raised above this desired design level. Although the same formulation can be used as a negative constraint function it has not been implemented as such within this program. There are numerous

ways the singular value formulation could be implemented within the program by changes of the code if design requirements forced such changes.

The pole placement and robustness design program is based on the ADS code discussed in Chapter 4 to implement the design variable selection procedures. The pole placement and robustness program consists of two separate programs. The first program is used to provide designs for state or output feedback problems while the second program is used for observer or filter designs.

For the state or output feedback design program the user must input the plant matrices \underline{A} , \underline{B} , \underline{C} and initial starting values for the feedback matrix \underline{F} . The matrices correspond to the following linear differential system:

$$\dot{\underline{x}} = \underline{A}\underline{x} + \underline{B}u \quad (5.8)$$

$$\underline{y} = \underline{C}\underline{x} \quad (5.9)$$

$$\underline{u} = -\underline{F}\underline{x} \quad (5.10)$$

A feed-forward matrix has not been considered in the current program. A feed forward matrix could be added to the procedure if required for specific design cases.

As the design program is currently coded the user may run output feedback or state feedback design by specifying the \underline{C} matrix as the diagonal(\underline{I}) matrix for state feedback. The program relies on initial starting values of the feedback gains, \underline{F} . As discussed in Chapter 4 there is no guarantee that the optimum found by the procedure each time is the global optimum or that the procedure will always

converge to an acceptable solution. The ability to select acceptable starting values for the feedback gains will make the procedure more efficient in operation. As currently employed, the program is used to obtain pole placement and robustness for a given set of starting gains and a selected optimization routine from the ADS program. If the optimizer is not able to meet the desired design goals on this program run two options are available. First, change to a different optimization routine from the list of available ADS routines and rerun the problem. This was usually successful in improving the design. Second, the designer uses a new set of starting values for the feedback gains and repeats the design procedure. Both options might be used on particularly difficult cases.

The pole placement and robustness design procedure has consistently been able to find improved designs; however the program does not always yield acceptable designs. Certain problems require changes in the optimizer routine and modification in the initial feedback gain starting values in order to obtain acceptable designs. Using the IBM 3033 time share system the pole placement and robustness routine requires about ten CPU seconds to work a second order problem and on the order of 15 to 60 CPU seconds to run a fourth order problem. The actual amount of time varies with optimization requirements and time share utilization.

The observer robustness design program requires two passes of the ADS program. In the first pass the feedback gains, F , of the controller are computed to obtain the desired pole locations. The second pass of the ADS routine is used to adjust the observer gains to recover the system robustness. The two pass procedure was chosen because it allows a smaller number of design variables at each stage of the optimization and much more efficient computer usage. Figure 5.2 shows how the observer is implemented. This diagram is algebraically stated as;

$$\begin{bmatrix} \dot{\underline{x}} \\ \dot{\underline{\hat{x}}} \end{bmatrix} = \begin{bmatrix} \underline{A} & -\underline{BK} \\ \underline{FC} & \underline{A}_c - \underline{BK} \end{bmatrix} \begin{bmatrix} \underline{x} \\ \underline{\hat{x}} \end{bmatrix} + \begin{bmatrix} \underline{B} \\ \underline{B} \end{bmatrix} r \quad (5.11)$$

$$\underline{A}_c = \underline{A} - \underline{FC}$$

where \underline{x} is the state, $\underline{\hat{x}}$ is the estimator variable, \underline{F} is the feedback gain and \underline{K} is the observer gain. The design of the feedback gains and the observer gains are accomplished as separate quantities in keeping with the separation prin-

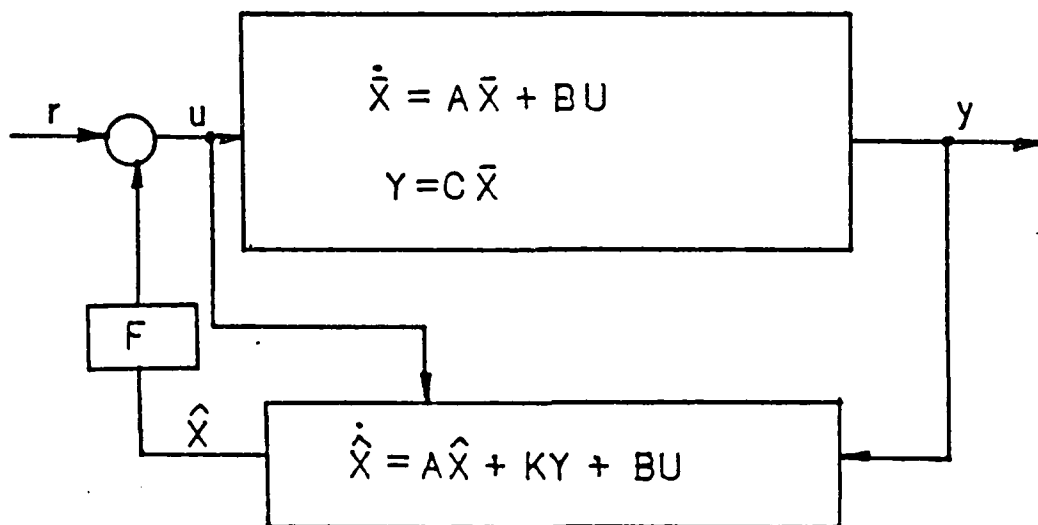


Figure 5.2 Observer Implementation.

ciple. In using the pole placement and robustness design procedure for the observer system, initial values of the F and K matrices must be input. The same or different optimization techniques from ADS may be employed.

The routines contained in this thesis have been based on the input additive singular value level. The pole placement and robustness design algorithm computes input additive,

output additive, input multiplicative, and output multiplicative singular values. Any of these singular values can be incorporated into the objective or constraint formulations but have not been for this version of the program.

In summary, the pole placement and robustness design procedure is a straight forward numerical optimization procedure for the practical application modern MIMO system analysis. The new aspects of the procedure are the implementation of both pole placement and robustness criteria within the same design program. The versatility of the pole placement and robustness design is obtained by incorporating a state of the art optimizer routine ADS, with currently available singular value computation routines. Using the optimizer format for the pole placement and robustness design gives the designer the ability to modify variables directly that affect both the time domain or performance of the system and the frequency domain or robustness of the system. The numerical optimization incorporated into the pole placement and robustness design is flexible enough to incorporate the double pass design technique using the separation of the feedback and filter gains to obtain robustness recovery for observer based controllers.

VI. INTRODUCTORY PROBLEM

The purpose of this introductory problem is to review some results of modern multivariable robustness theory using a simple problem. This same simple system is then used as a test problem for the optimization technique developed for this thesis. The problem provides excellent insight into the cross-coupling problem and demonstrates how effectively the pole placement and robustness design procedure can be in dealing with the cross perturbation terms.

The problem chosen for this introductory analysis comes from [Ref. 9]. Figure 6.1 is a diagram of this basic system. In this problem a simple plant is specified by the following linear system:

$$\begin{bmatrix} \dot{x}_1 \\ \dot{x}_2 \end{bmatrix} = \begin{bmatrix} -1 & 0 \\ 0 & -1 \end{bmatrix} \begin{bmatrix} x_1 \\ x_2 \end{bmatrix} + \begin{bmatrix} 1 & b_{12} \\ 0 & 1 \end{bmatrix} \begin{bmatrix} u_1 \\ u_2 \end{bmatrix} \quad (6.1)$$

where

$$\begin{aligned} y_1 &= x_1 \\ y_2 &= x_2 \end{aligned} \quad (6.2)$$

A feedback compensation of the form of equation 6.3 was assumed.

$$\begin{bmatrix} u_1 \\ u_2 \end{bmatrix} = - \begin{bmatrix} x_1 \\ x_2 \end{bmatrix} + \begin{bmatrix} uc_1 \\ uc_2 \end{bmatrix} \quad (6.3)$$

Which gives a closed-loop system, equation 6.4

$$\begin{bmatrix} \dot{x}_1 \\ \dot{x}_2 \end{bmatrix} = \begin{bmatrix} -2 & b_{12} \\ 0 & -2 \end{bmatrix} \begin{bmatrix} x_1 \\ x_2 \end{bmatrix} + \begin{bmatrix} 1 & b_{12} \\ 0 & 1 \end{bmatrix} \begin{bmatrix} uc_1 \\ uc_2 \end{bmatrix} \quad (6.4)$$

This system has eigenvalues at $-2, -2$ and is therefore stable. Using equation 6.5

$$\underline{G} = \underline{C}(s\underline{I} - \underline{A})^{-1}\underline{B} \quad (6.5)$$

the transfer matrix may be written as equation 6.6.

$$\underline{G} = \begin{bmatrix} 1/s+1 & b_{12}/s+1 \\ 0 & 1/s+1 \end{bmatrix} \quad (6.6)$$

which gives the return difference matrix, equation 6.7.

$$\underline{I} + \underline{G}(s) = \begin{bmatrix} s+2/s+1 & b_{12}/s+1 \\ 0 & s+2/s+1 \end{bmatrix} \quad (6.7)$$

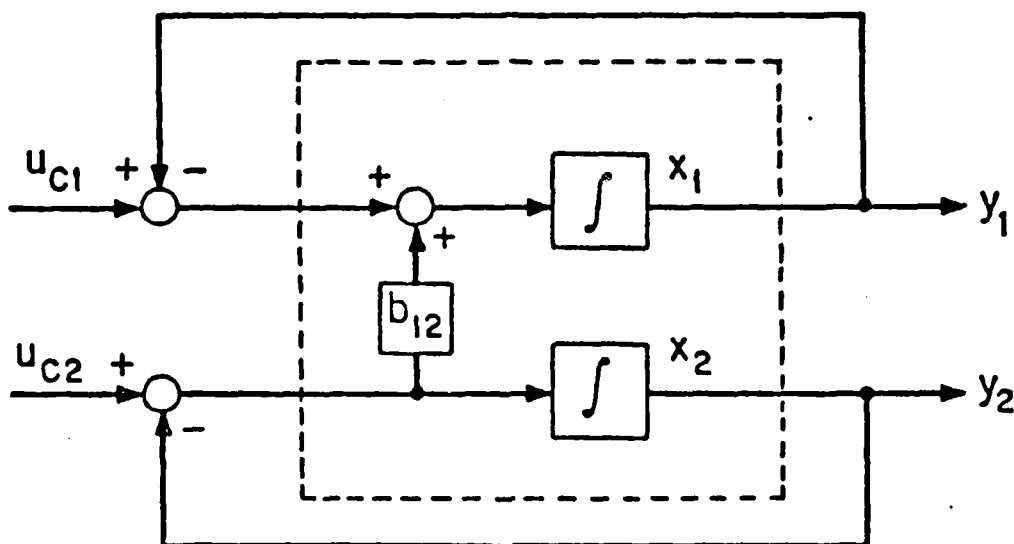


Figure 6.1 Basic Multi-input Multi-output System.

The problem shows the inadequacies of classical methods in establishing the robustness of the system. A brief review

of the results will be presented. Using the return difference matrix $(\underline{I}+\underline{G})$, the determinant may be written as equation 6.8.

$$\det(\underline{I}+\underline{G})^{-1} = 2s+3/(s+1)^2 \quad (6.8)$$

Therefore, the multivariable Nyquist diagram will be as

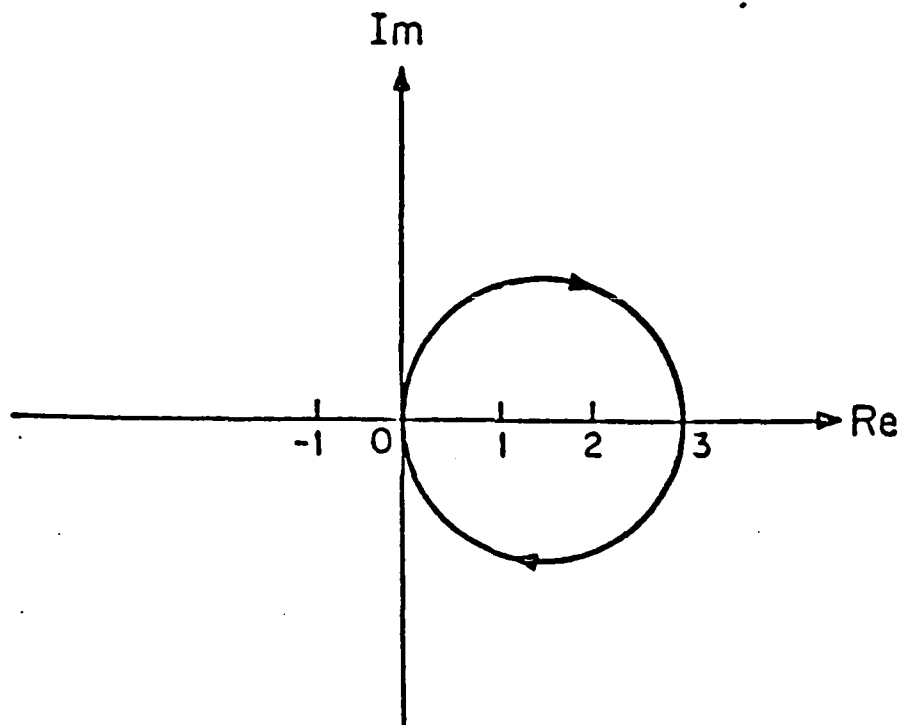


Figure 6.2 Multivariable Nyquist for $2s+3/(s+1)^2$.

shown in figure 6.2. The diagram does not encircle the $(-1,0)$ point and is indicative of a closed-loop stable system. Considered as a SISO system one has a gain margin of $-1/3$ to ∞ and a phase margin of ± 106 degrees. Under this criteria one can conclude that this is a good design. This will be shown later not to be the case.

Multi-input systems are often designed a loop at a time. Applying loop design to the system the transfer function for either loop taken separately becomes equation 6.9

$$G=1/s+1$$

(6.9)

Figure 6.4 shows the Nyquist diagram of this problem. Using this Nyquist diagram the system is indicated to be stable and have phase and gain margins of $GM=(-1, \infty)$ and $PM=(\pm 180)$. This analysis does not show the true nature of the robustness of the system. Since the factor b is not a parameter in either of the Nyquist curves it plays no part in the stability determination using these diagrams.

Using the criteria of singular values discussed in Chapter 3 a measure of the nearness to instability for this problem may be obtained by plotting the minimum singular value of $(I+G), \underline{Q}$. (For numerical calculations a value of $b_{12} = 50$ is assumed). Figure 6.3 shows the plot of this value vs. frequency. This gives a minimum singular value of about -23 db or 0.071 which corresponds to a gain margin of about 0.93 to 1.08 and a phase margin of ± 4.1 degrees. These phase and gain margins are quite small and are evident in the cross-feed perturbation problem.

A perturbed system as shown in figure 6.5 can be produced which will lead to stability problems with very small values of perturbation. The closed-loop system if perturbed by a small perturbation, $5/b_{12}$, where b_{12} is a large number, will have as a characteristic equation, equation 6.10

$$(sI - \underline{A}) = s^2 + 4s + 9 \quad (6.10)$$

with the eigenvalues of $s = -2 \pm \sqrt{5}$. There is one positive root in this solution and the system is unstable.

To determine the nature of the robustness of this system the return difference matrix must be considered. If the return difference matrix of the transfer function $(I+G(j\omega))$

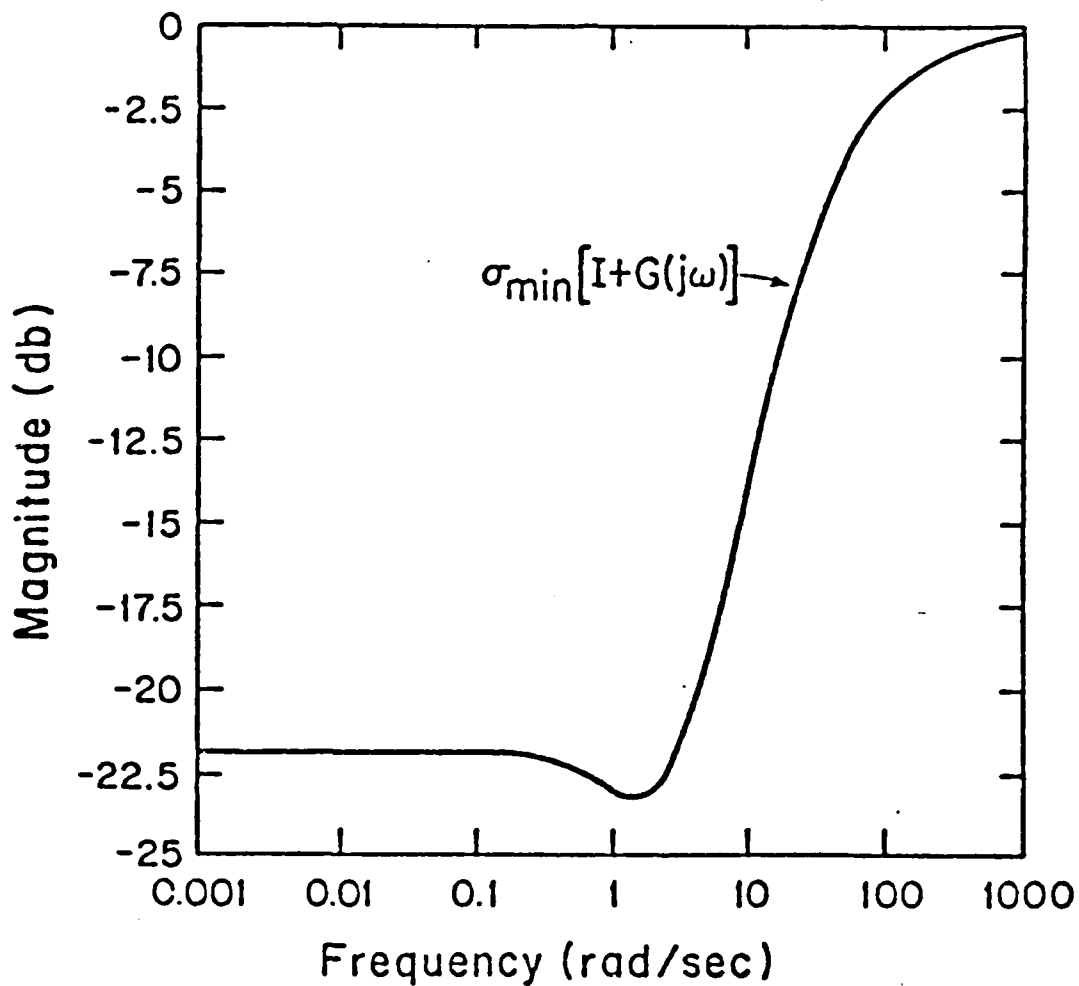


Figure 6.3 Minimum Singular Value Plot, Example Problem.

is nearly singular at some frequency ω_0 , then the multivariable system will not be robust with regard to any modelling errors within the system. This is because any small change in $\underline{G}(j\omega)$ can then make $\underline{I}+\underline{G}(j\omega)$ singular and the $\det(\underline{I}+\underline{G})$ becomes zero, thus changing the encirclements of the Nyquist stability point and indicating a system instability. Using equation 6.1 the pole placement and robustness design method

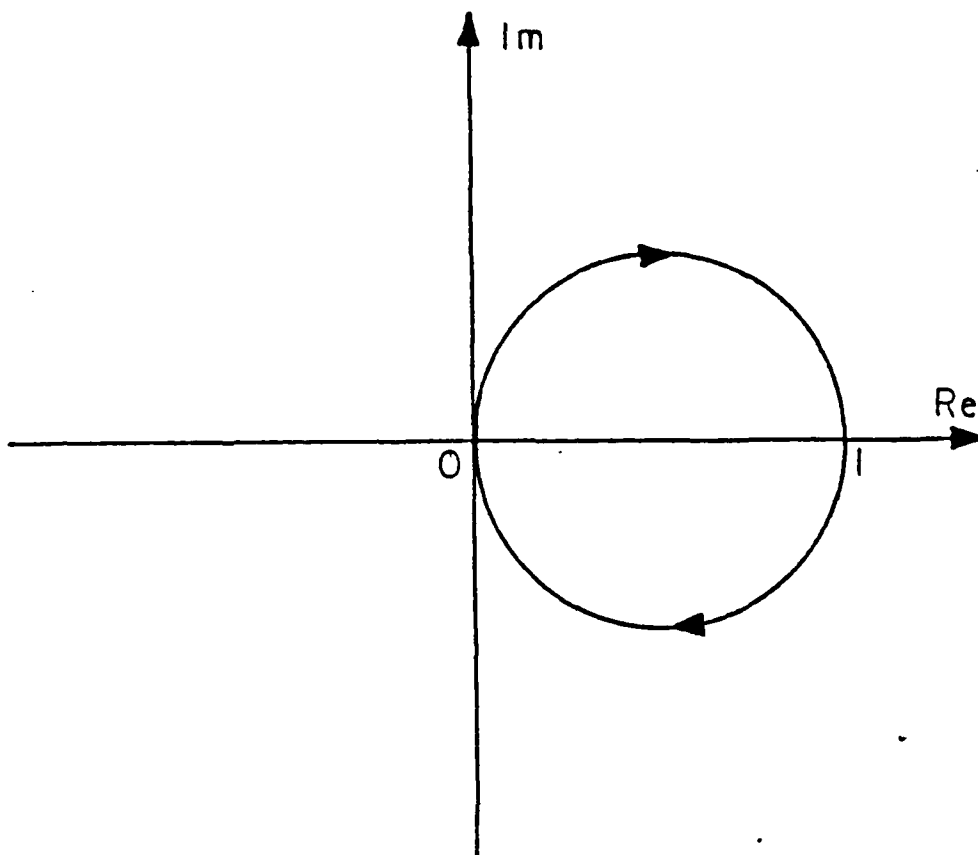


Figure 6.4 Nyquist Diagram of $1/s+1$.

can be demonstrated . The first step is to establish a baseline for the design. The state unity feedback model in this simple problem gives pole locations of -2 and -2 . This set of eigenvalues -2 , -2 were chosen as the baseline for the system. Since a second order system requires only two feedback gains to place the poles, the diagonal feedback gains were chosen for pole placement purposes. The pole placement and robustness design program was then used to place the poles and in the process obtained the gains required to do this (1,1). A plot of some of the singular value criteria obtained is shown in figure 6.6. Pole-zero plots of the

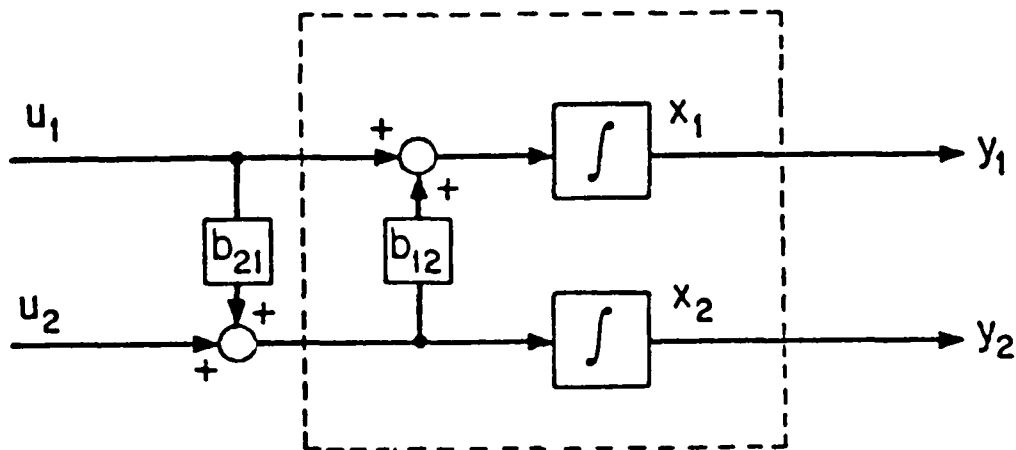


Figure 6.5 Perturbed System.

closed-loop transfer functions of the closed-loop transfer matrix are shown in figure 6.7. In this case the poles and a zero are clustered about the -2 point and in the input two to output one channel a zero is located at the -1 point on the pole-zero diagram. This point closely corresponds to the minimum singular value frequency. The only significant observations are the ability of the pole placement and robustness routine to place the poles and the relatively poor singular values indicative of low robustness.

Since there is a requirement for two feedback parameters to set the poles of a second order system there should be no additional freedom in design to account for robustness. Case two was a run to demonstrate this fact. Again allowing only two design variables for the problem the pole placement and robustness design program was run but with an objective function formulated to adjust the singular value above a

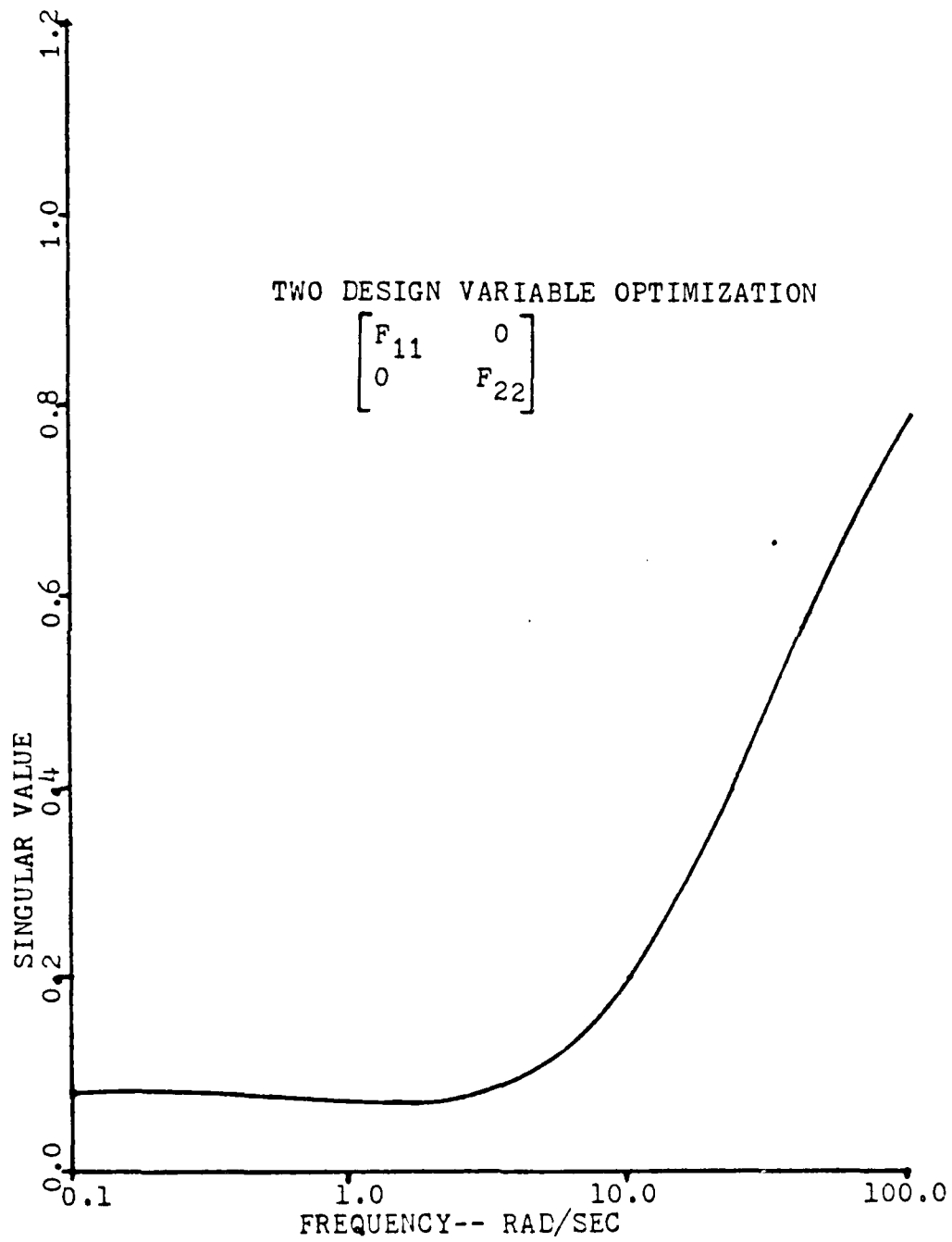


Figure 6.6 Singular Value Plot for Simple Problem.

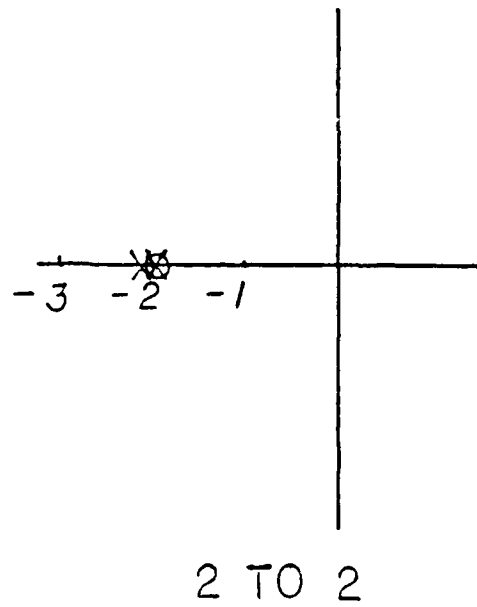
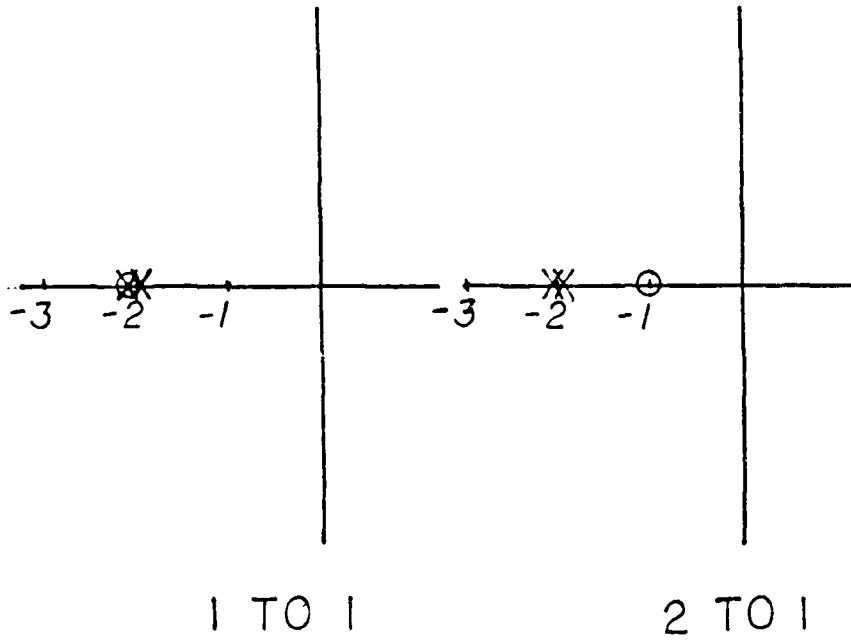


Figure 6.7 Closed-loop Poles for Pole Placement Only Case.

base level of 0.6. This level would correspond, using the universal gain margin chart, to a gain margin of -4 db to 3 db and a phase margin of ± 35 degrees. With only the two design variables to work with the pole placement and robustness design program was unable to place the poles and adjust the singular value level to the required value. The poles were placed at -2, -2 but the singular value minimum was still on the order of -23 db or 0.07. The pole-zero plot remained almost unchanged. It is clear that additional degrees of freedom for the pole placement and robustness design program must be opened if robustness is to be accounted for.

Case three was then run on the pole placement and robustness program by adding on additional degree of freedom. This case used the f gain as the additional design variable. A good choice as will be seen. Allowing the optimizer routine the extra freedom to adjust the additional feedback gain term an excellent design was found. The singular value minimum became 0.885 as shown in figure 6.8. Using the universal gain margin chart this corresponds to gain and phase margins of -6 db - 18 db and ± 52 degrees respectively. This is a considerable improvement over the original design. The factor that changed the design was the upper diagonal feedback term which provides a cancelling factor for the cross-coupling term $b_{12} = 50$. This can be seen by looking at the system matrix equation 6.11.

$$\underline{A}_c = \underline{A} - \underline{BF} \quad (6.11)$$

where equation 6.12 gives \underline{A} .

$$\underline{A} = \begin{bmatrix} -1-f_{11} & -f_{12} - b_{12} f_{22} \\ 0 & -1-f_{22} \end{bmatrix} \quad (6.12)$$

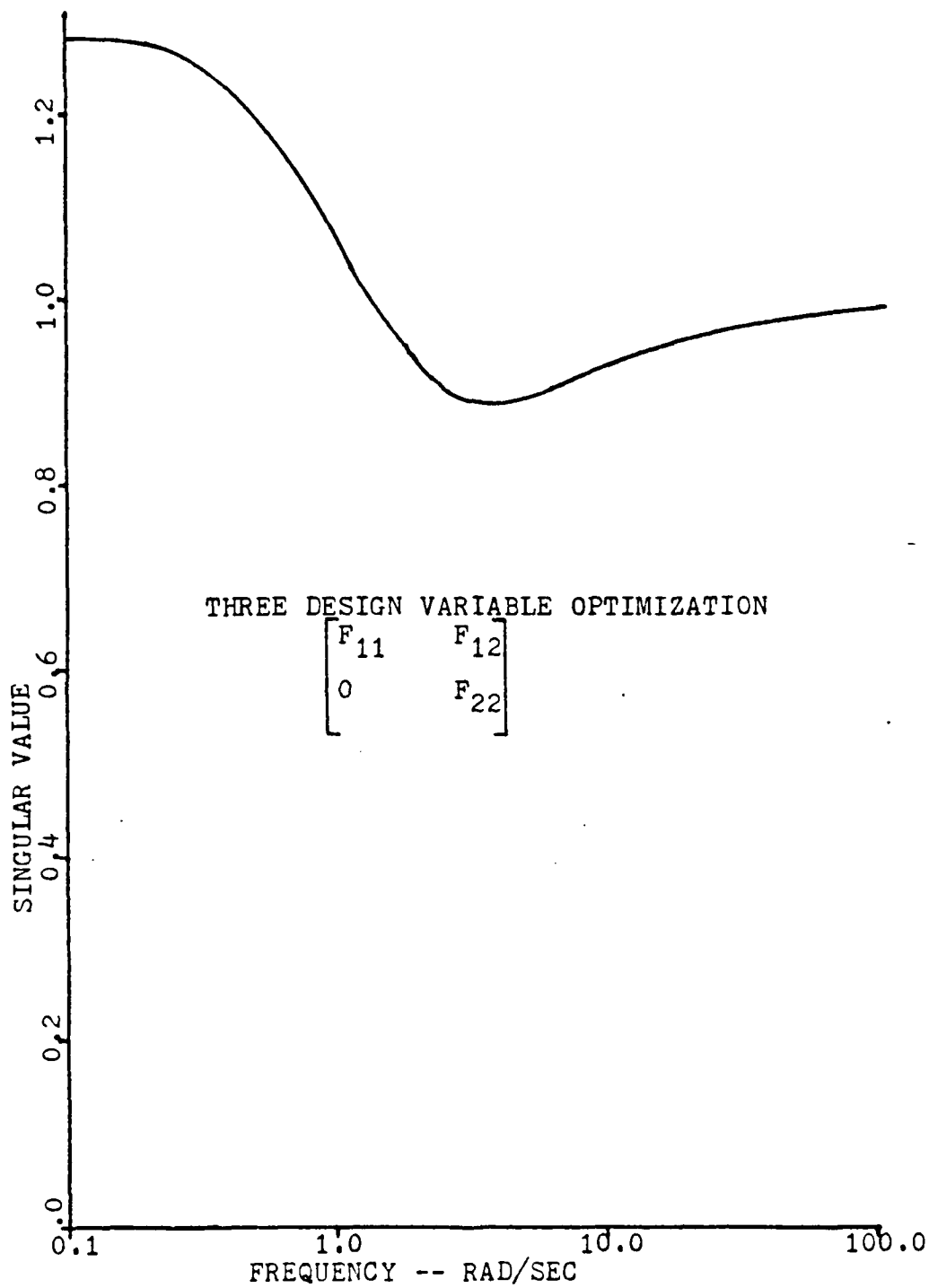


Figure 6.8 Singular Value Plot Case Three.

If the upper diagonal term of the matrix can be driven to zero the system will be decoupled into a diagonal system. To place the poles of this system at $-2, -2$ the diagonal feedback gains must be one. The optimizer feedback gains for this case were $f_{11} = 1.00006$, $f_{22} = 0.99998$ and, most importantly, $f_{12} = -51.83401$. Using these values in the A matrix

$$A = \begin{bmatrix} -2.00006 & 1.83501 \\ 0.0 & -1.99998 \end{bmatrix}$$

The value in the upper right position in the system matrix has been lowered considerably from the value of near 50 that appears in this position in the low singular value cases. Lowering this system gain value decreases the cross-coupling perturbation effects on the system. This can be more graphically demonstrated by figures 6.9 and 6.10. In figure 6.9 the transfer function shows a high gain of approximately 35 db and a bandwidth of 50 rad/sec. In figure 6.10 this gain has been reduced to 6.0 db with a bandwidth of almost 2 rad/sec. Two things are indicated by the figures, one, the open-loop Bode plot of the transfer function of the cross-coupled channel can be used to indicate the robustness problem as evidenced by the high gain and bandwidth relative to the other feedback gains and, two, the mechanism used by the pole placement and robustness design procedure to recover robustness is to reduce the relative gain and associated bandwidth within the affected channel. Figures 6.11 and 6.12 which are for the input one to output one channel are approximately the same as are the Bode plots for the input two to output two channel which are not shown. These figures indicate that no problem exists in the diagonal or direct coupling terms. The pole-zero diagram for optimization run case three is included in figure 6.13. The only significant change in this plot as compared to figure 6.7 is the movement of the zero in the off diagonal pole-zero plot. The zero is seen to shift to one of the pole locations

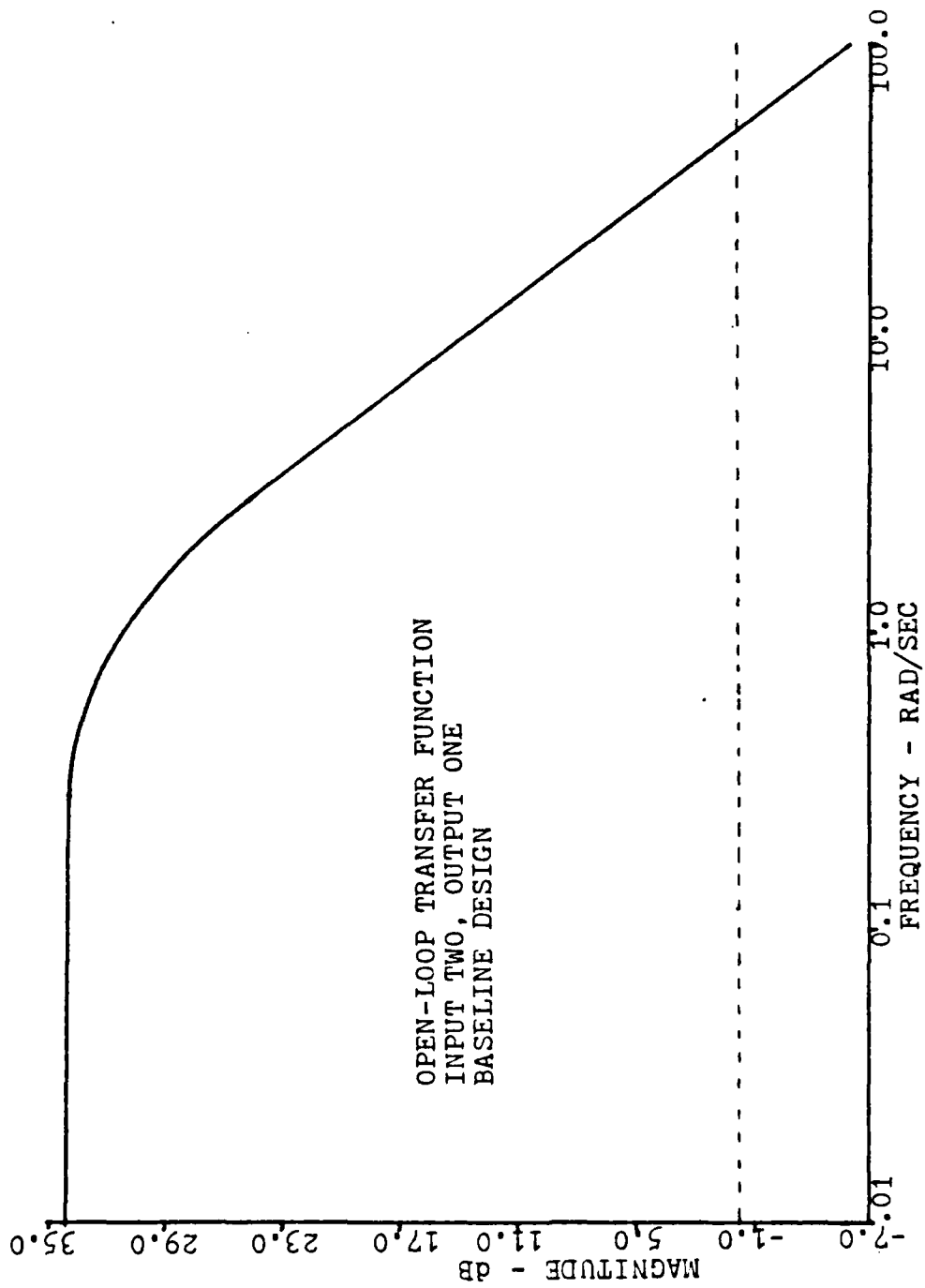


Figure 6.9 Open-loop Transfer Function 2-1 for Baseline.

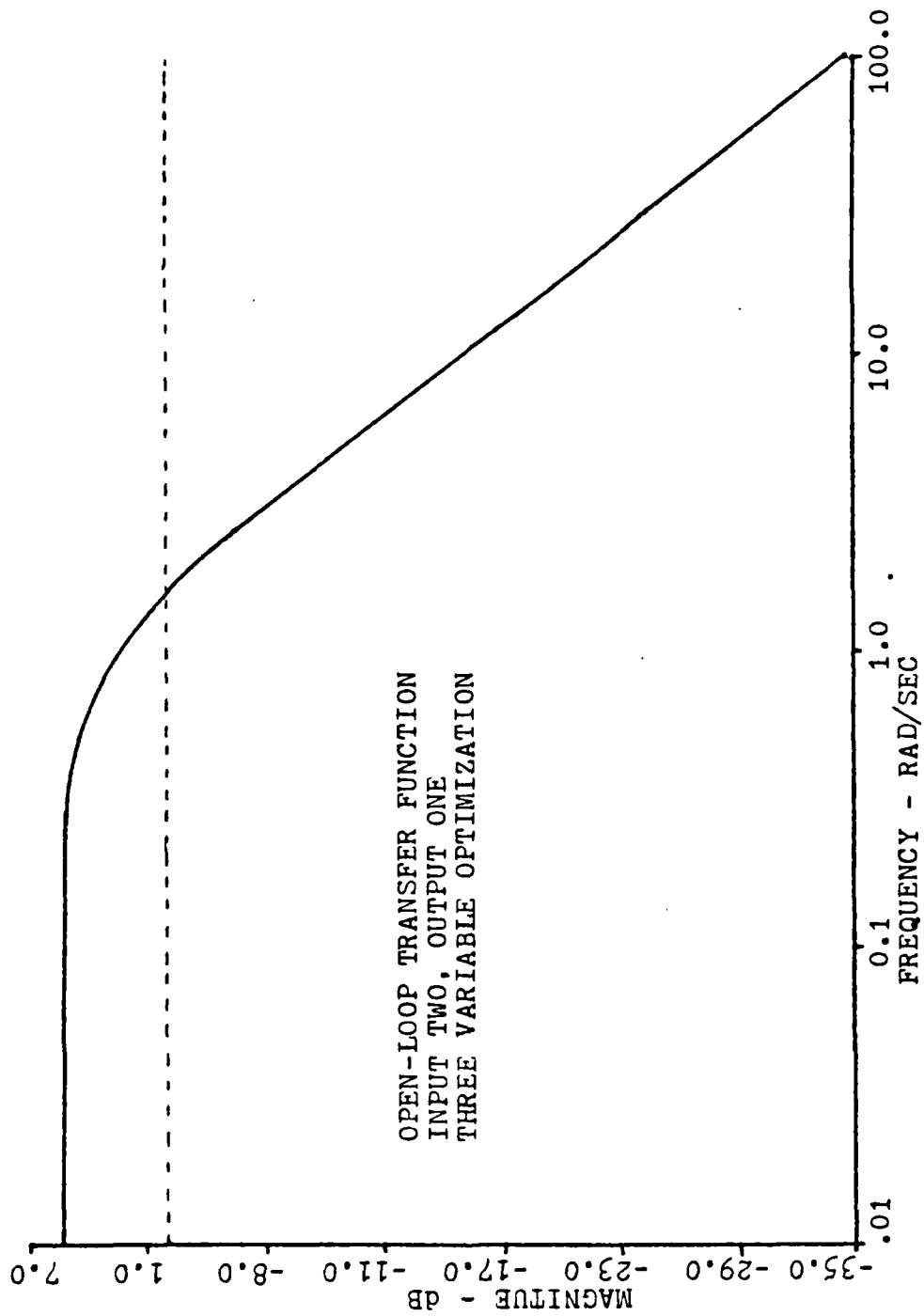


Figure 6.10 Transfer Function 2-1 Optimized (3 Var).

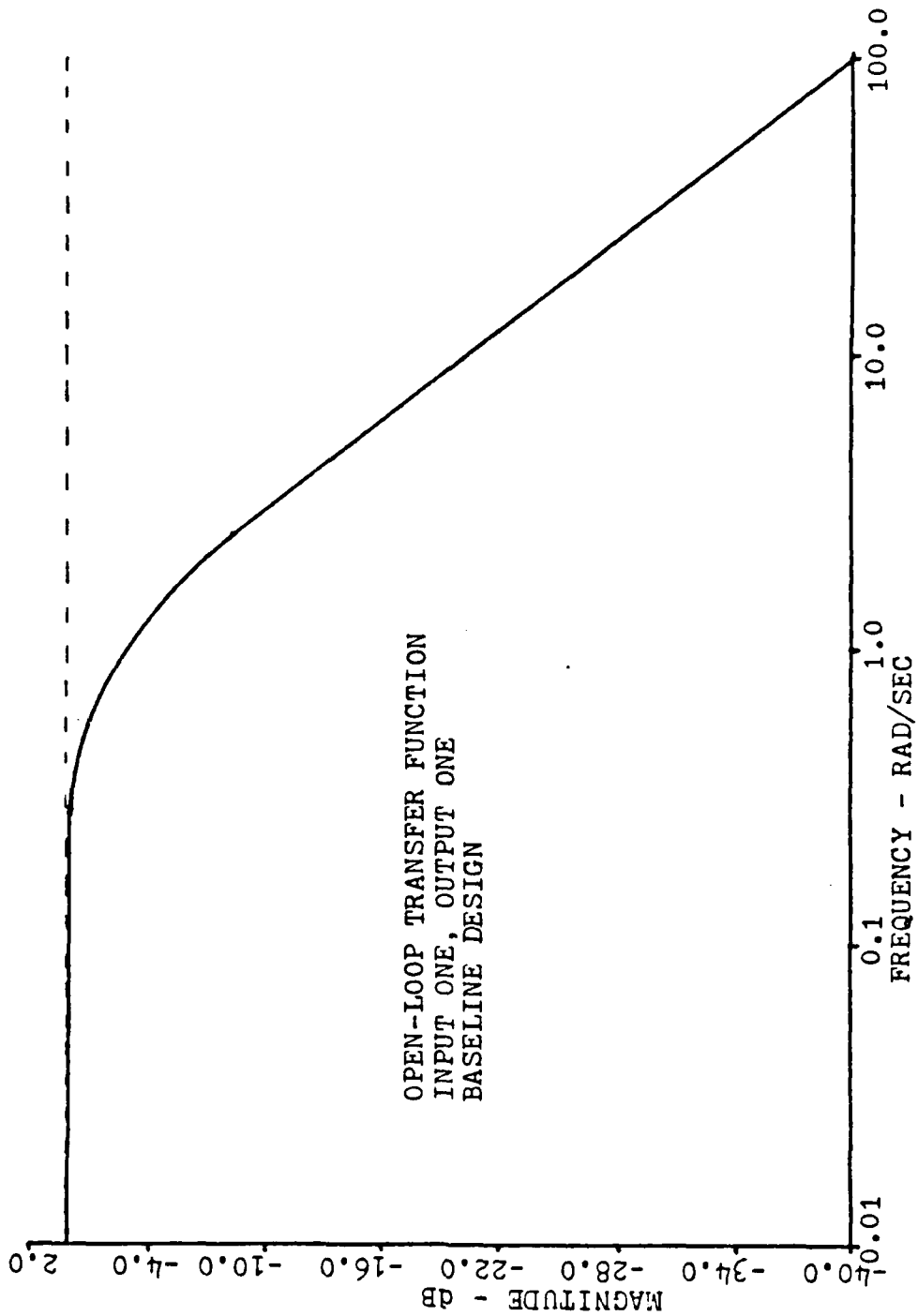


Figure 6.11 Transfer Function 1-1 Baseline.

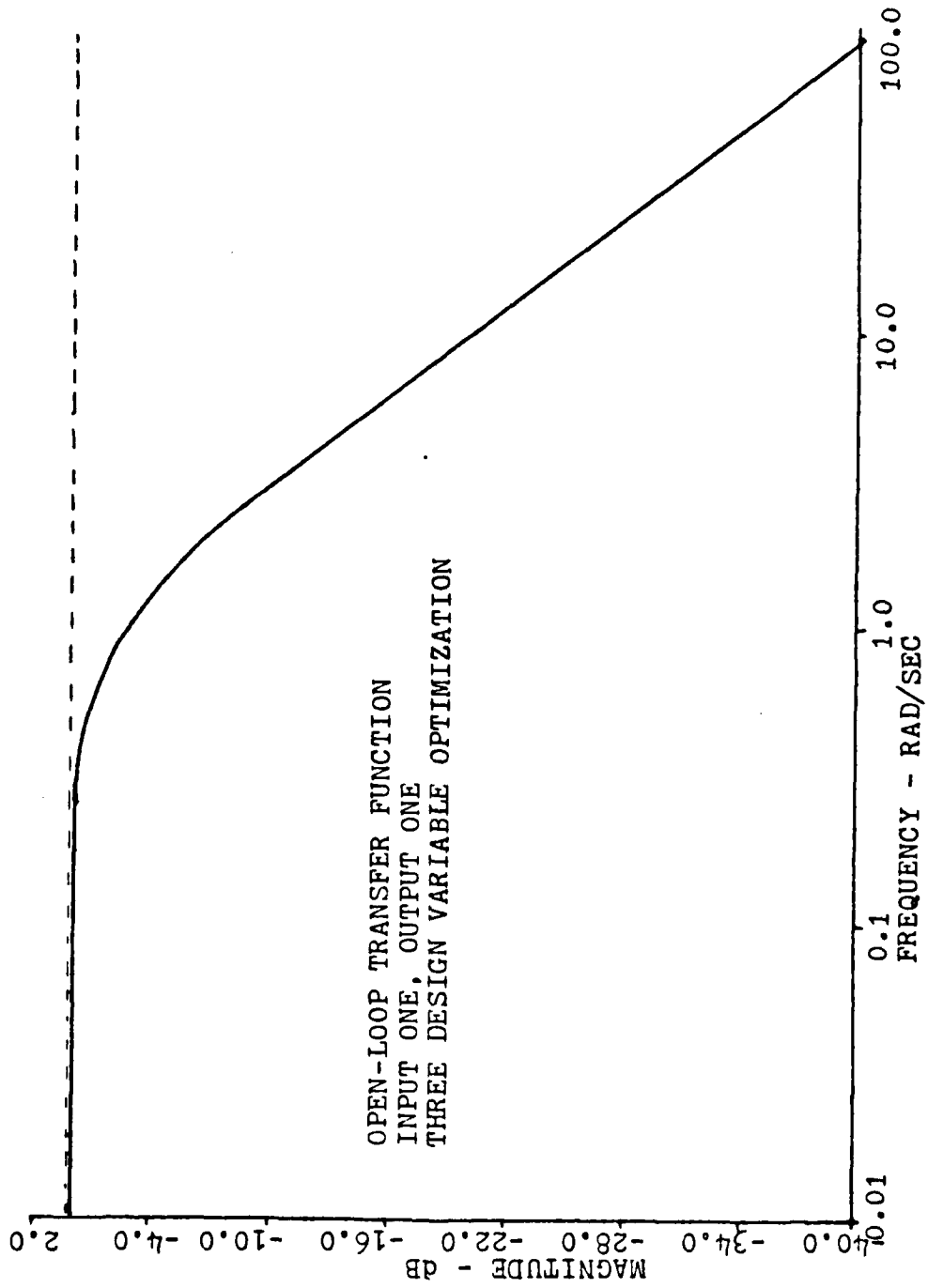


Figure 6.12 Transfer Function 1-1 Optimized (3 variables).

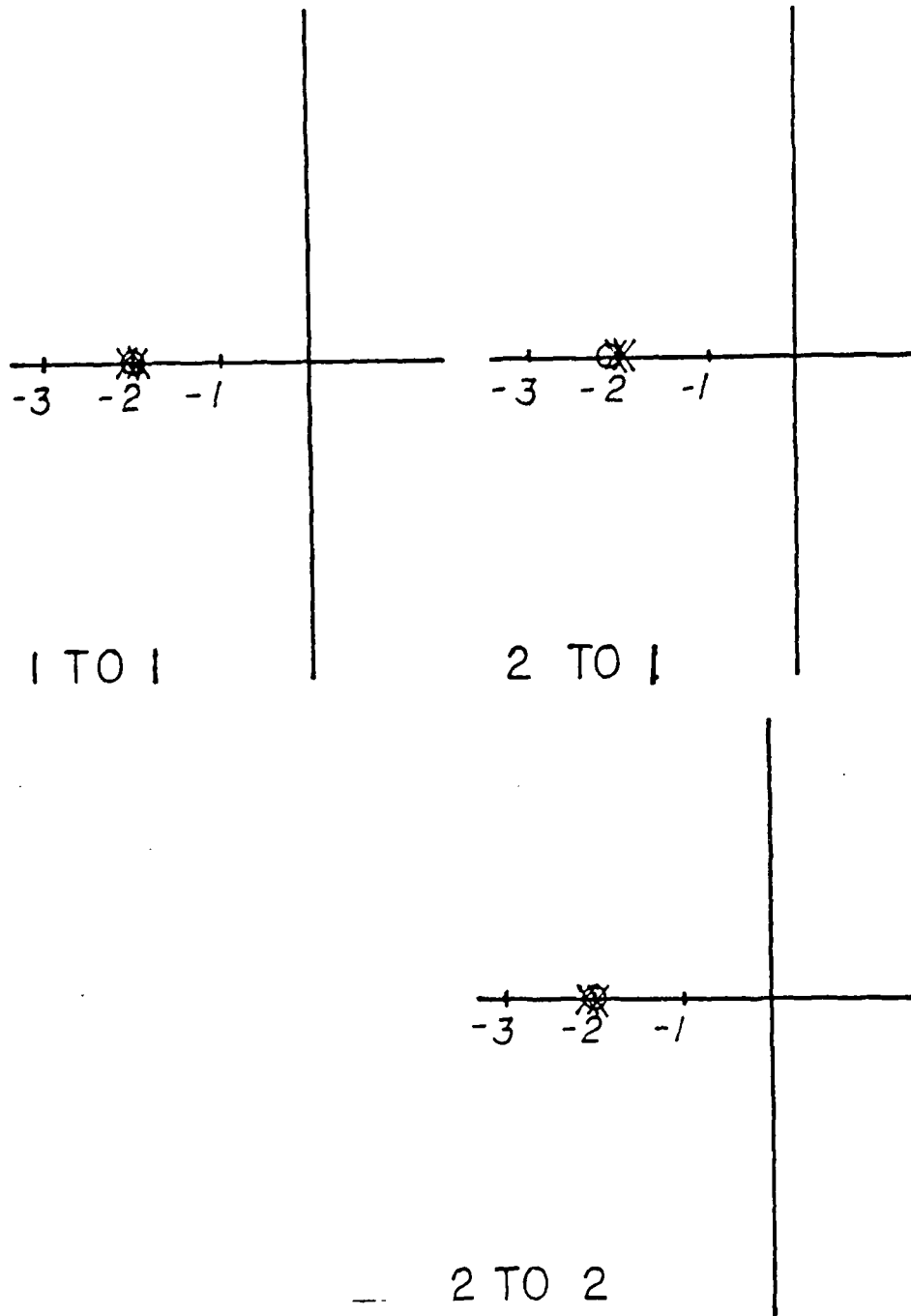


Figure 6.13 Closed-loop Pole-Zero Plot Case 3.

during the optimization. This zero shift has the effect of smoothing the frequency response curve in the vicinity of the frequency of the minimum singular value providing a more uniform gain distribution around this point. Table 1 shows comparison results for the feedback gains for several cases of this basic problem.

The logical extension of the problem to the general case is to allow all four feedback gains to become design vari-

TABLE 1
Comparative Results Simple Problem

	Feedback Gains			
	f_{11}	f_{12}	f_{21}	f_{22}
f_{12} variable $f_{21}=0$	1.00006	-51.83401	0.0	0.9998
f_{21} variable $f_{12}=0$	0.25254	0.0	-0.01071	1.52332
f_{21} variable $f_{12}=-50$.99960	-50.0	0.00025	0.99038
All f's variable	1.11936	-60.4718	0.00280	0.75478

ables. The pole placement and robustness routine can then use full freedom in choosing all four of these feedback gains to compensate for any cross-coupling effects within the system. Based on the previous analysis the two diagonal gains would be expected to approach 1 while the upper off diagonal gain moves to -50 and the lower one moves to 0. The flexibility of the ALS program was required for the four design variable study. Several runs were made with various combinations of starting parameters for the feedback gains and optimizer routines before a good design for the case

incorporating all four feedback gains as variable was obtained. While this points out one of the limitations of optimization design routines the program was able to develop an improved design over the baseline while employing four design variables. In the design produced for this case the singular value level was placed above 0.6 for a gain margin of -4 db to 9 db and phase margin of ± 35 degrees. In this formulation the optimizer was able to place the poles and meet the design singular value level. The feedback gains produced by the optimizer were:

1.11936	-60.4718
0.0028	0.75478

which are approaching the analytic design gains. After obtaining the feedback gains the OPTSYS program was used to obtain the necessary data to do a closed-loop pole-zero map. This plot is shown in figure 6.14. These plots indicate a similar pole-zero location to that found in the previous three design variable problem. Again the gain in the affected channel has been reduced to compensate for the high cross-coupling perturbation within the system.

The design studies presented to this point have been based on breaking the system loop at the input as shown in figure 6.15. In multivariable theory the location of the break in the loop changes the return difference for the system and the transfer function formulation. In the figure number 1 depicts a system with an input loop break point while number 2 is an output loop break point for output return difference determination. The return difference function for the point 1 is written as $\underline{I} + \underline{FQ}$ while the return difference for point 2 is $\underline{I} + \underline{GF}$. The baseline system not only has low singular values of the input return difference matrix, the lowest being 0.0706, but also has low singular values for the output return difference matrix of point 2 of about the same order. To demonstrate the versatility of the

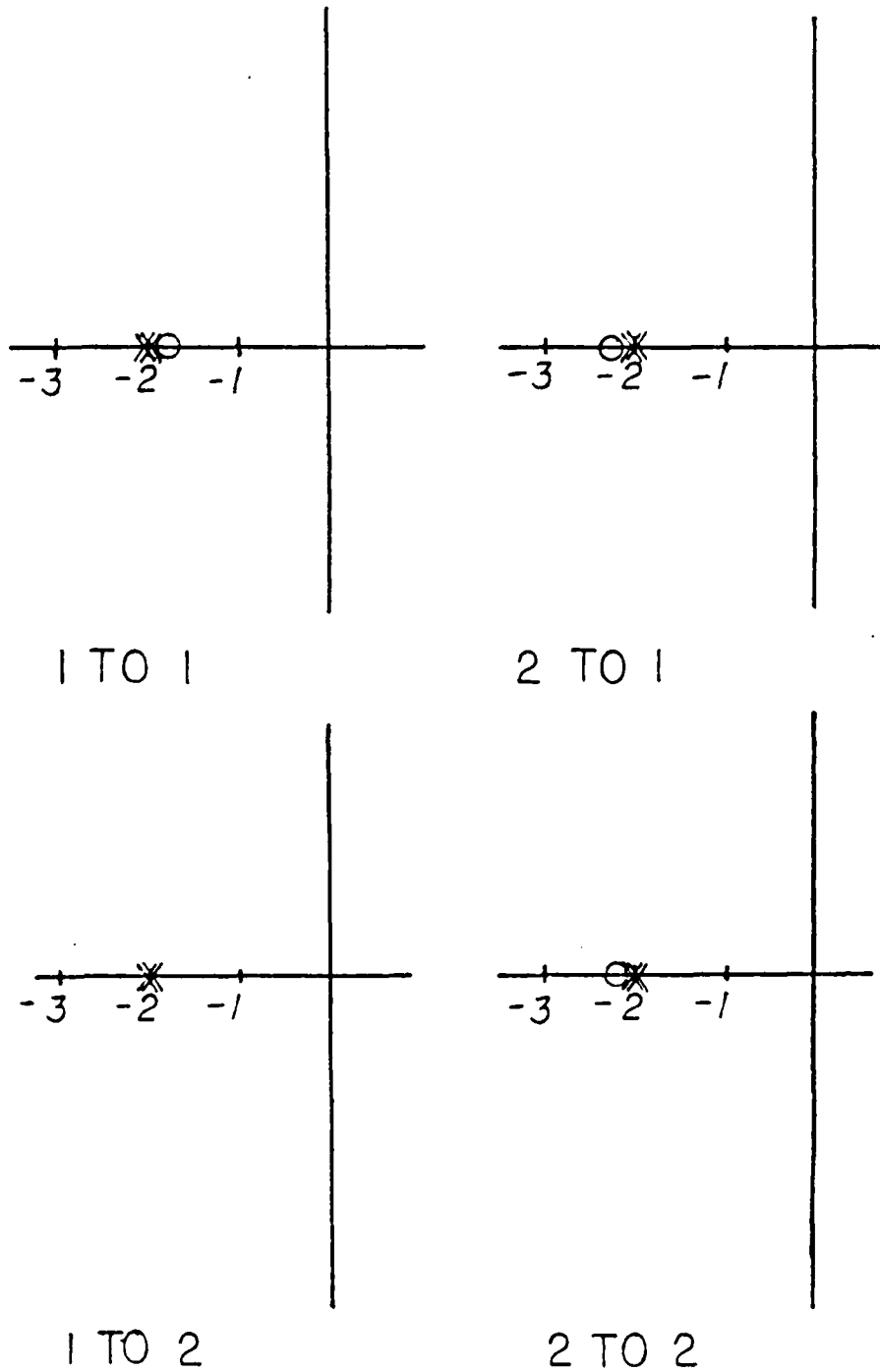


Figure 6.14 Pole-Zero Plot Simple Problem (4 Variables).

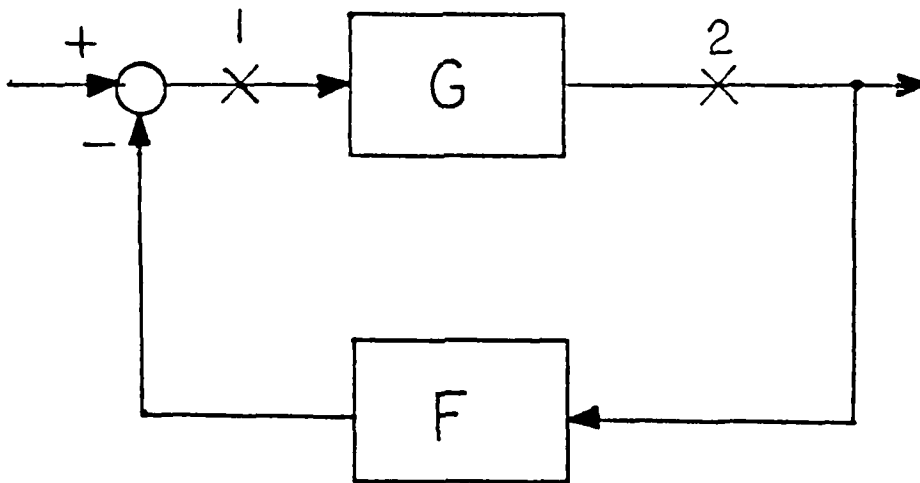


Figure 6.15 System Block Diagram.

pole placement and robustness routine a design was made in which the output singular values were specified instead of the input values. The pole placement and robustness routine produced a design with gains that provided a highly robust system on the output side with gain and phase margin of -6 db to and phase margin of ± 60 degrees. The design was not robust on the input side. Thus, designing for robustness at one point in the system does not necessarily give robustness at all points within the system.

One final case that should be discussed is that of setting both input and output robustness criteria at the same time. Excellent results were obtained for this case. The design routine placed the poles at $-1.97 \pm j0.009$ with feedback gains of

0.85793	-45.91757
0.00425	0.87137

The input singular values were raised to a level of 0.74984 or -4.5 db to 12 db gain margin and ± 43 degrees phase

margin. The output values were raised to above 0.822 which corresponds to -5 to 15 db gain margin and ± 49 degrees phase margin.

To summarize, it can be stated that the robustness problem for this system exists in the upper cross-coupling channel (input two, output one). The lack of robustness can be discovered in two ways. The first method is to plot the open-loop Bode plots of each element of the transfer matrix and look for extremely high gains and bandwidths relative to the other transfer functions. The second method examines the singular values of the return difference matrix for magnitude. Low singular values correspond to low robustness. The pole placement and robustness design routine can increase robustness by modifying feedback gains to reduce the effect of cross-coupling within the system. Observing the gain modification made by the pole placement and robustness routine the critical channel within the system that affects the robustness may be determined from the Bode plots. The pole placement and robustness routine feedback gain changes also cause zero shifts during the robustness recovery. The gain on the open loop Bode plot for the affected cross-coupling channel is adjusted and the closed-loop zeros, as seen on the pole-zero diagram, are shifted. This zero shift is in a direction which will combine with system poles to smooth the frequency response diagram in the vicinity of the minimum singular value.

VII. A HELICOPTER STABILITY PROBLEM

This chapter will deal with a more practical application of the numerical optimization program. In this problem the combined pole placement, robustness design procedure will be applied to the linear lateral dynamic channels of a CH-47 helicopter. The model is a highly coupled two-input two-output system that has been studied for its basic robustness characteristics [Ref. 16]. The usual procedure for design of highly coupled systems is to obtain a diagonally dominant closed-loop system. This diagonal system will be stable but not robust to cross-feed parameters. Sandell, et al, produced three designs. Two of these designs, while meeting basic performance criteria, had poor robustness. The third design was a relatively good design. The numerical optimization technique developed in the thesis was applied to the two poor designs and shown to provide substantial improvement in robustness.

The systems were designed to satisfy specifications to step input response and stability margins as stated in military specifications. Specific design parameters for each of the three designs presented were not available. The designs were all considered to meet the performance specification criteria and stability margin requirements. It was shown that two of these designs were extremely sensitive to model errors. The classic Nyquist techniques did not predict this sensitivity. The singular value analysis did indicate sensitivity problems.

The model is that of a CH-47B helicopter lateral dynamic system in hover. The dynamic model of the system is

$$\dot{\underline{x}} = \underline{A} \underline{x} + \underline{B} \underline{u} \quad (7.1)$$

$$\underline{x} = (v, p, r, \psi) \quad (7.2)$$

$$\underline{u} = (\delta_B, \delta_C) \quad (7.3)$$

where

$$\underline{A} = \begin{bmatrix} 2.27 & -1.42 & -0.15 & 31.99 \\ 0.01 & -0.7 & -0.07 & 0 \\ 0.04 & -0.05 & -0.5 & 0 \\ 0 & 1 & 0.11 & 0 \end{bmatrix}$$

and where

$$\underline{B} = \begin{bmatrix} 0.12 & 0.95 \\ 0.04 & -8.37 \\ .34 & 0.02 \\ 0 & 0 \end{bmatrix}$$

with full state available for feedback. Table 3 is a summary of parameters. The system is not open-loop stable.

Three control laws are formulated to satisfy the desired performance specifications. Equation 7.4 is the basic control law.

$$\underline{u} = -\underline{F}_i \underline{x} + h_i \psi_c \quad (7.4)$$

$i=1, 2 \text{ or } 3$

where the following values of F and h were are:

$$\underline{F}_1 = \begin{bmatrix} -1.72 & -23.5 & 70.6 & 595. \\ 0.024 & -2.71 & 0.368 & -7.99 \end{bmatrix}$$

$$\underline{F}_2 = \begin{bmatrix} 0.198 & 154.0 & 18.3 & 142.0 \\ -0.01 & -1.592 & -0.189 & -1.47 \end{bmatrix}$$

$$\underline{F}_3 = \begin{bmatrix} 0 & 0 & 25.5 & 0 \\ 0 & -4 & 0 & -27 \end{bmatrix}$$

TABLE 2
CH-46 Helicopter Parameter Definitions

Variable	Units	Description
v	ft/sec	Vehicle body y-axis earth relative velocity component
p	rad/sec	Roll rate
r	rad/sec	Yaw rate
ϕ	rad	Roll attitude angle
δ_B	in	Yaw rate rotor deflection control
δ_C	in	Roll rate rotor deflection control

$$h_1 = \begin{bmatrix} 597.0 \\ -7.99 \end{bmatrix}$$

$$h_2 = \begin{bmatrix} 142.0 \\ -1.47 \end{bmatrix}$$

$$h_3 = \begin{bmatrix} 0 \\ -27 \end{bmatrix}$$

The ψ_c is a step input command that must track. Figure 7.1 is a diagram of the control structure for the feedback control laws. Figure 7.2 is a detailed layout of the system. All three of the designs have negative real eigenvalues and provide stable overdamped responses. All three of the above designs meet the desired design specifications.

The loop Bode plots, [Ref. 16], indicate all three designs to have good stability margins when considered a loop at a time. Since these designs were all full state LQ

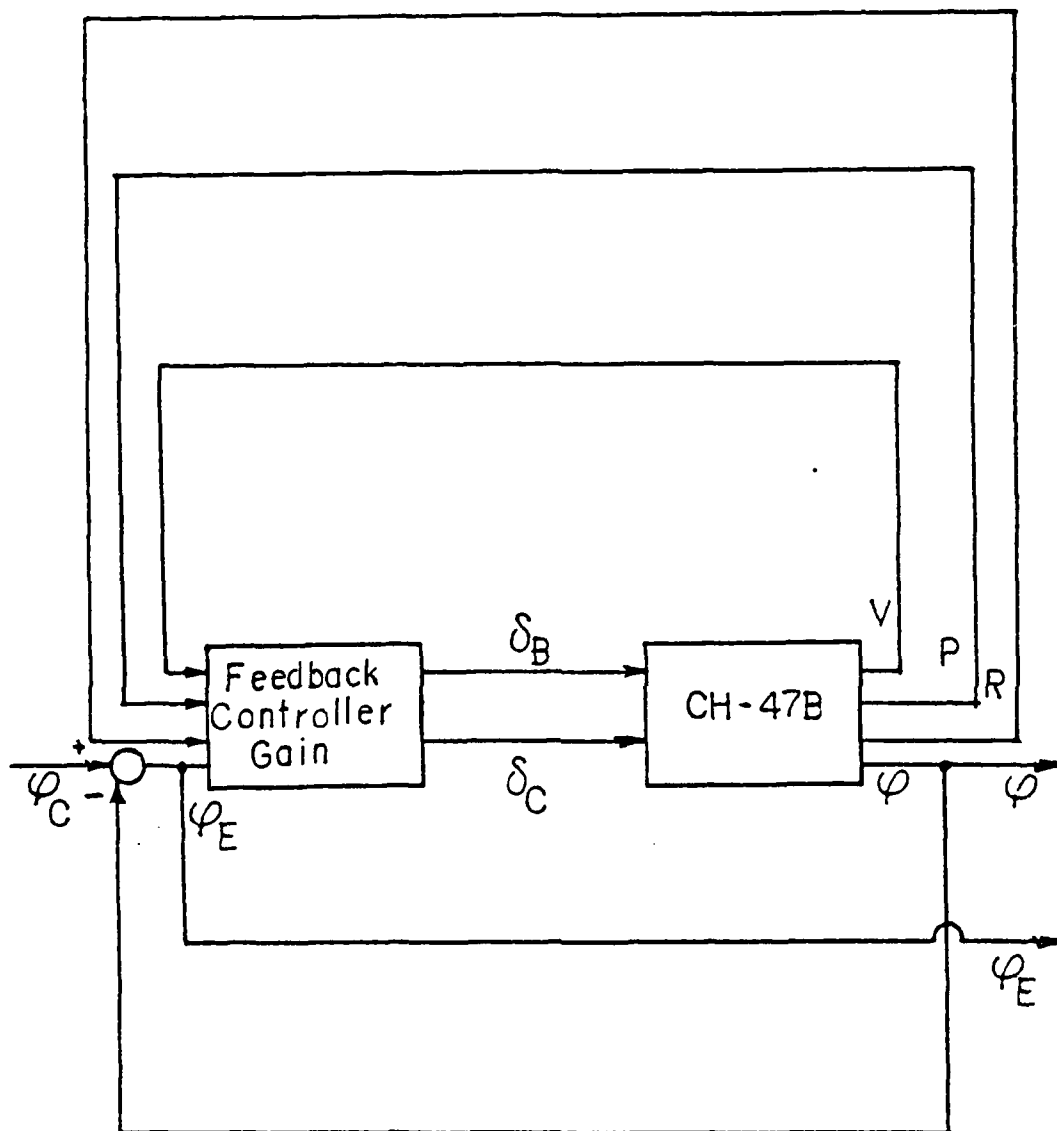


Figure 7.1 Feedback Control Structure.

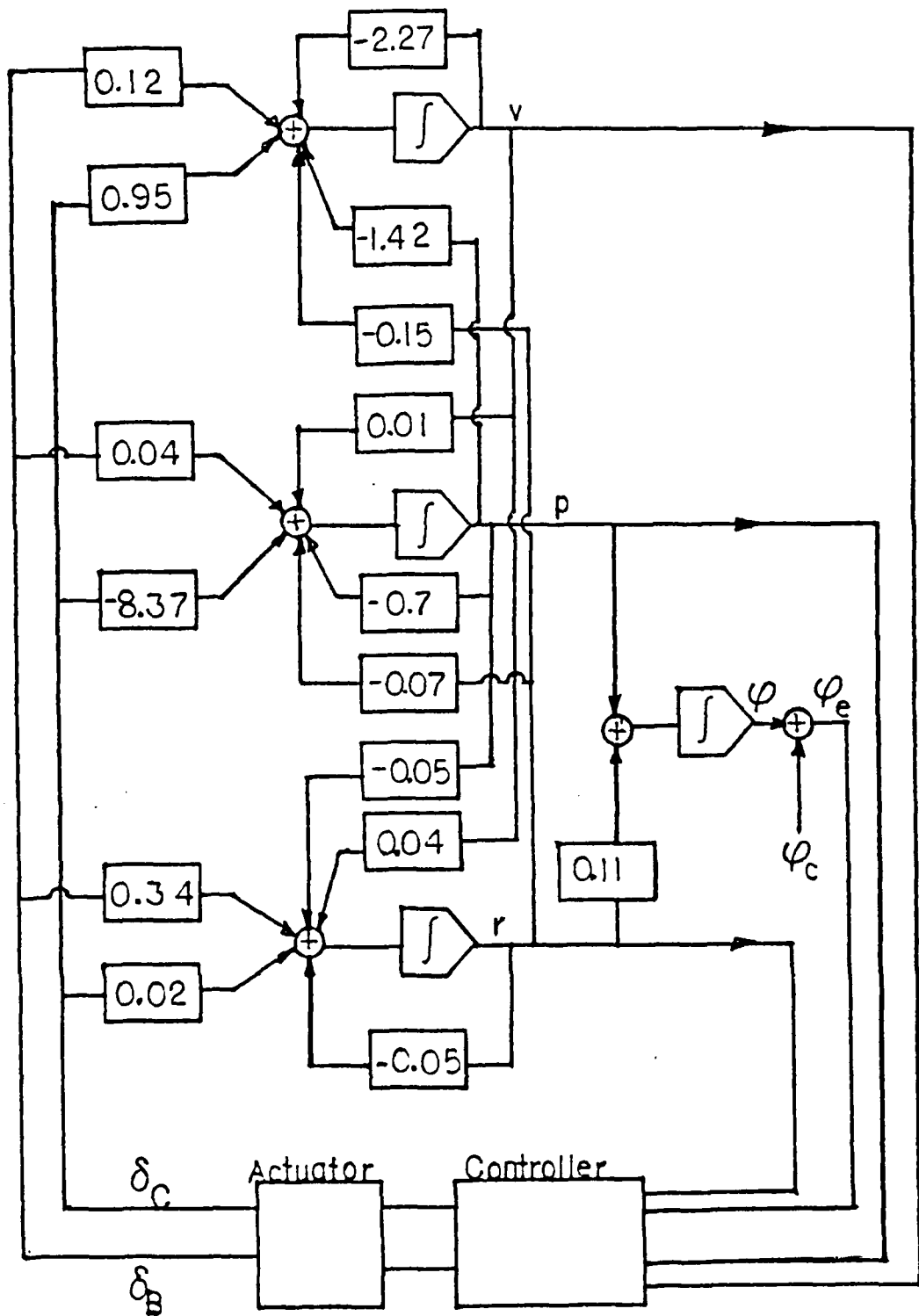


Figure 7.2 System Diagram.

designs with a diagonal control weighting matrix they should possess at least -6 db to infinite gain margin and 60 degrees of phase margin. When the singular values of the three designs are computed a robustness problem is indicated by low singular values of two of the designs. Figure 7.3 presents singular value plots of all three designs. This plot shows that designs 1 and 2 both have very low minimum singular values for the return difference matrix. Design 1 goes as low as -20 db near 10 rad/sec in frequency while design 2 is down to -34 db at frequencies up to 1000 rad/sec. Design 3 is a good design with singular values that remain above one throughout the frequency range of interest. Using the universal gain and phase diagram as discussed in Chapter 6 this equates to a gain margin of about -6 db to infinity and a phase margin of 60 degrees as expected.

The system stability in design 1 may be affected by perturbations occurring in the actuators as shown in figure 7.4. If the output axis coupling from δ_c spills into δ_B in the frequency range from 0.5 to 50.0 rad/sec with a magnitude of 0.12 and a phase of 60 degrees then the system can become unstable. This could be caused by nonlinear terms, worn parts, or system saturation.

The second design as shown in figure 7.5 may have a stability derivative variation between δ_B and p . If this derivative varies from about 0.04 to -0.96 the system can become unstable. The center of gravity location, trim of the aircraft and rotor coupling can all affect this derivative.

The pole placement and robustness design technique developed for this thesis research was applied to designs 1 and 2 to obtain an improved robustness for these designs. Design 1 will be considered first. In this design a cross-feed perturbation through the actuator can produce instability as indicated by the low singular values at lower frequencies. To study this problem with the pole placement

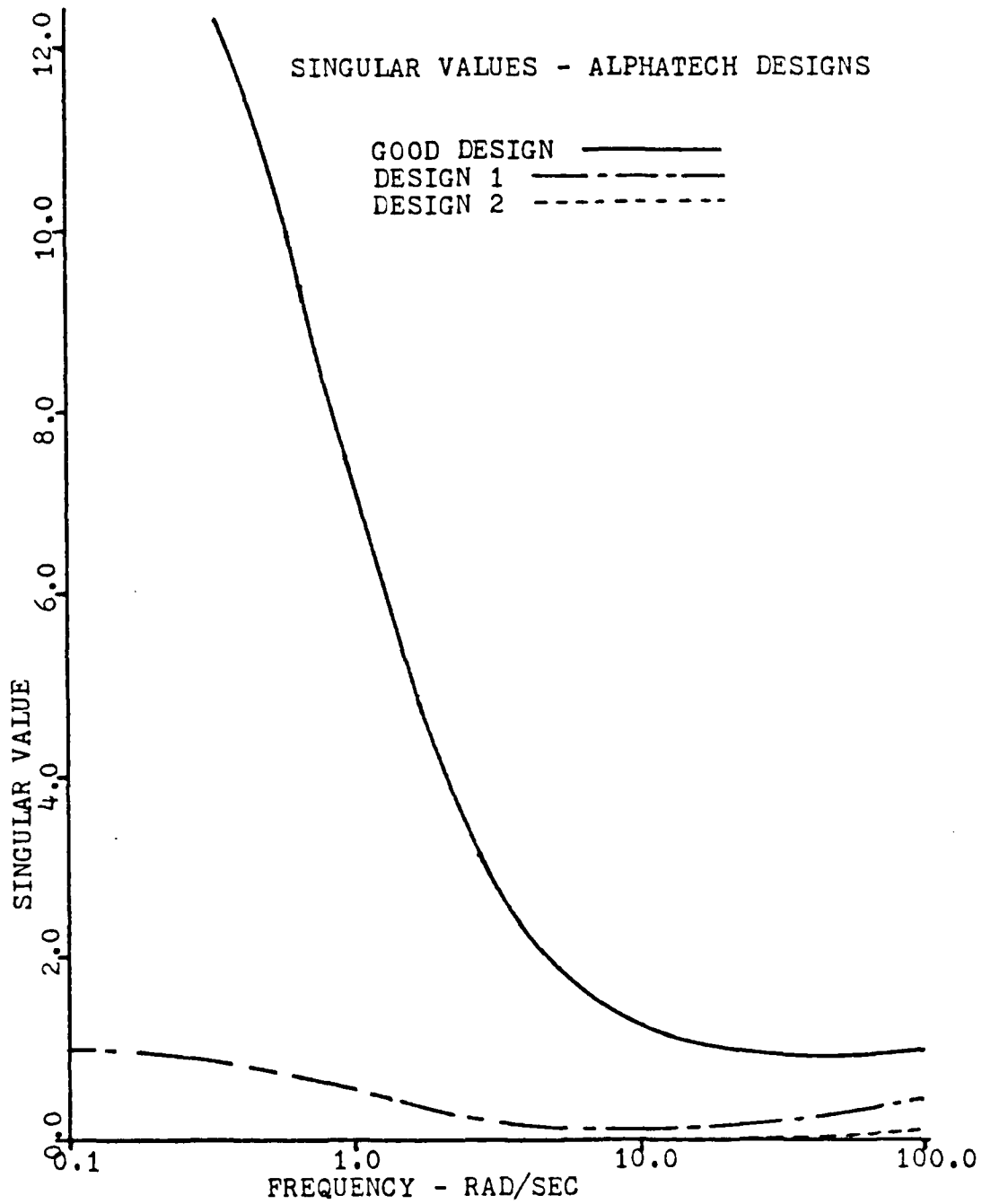


Figure 7.3 Alphatech Design Singular Value Plots.

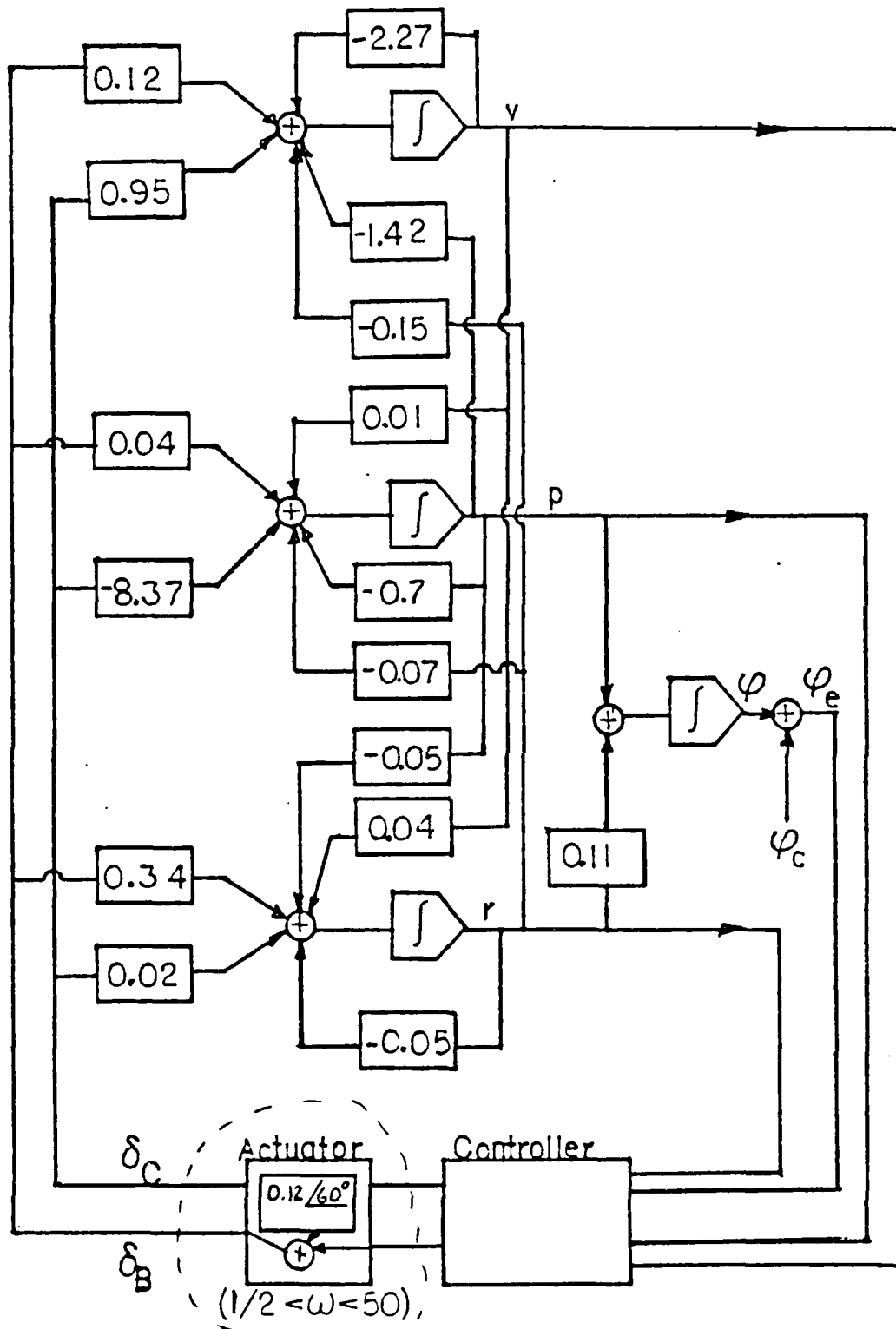


Figure 7.4 Design One Perturbation Input.

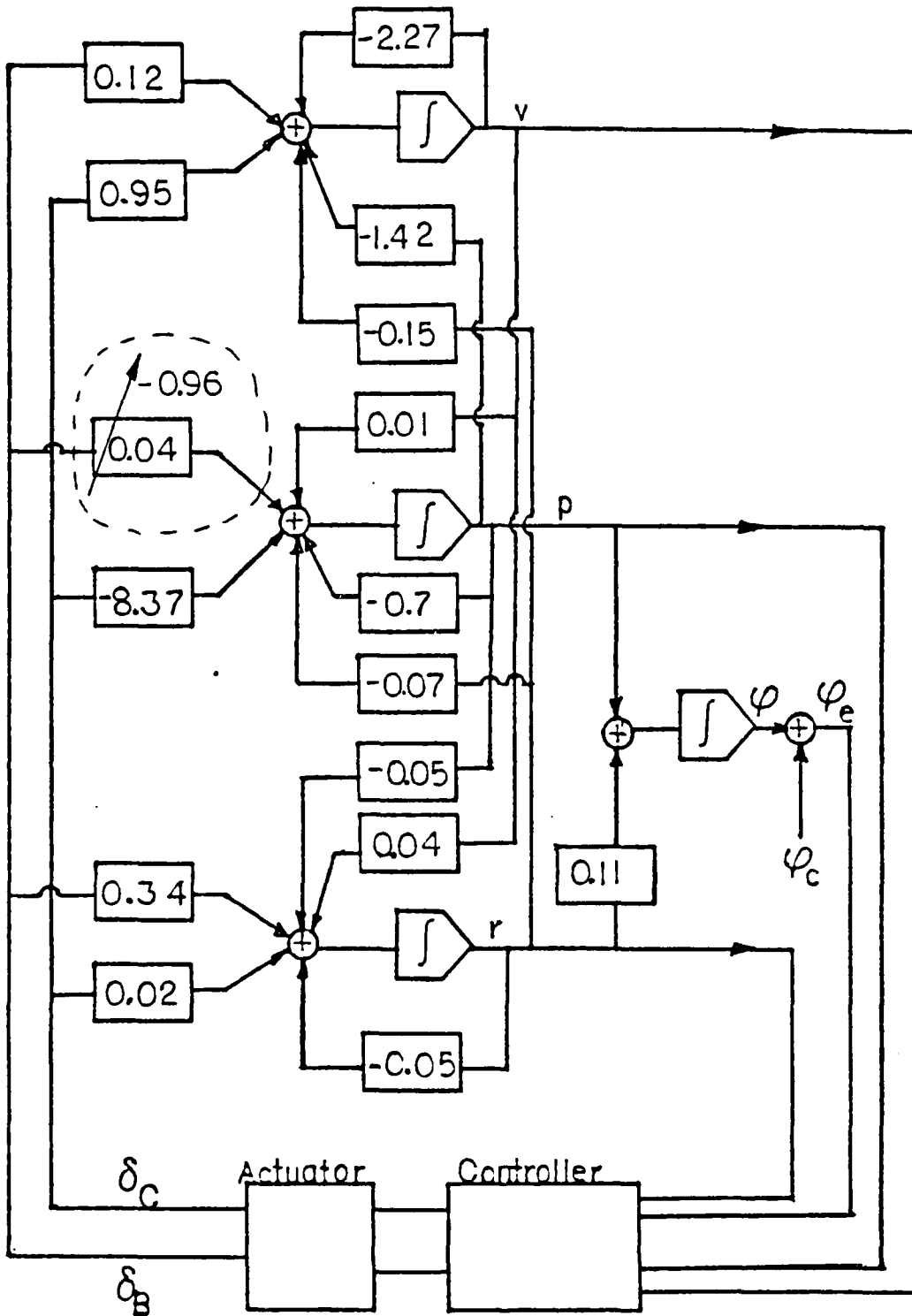


Figure 7.5 Design 120 Perturbation Input.

and robustness design method it is assumed that the eigenvalues (pole locations) of the system as developed in [Ref. 16]. are the required poles for the performance criteria. Once the pole locations are set, robustness criteria must be selected. From the universal gain and phase margin curve discussed earlier two choices of singular value levels were made for this problem. The first singular value level chosen was 0.6. This corresponds to a gain margin of -4.0 db to 8 db and a phase margin of about 35 degrees. The second value chosen was 1.0. With corresponding gain margin of -6 db to ∞ and a phase margin of 60 degrees which are the characteristics of a LQ regulator design with diagonal weighting matrices.

For singular value level 0.6 the pole placement and robustness design routine places the poles as shown in table 2. The slight differences in these pole locations appear to have insignificant effect on the performance as shown in the response curves of the system. The feedback gain adjustment moves the minimum singular value from about 0.11 with very poor phase and gain margins to a level of 0.66. This is above the desired values of gain and phase. The improvement in robustness came from modifying the feedback gains in channel δ_B . By greatly reducing the gains in channel δ_B the optimizer minimizes the influence of the cross-coupling from channel δ_C . In this way a much larger spill over of channel δ_C may be tolerated through the actuator before the system will become unstable.

The primary mechanism of robustness improvement in this problem was a reduction in the gain levels of the affected channel. The feedback gains presented in table 4 show the modification of these gains from those utilized in [Ref. 16]. While all the gains are modified the f_{14} gain undergoes a significantly larger change than the other design 1 case 1 feedback gains. Looking at the open-loop

TABLE 3
Design One Pole Placement

Pole	Desired Location	Actual Location
1	-24.7977	-24.7893
2	-11.3635	-12.0083
3	-10.3288	-10.7752
4	- 2.1005	- 2.1181

transfer functions of this optimized problem and comparing them with a non-optimized set of transfer functions for δ_B to as shown in figure 7.6 and 7.7 show very little change in the system gain, both are around 42.0 db, and a bandwidth of about 20 rad/sec. There is a significant change in the phase diagram which is caused by the zero location shift.

The transfer function for δ_C to δ_C depicted a gain increase of about 3 db for the optimized design while the phase remained similar for both transfer functions. In transfer function δ_C to δ_B some important aspects of the problem are observed. The Bode diagram of the open-loop transfer function of δ_C to δ_B clearly indicates the cross-coupling problems and the pole placement and robustness design routine's mechanism of optimizing the system gains to increase robustness. The gain is reduced from 93 db to about 78 db and the bandwidth is reduced from above

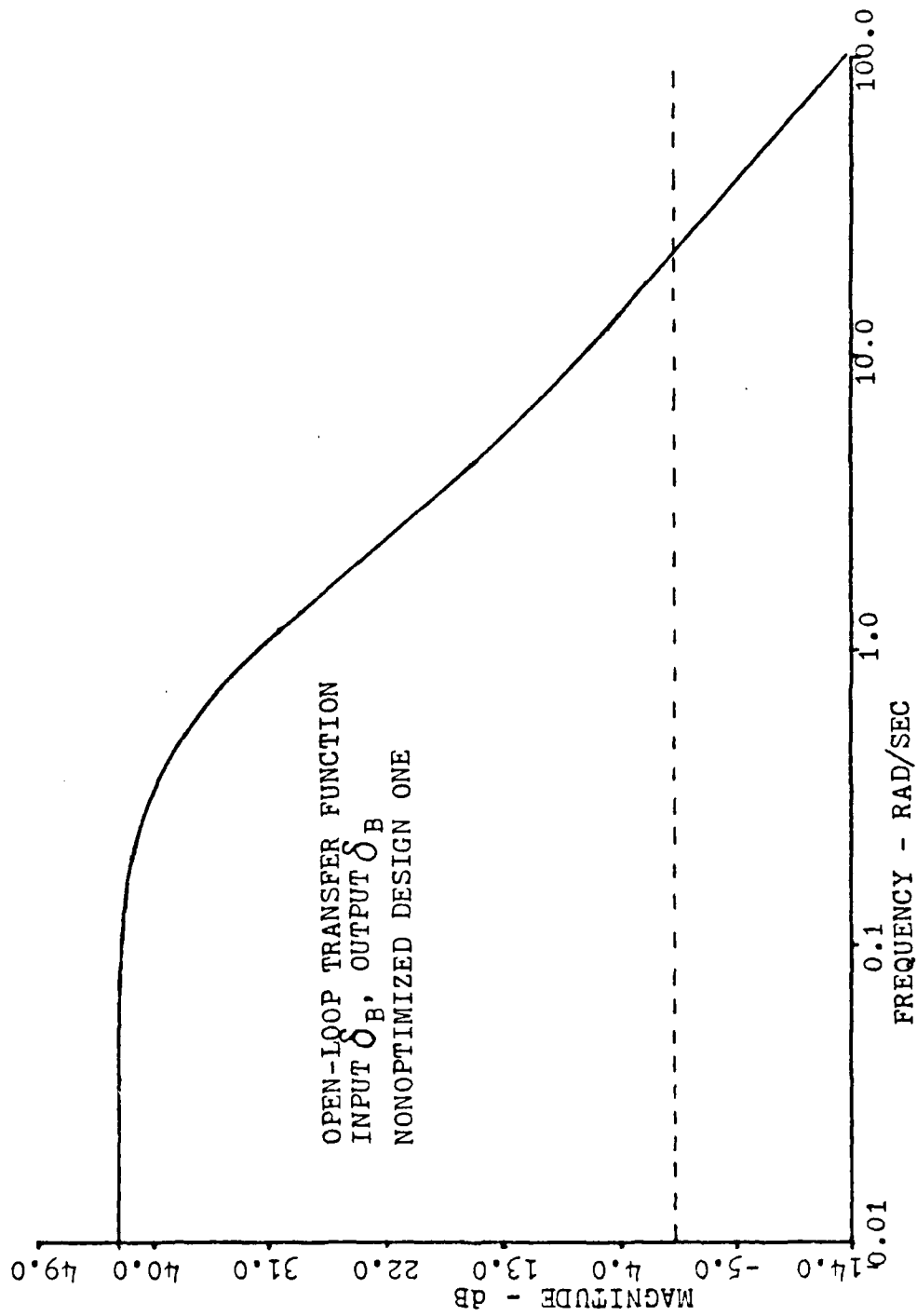


Figure 7.6 Transfer Function $\delta_B - \delta_B$ Design One, Nonoptimized.

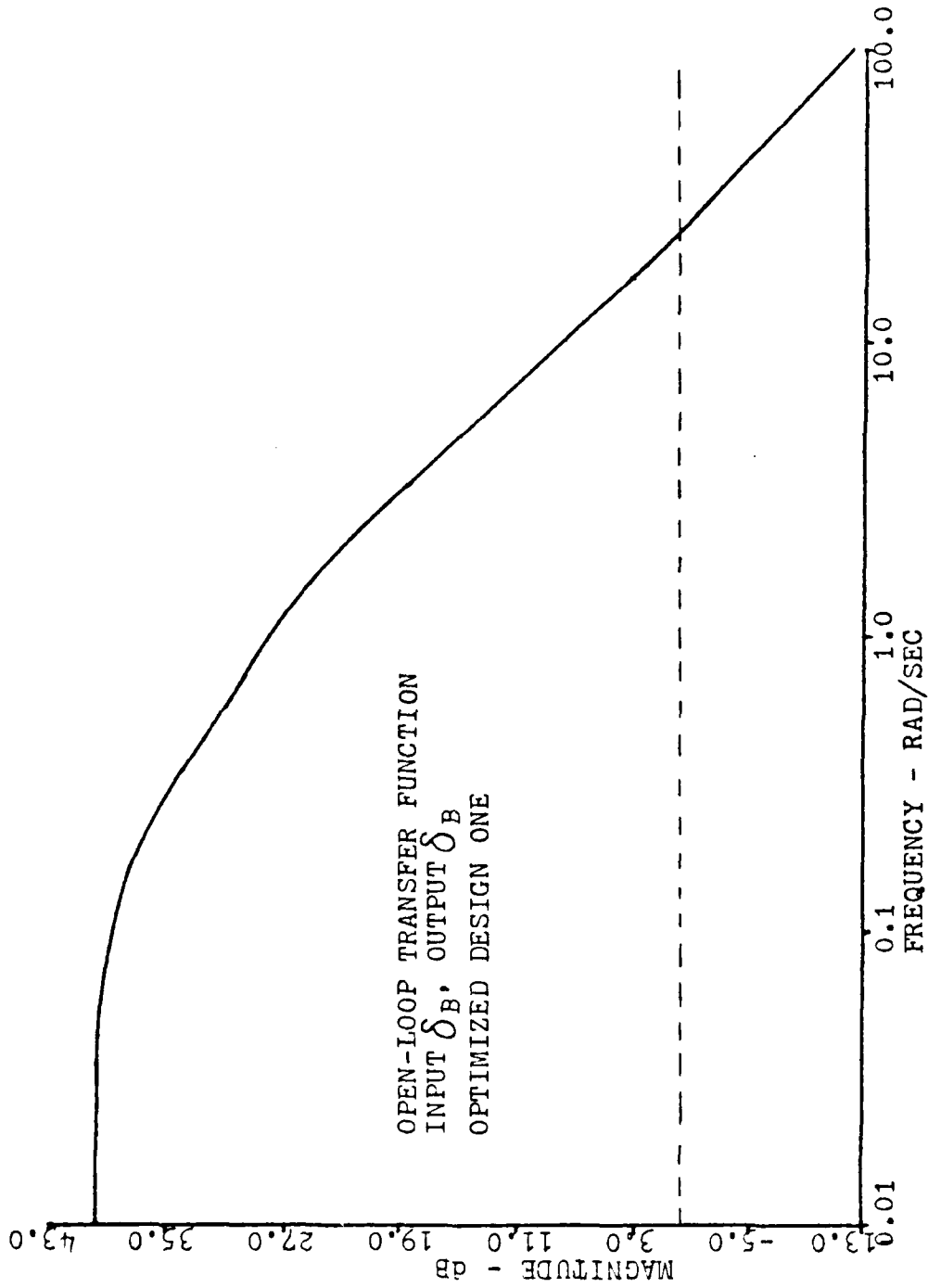
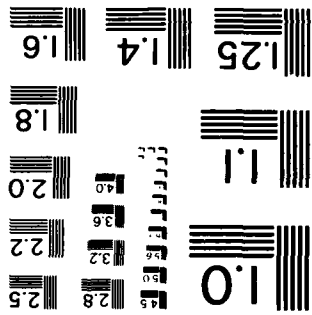


Figure 7.7 Transfer Function $\delta_B - \delta_B$ Design One, Optimized.

100 rad/sec to about 30 rad/sec. The reduction of bandwidth and gain in the loop δ_c to δ_B yields an increased tolerance to perturbation. The transfer function for δ_c to δ_B is shown in figures 7.8 and 7.9. In the transfer functions for δ_B to δ_c the bandwidth is slightly increased from 0.6 to 0.8 rad/sec and the gain actually increased from 9 db to 14 db. The big change in the overall system, however, is in the transfer function from δ_c to δ_B . This is the channel that the destabilizing perturbation enters and by greatly reducing the gain and bandwidth in this channel through a change in feedback gain, the optimizer routine has brought the entire system gains to more balanced conditions and recovered a highly robust design.

The gain changes associated with the robustness improvement cause the zeros of the various closed-loop pole-zero diagram to move. A comparison of the eight pole-zero diagrams is shown in figures 7.10 to 7.13. The significant feature of these pole-zero diagrams is the shift of the zeros of the optimized design in a direction that attempts to equalize or balance the frequency response for frequencies in the vicinity of the minimum singular values. The pole-zero diagram of δ_B to v will be discussed as an example of this effect. In 7.10 the nonoptimized zeros are located about $-2 \pm 4.5j$ and -19.8 . When the pole placement and robustness routine has completed the feedback gain modification these zeros have shifted near -11 and $-6 \pm 3j$. The effect of these zero shifts is to combine with the pole locations to equalize the frequency response as depicted in figures 7.14 and 7.15. Zero shifts for the remainder of the transfer functions provide similar results in the other channels. By moving toward the frequencies associated with the minimum singular values the zeros have balanced the overall frequency response of the system in each channel. While the channel gain modification is the primary mechanism

MICROCOPY RESOLUTION TEST CHART
NATIONAL BUREAU OF STANDARDS-1963-A



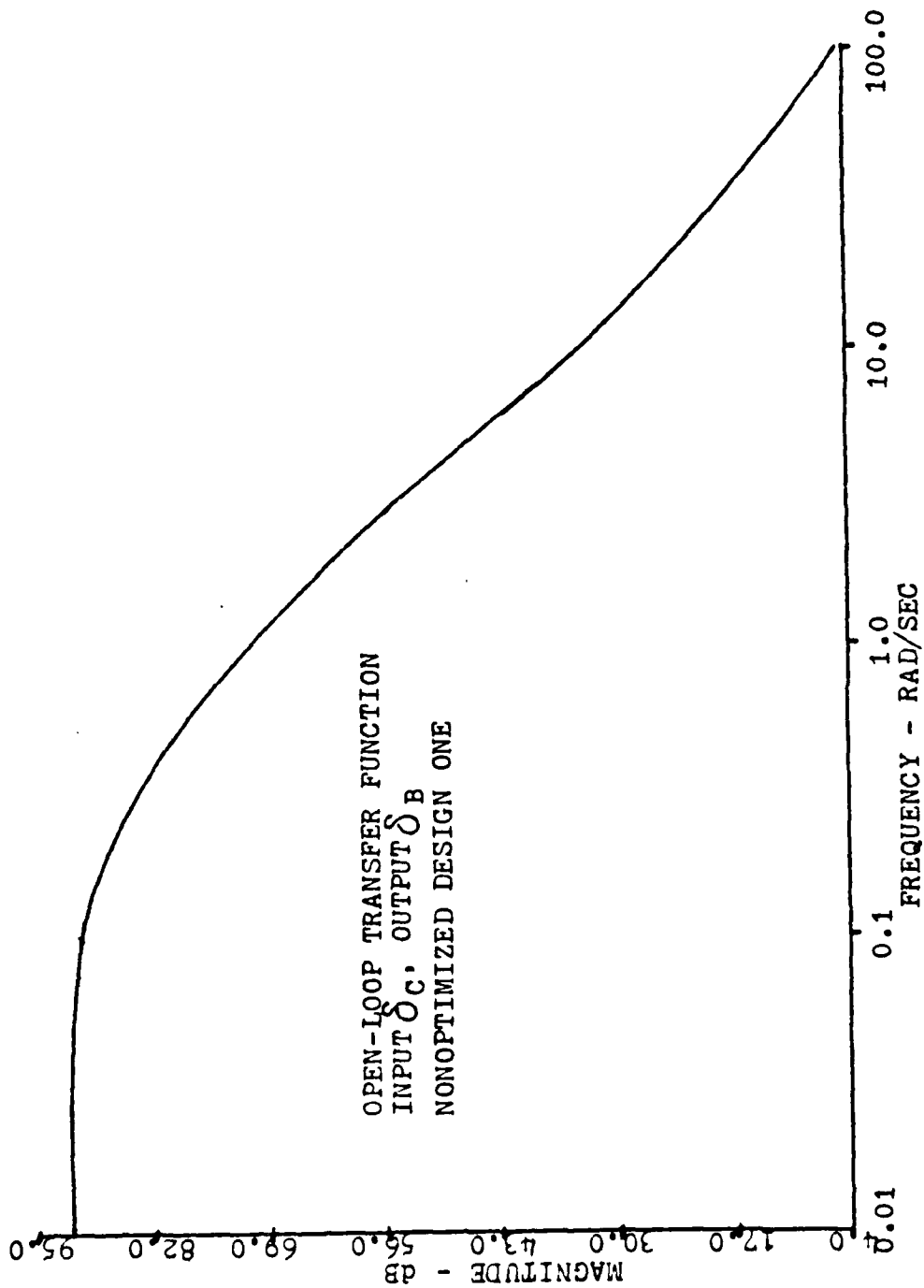


Figure 7.8 Transfer Function $\delta_C - \delta_B$ Design One, Nonoptimized.

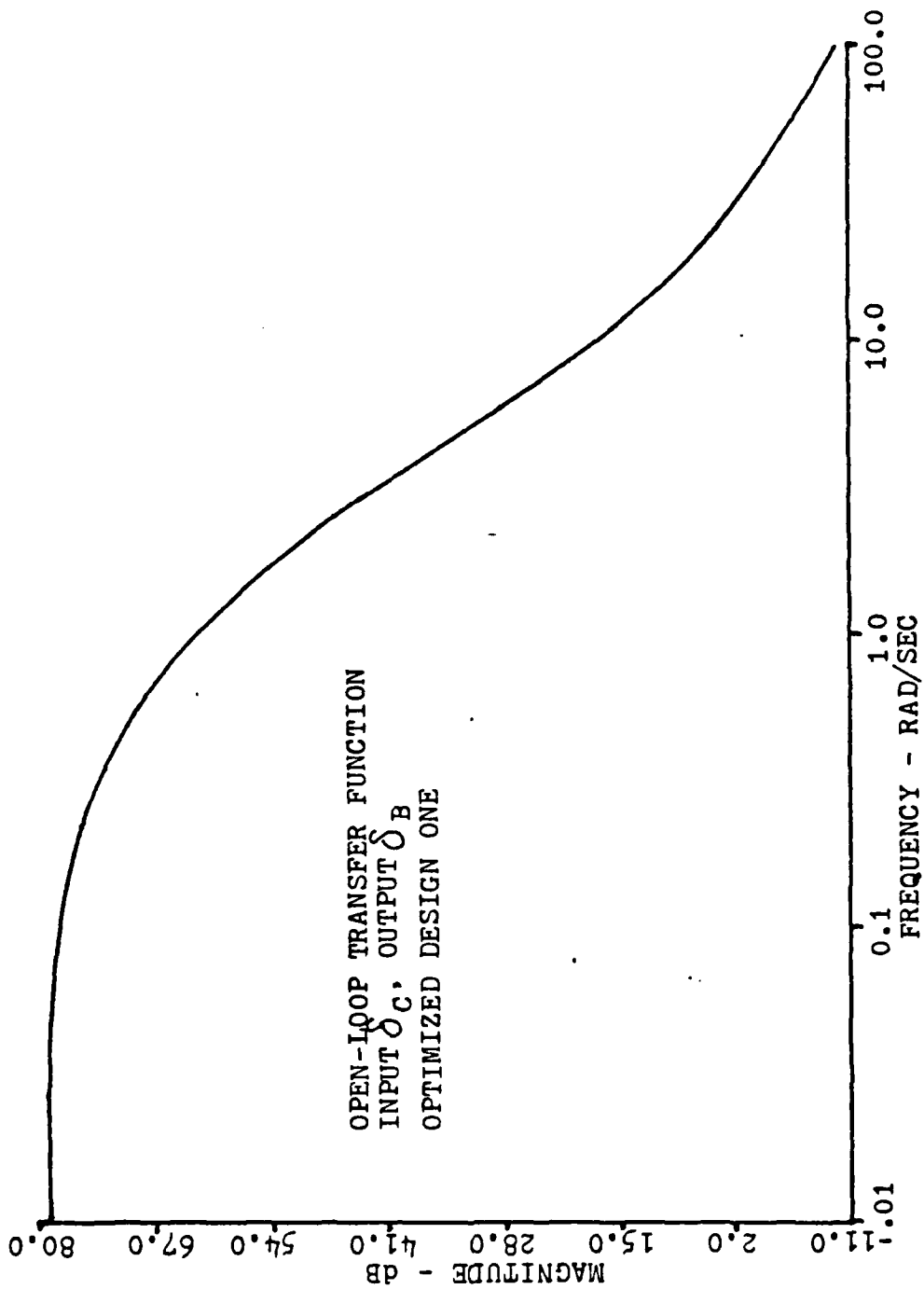


Figure 7.9 Transfer Function $\delta_c - \delta_B$ Design One, Optimized.

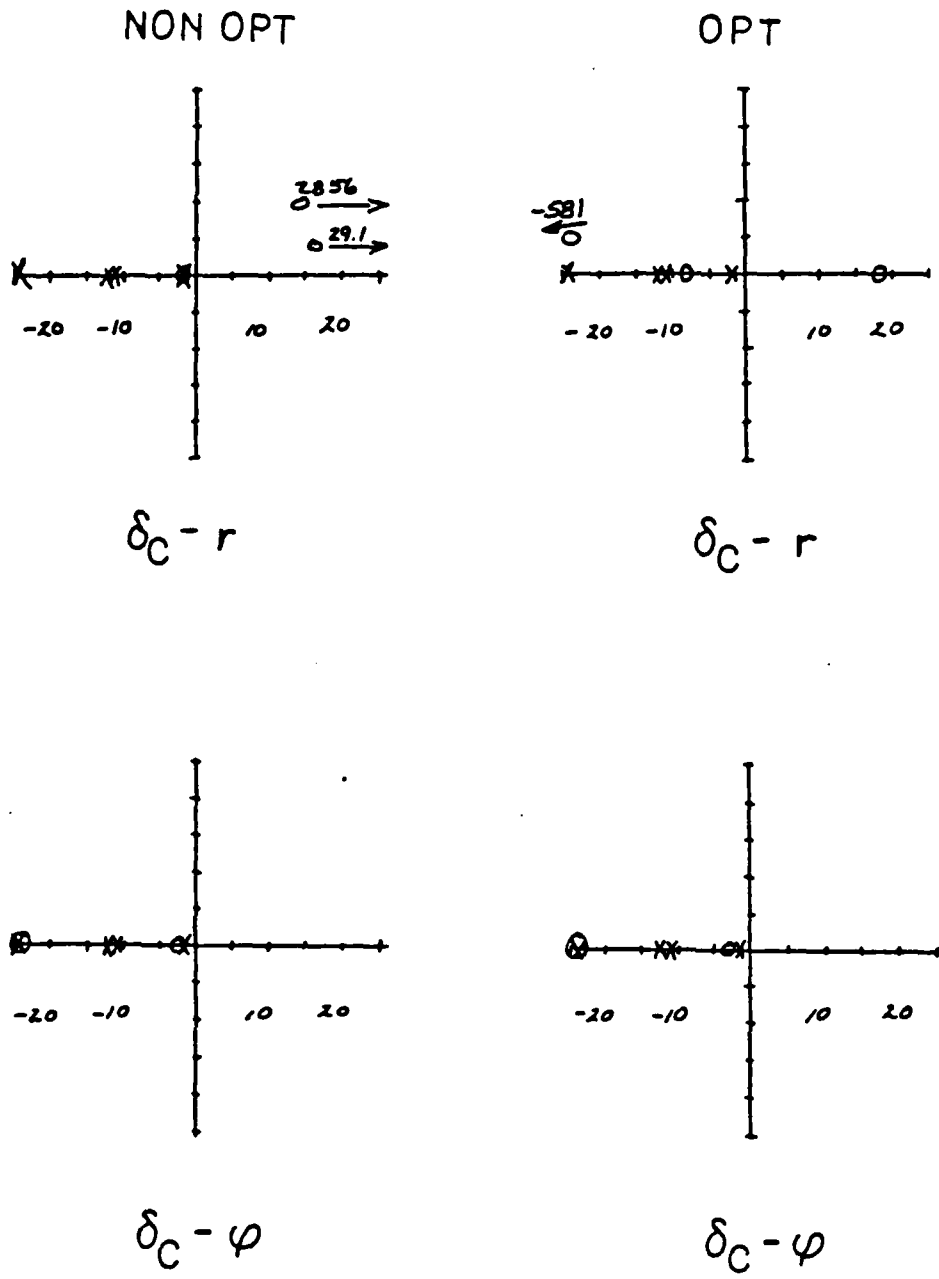


Figure 7.10 Pole-Zero Plots for Design 1.

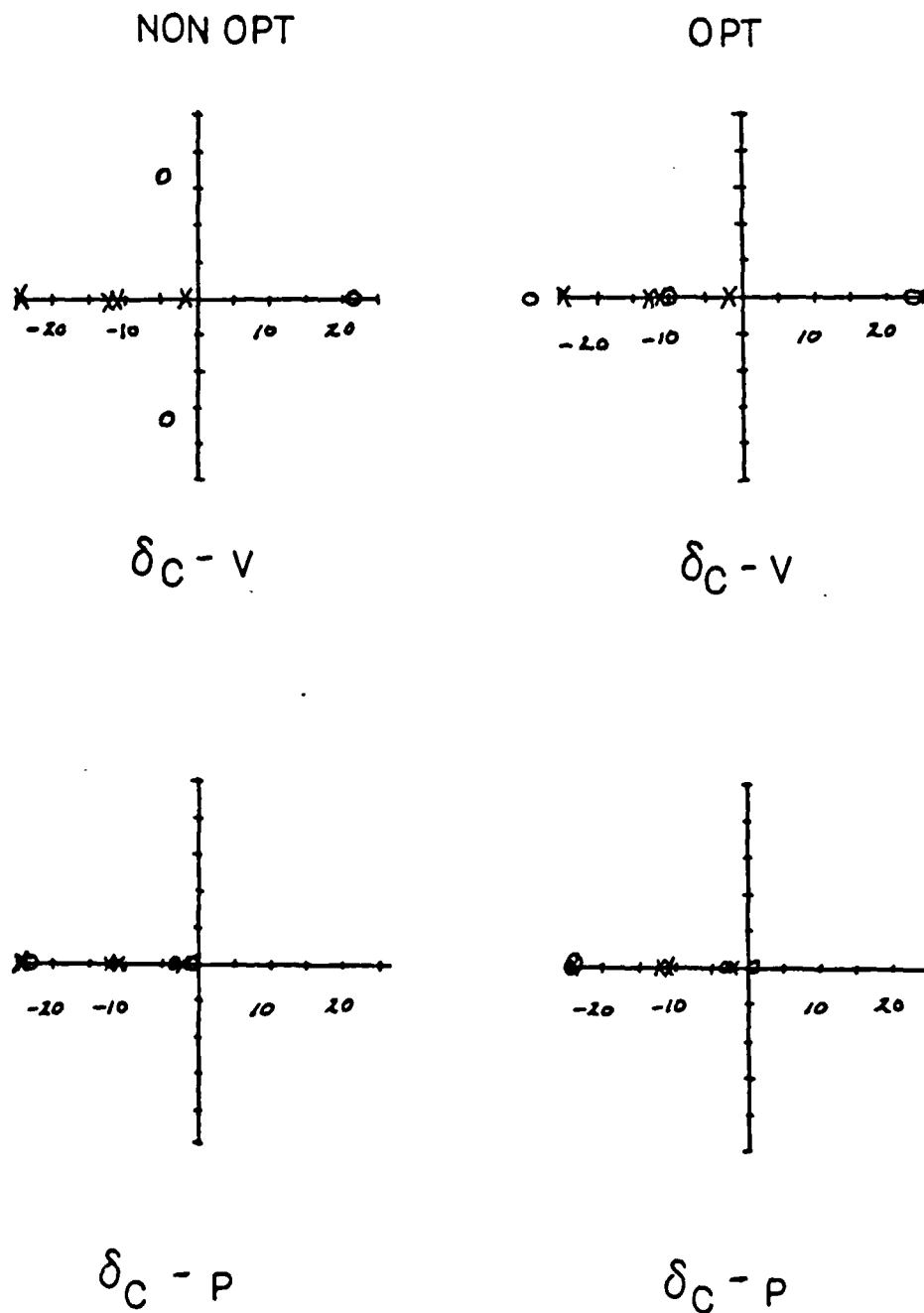
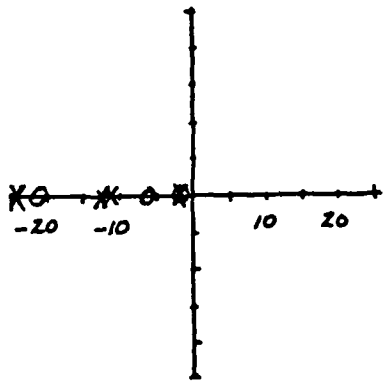


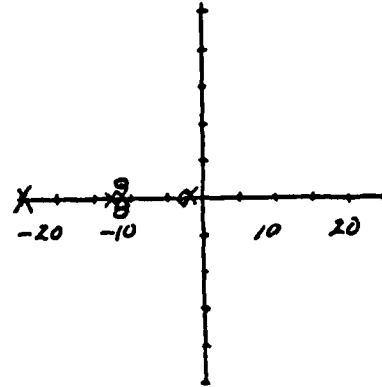
Figure 7.11 Pole-Zero Plots for Design 1 (cont.).

NON OPT

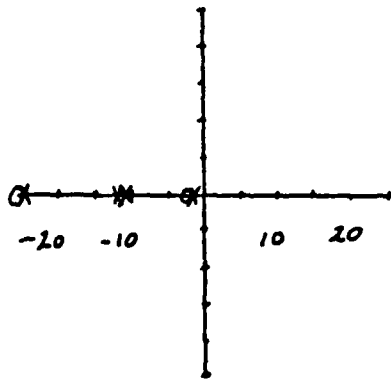


$\delta_B - r$

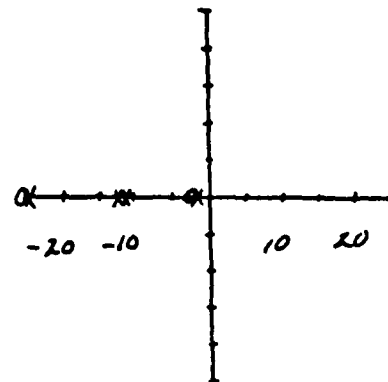
OPT



$\delta_B - r$



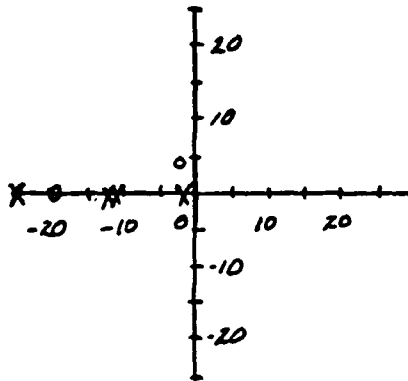
$\delta_B - \varphi$



$\delta_B - \varphi$

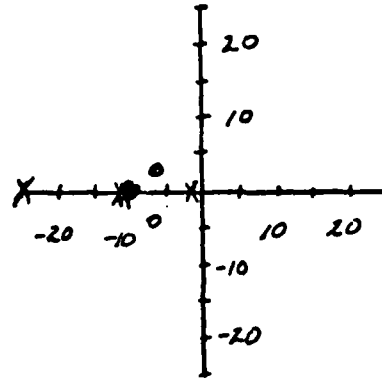
Figure 7.12 Pole-Zero Plots for Design 1 (cont.).

NON OPT

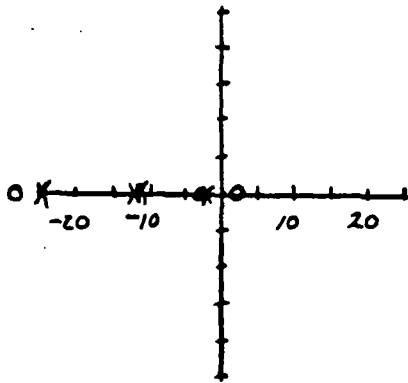


$\delta_B - V$

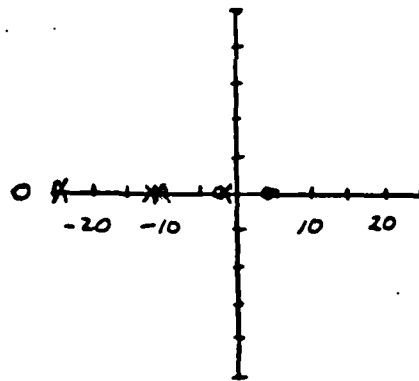
OPT



$\delta_B - V$



$\delta_B - P$



$\delta_B - P$

Figure 7.13 Pole-Zero Plots for Design 1 (cont.).

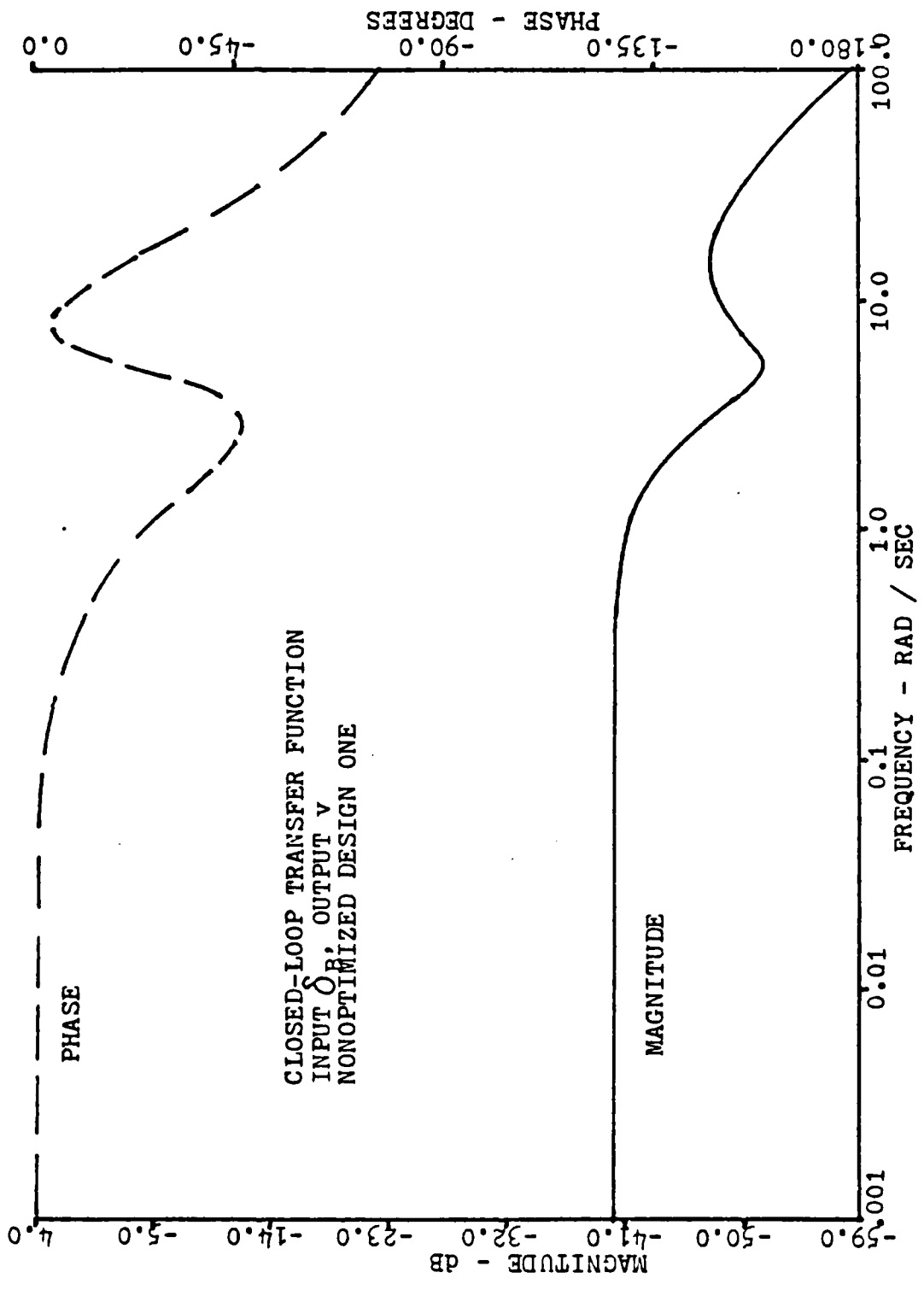


Figure 7.14 The δ_B to v Frequency Response, Nonopt..

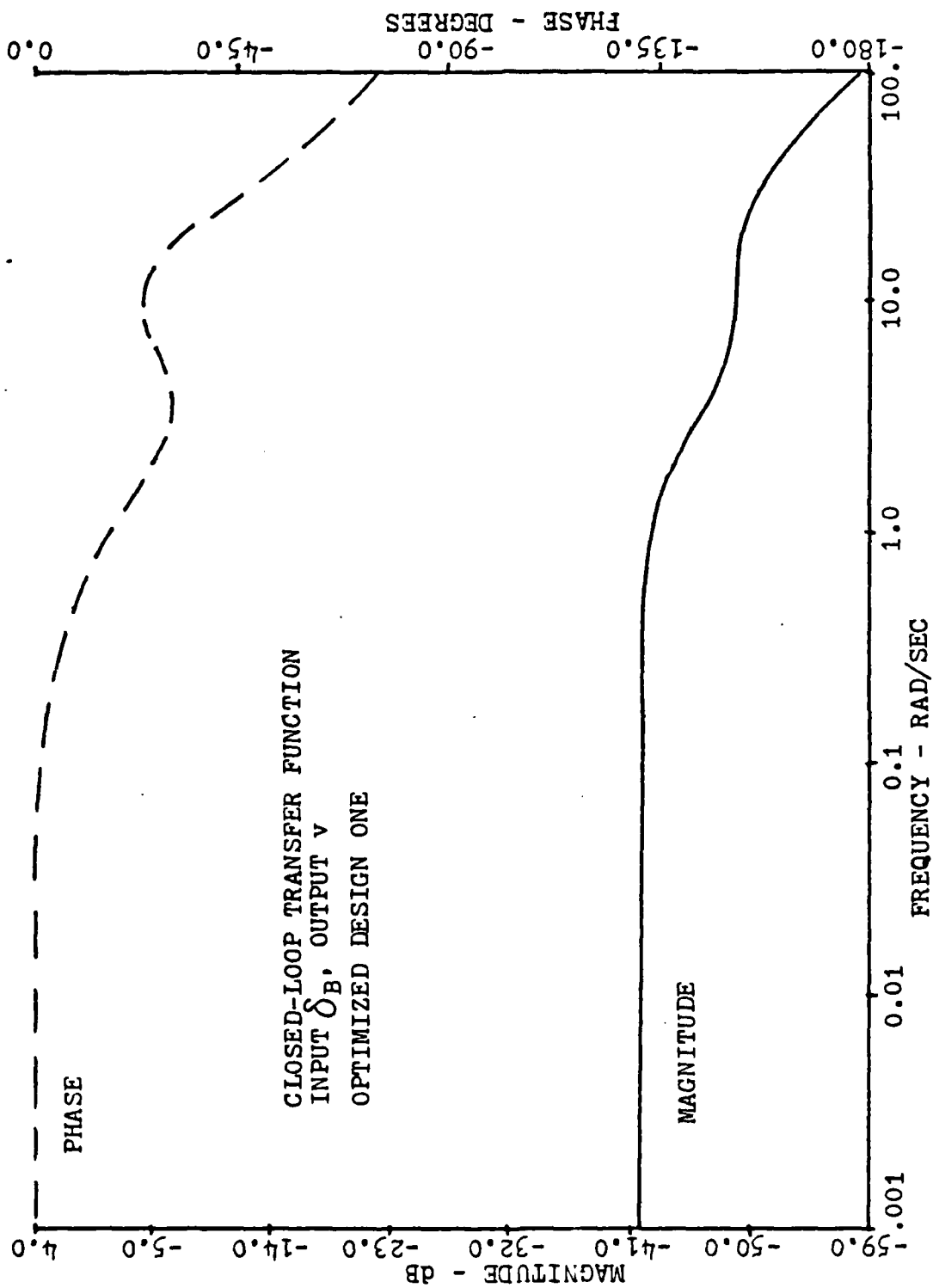


Figure 7.15 The δ_B to v Frequency Response, Optimized.

for robustness recovery the zero shift associated with the feedback gain changes is directly related to the overall frequency response of the system.

In design 1 case 2 the minimum singular value level was increased from 0.6 to 1.0. The pole placement and robustness design procedure also gave a better design for case 2

TABLE 4
Helicopter Problem Feedback Gains

DESIGN	GAIN VALUES $\begin{bmatrix} f_{11} & f_{12} & f_{13} & f_{14} \\ f_{21} & f_{22} & f_{23} & f_{24} \end{bmatrix}$			
One Case 1	-14.77726 -0.00567	2.15858 -2.55646	77.96629 0.39039	-32.91595 -15.04805
One Case 2	-6.36249 0.00813	-1.53746 -2.60073	72.85013 0.65395	74.20387 -13.47128
Two	-0.96660 0.00916	-4.54597 -3.03069	0.75436 -0.36391	11.96808 -0.34991

by modifying the feedback gains as shown in table 4. The change in the transfer functions for δ_c to δ_B (figure 7.16 and 7.17) is similar to the change seen in figures 7.8 and 7.9. The gain was reduced from above 90 db to about 75 db and the bandwidth cut from above 100 rad/sec to about 25 rad/sec. The added requirement of increased robustness did not result in a significant change in performance. [Ref. 16].

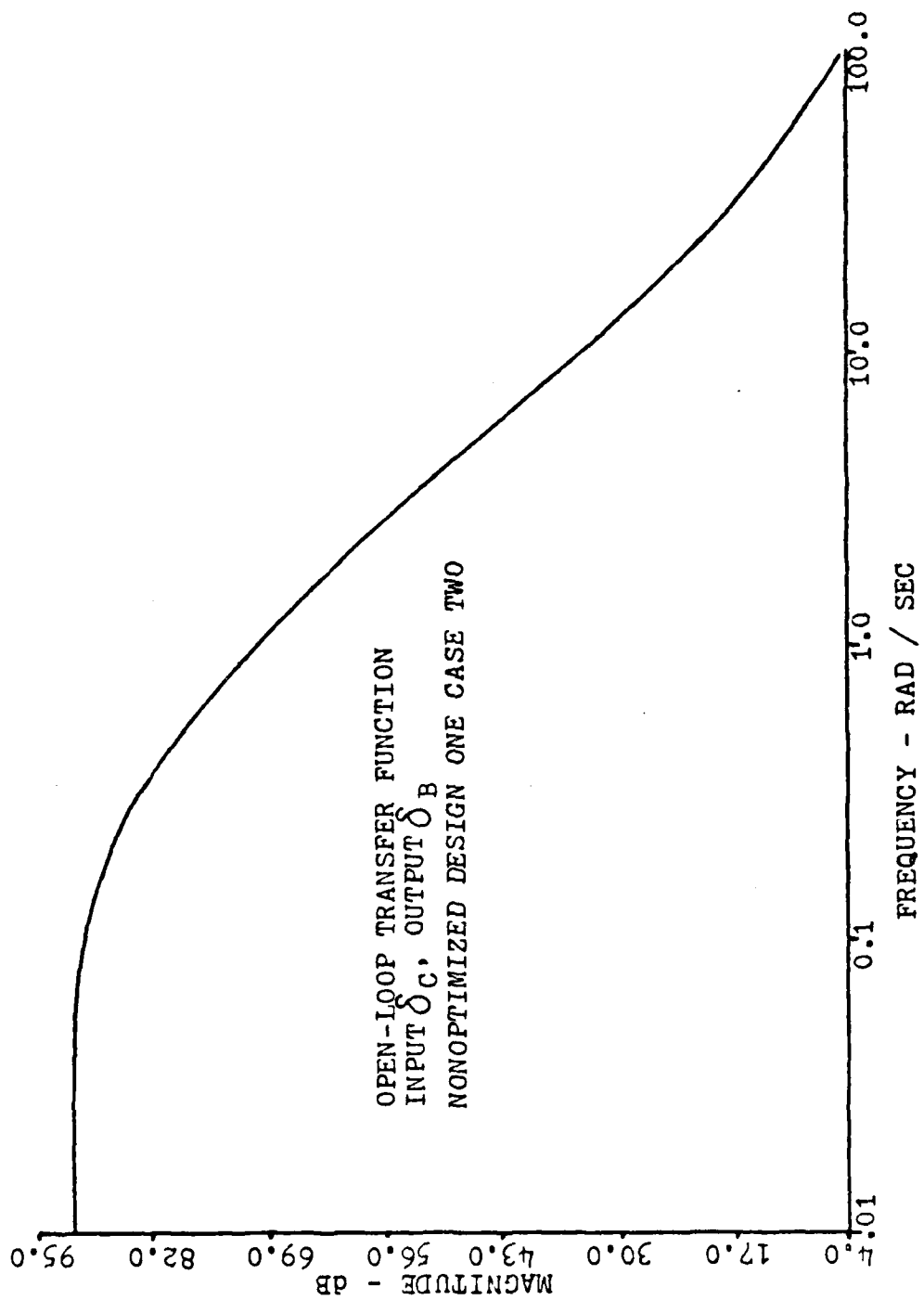


Figure 7.16 Transfer Function $\delta_c - \delta_b$ Design 1 Case2, Nonopt..

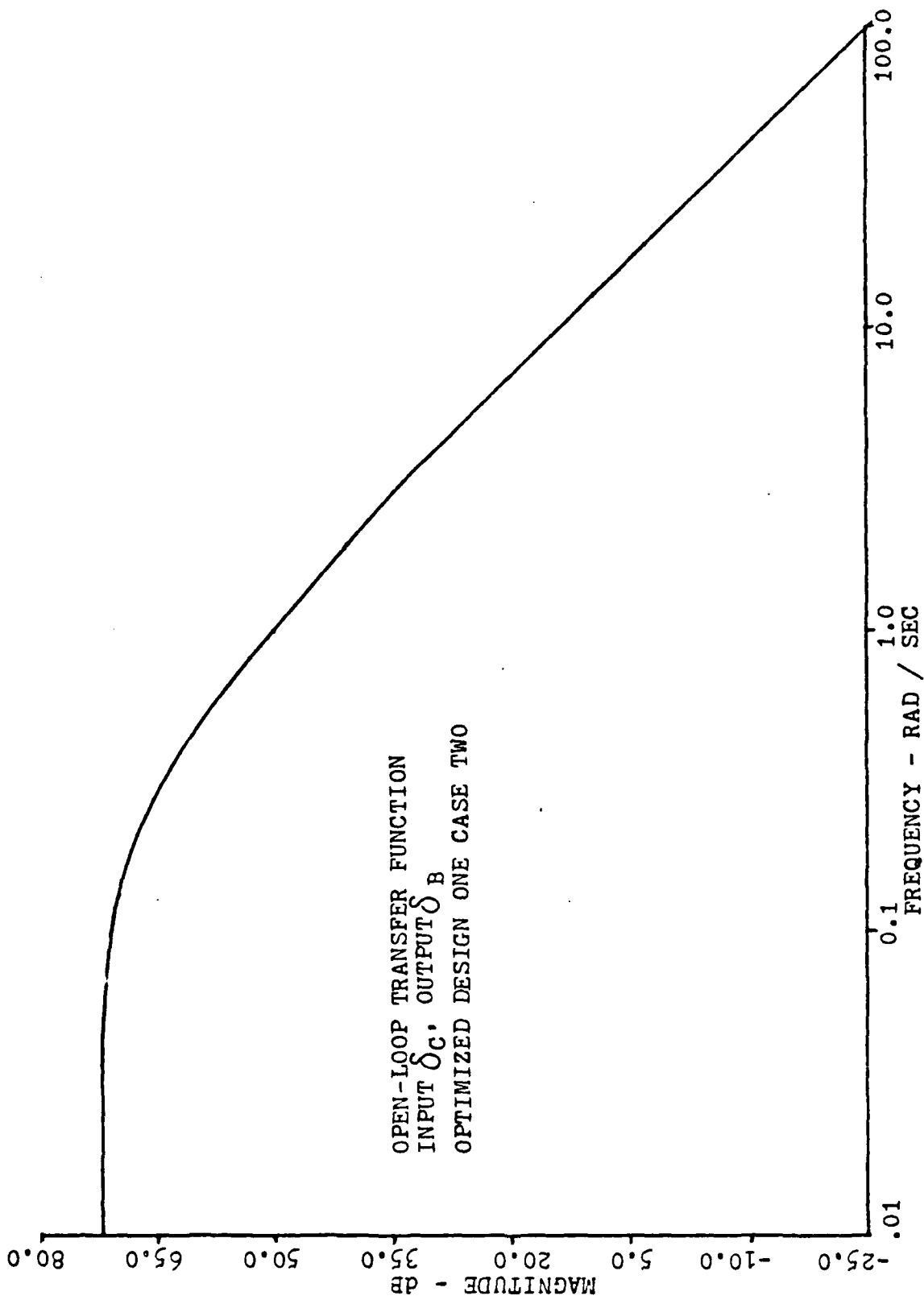


Figure 7.17 Transfer Function $\delta_C - \delta_B$ Design 1 Case 2, Opt.

Design two which is the design that is subject to parameter uncertainty in the δ_B to p channel was also studied using the pole placement and robustness design routine. In this design the singular values were very low until frequencies above 100 rad/sec were reached. To improve the design it was assumed that the pole locations that corresponded to [Ref. 16] were the required pole locations and that a robustness singular value level of 0.6 would provide adequate gain and phase margin for the design. The pole placement and robustness routine adjusted the gains in this problem until a minimum singular value of 0.6 was obtained. During this adjustment the gains in channel δ_B were considerably reduced to offset the cross-coupling between the two channels. Again, in this design as before the channel cross-coupling between δ_C and δ_B shows a marked change in bandwidth and gain from above 100 to 35 rad/sec and about 78 db to 22 db respectively. Figures 7.18 and 7.19 show the transfer function plots for this term. Figure 7.20 shows the singular value improvement. In figure 7.21 the time response is plotted. As can be seen in the plot the improvement in robustness for this problem results in very sluggish response and degraded performance.

To summarize for this problem, a given performance level has been chosen in terms of pole locations. The level of robustness has been set for a desired gain and phase margin based on the universal gain and phase margin curve. The pole placement and robustness routine has been able to improve the robustness level by changing the feedback gains that affect the channel δ_C cross-coupling. This robustness recovery is affected by modification of the system feedback gains in such a manner that cross coupling gains are reduced so that small cross-coupling perturbations do not drive the system into instability. The open-loop transfer function plots have been used to indicate how this mechanism operates

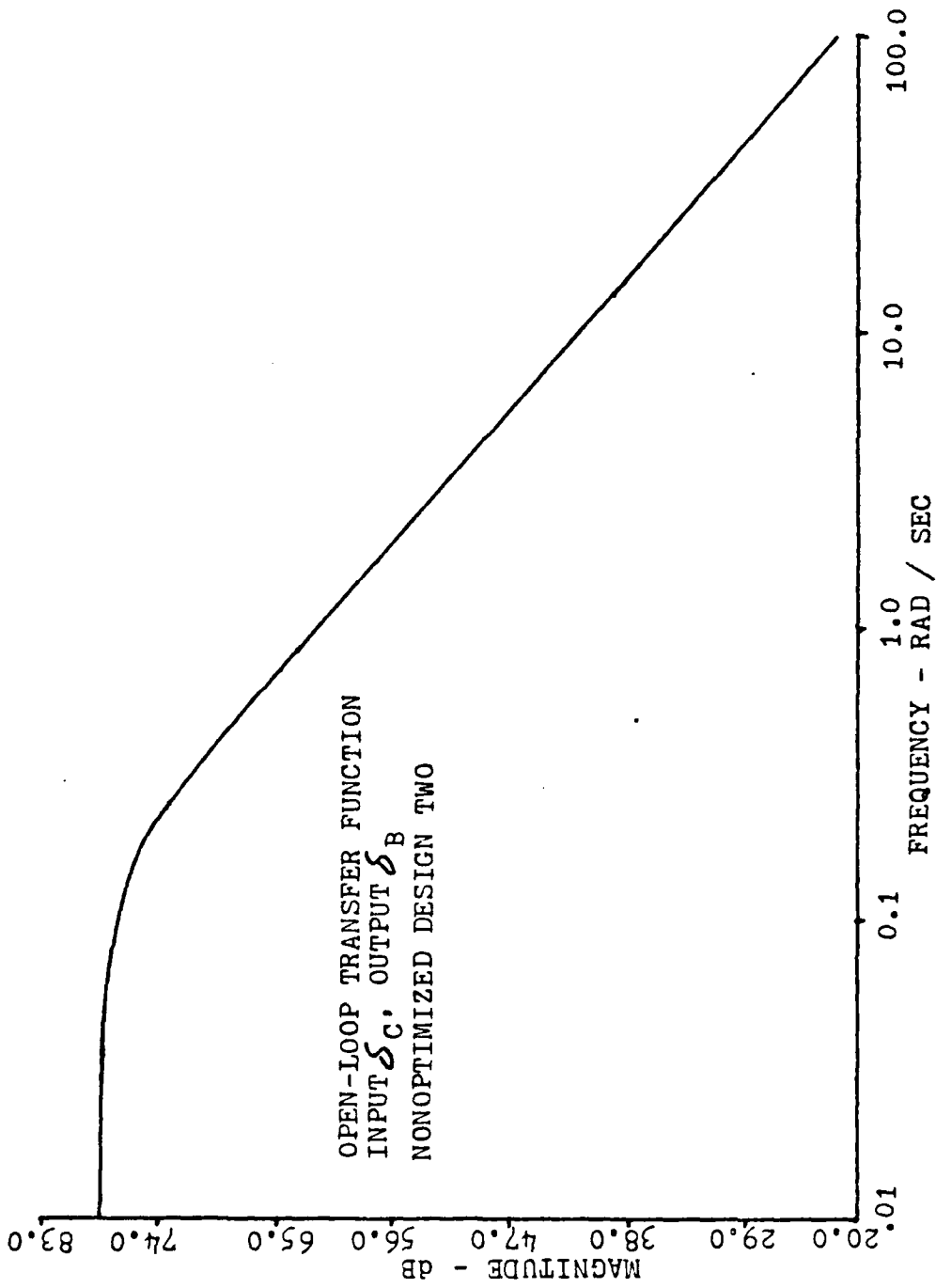


Figure 7.18 Transfer Function $\delta_C - \delta_B$ Design Two, Nonopt..

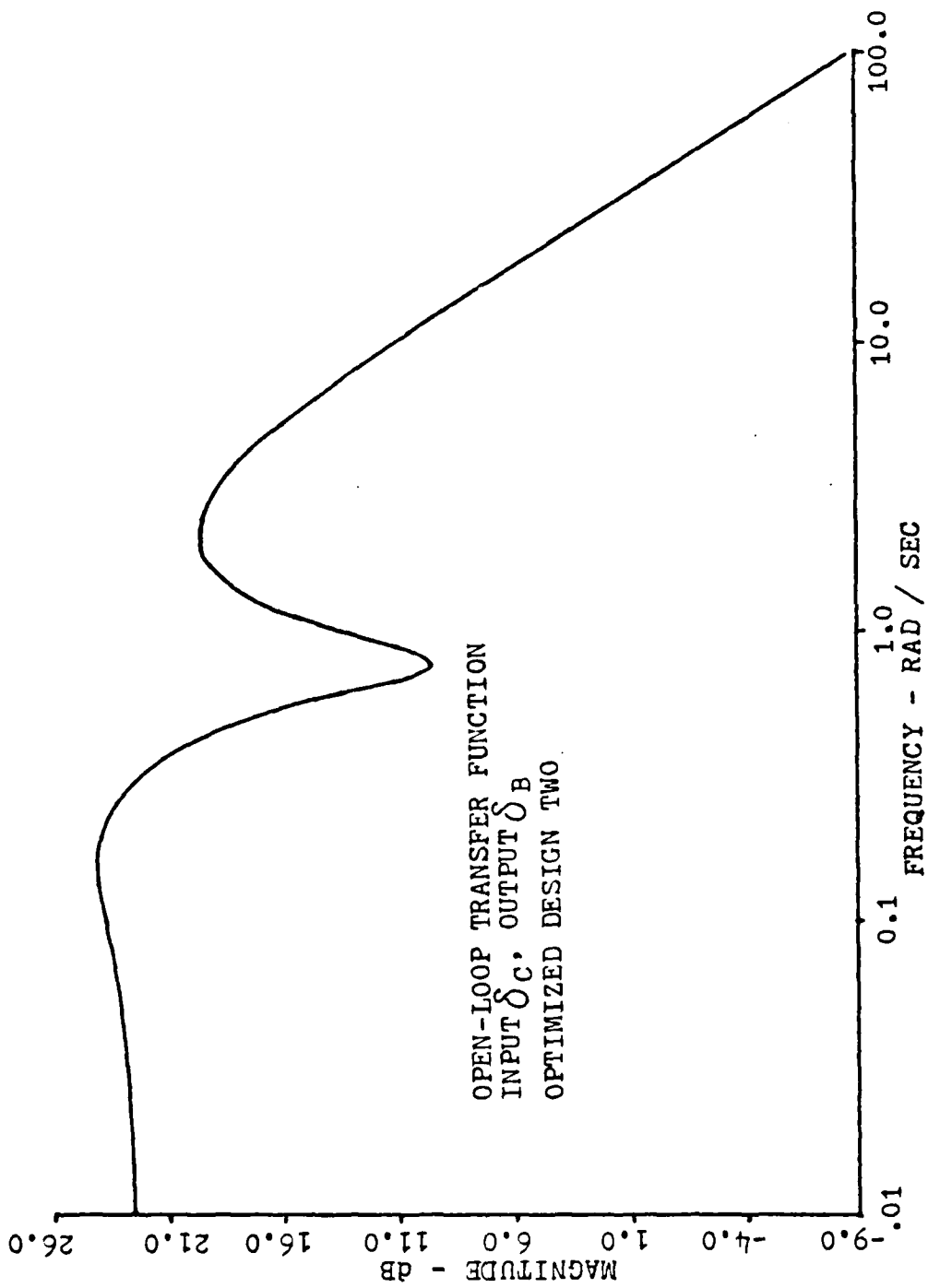


Figure 7.19 Transfer Function $\delta_C - \delta_B$ Design Two, Optimized.

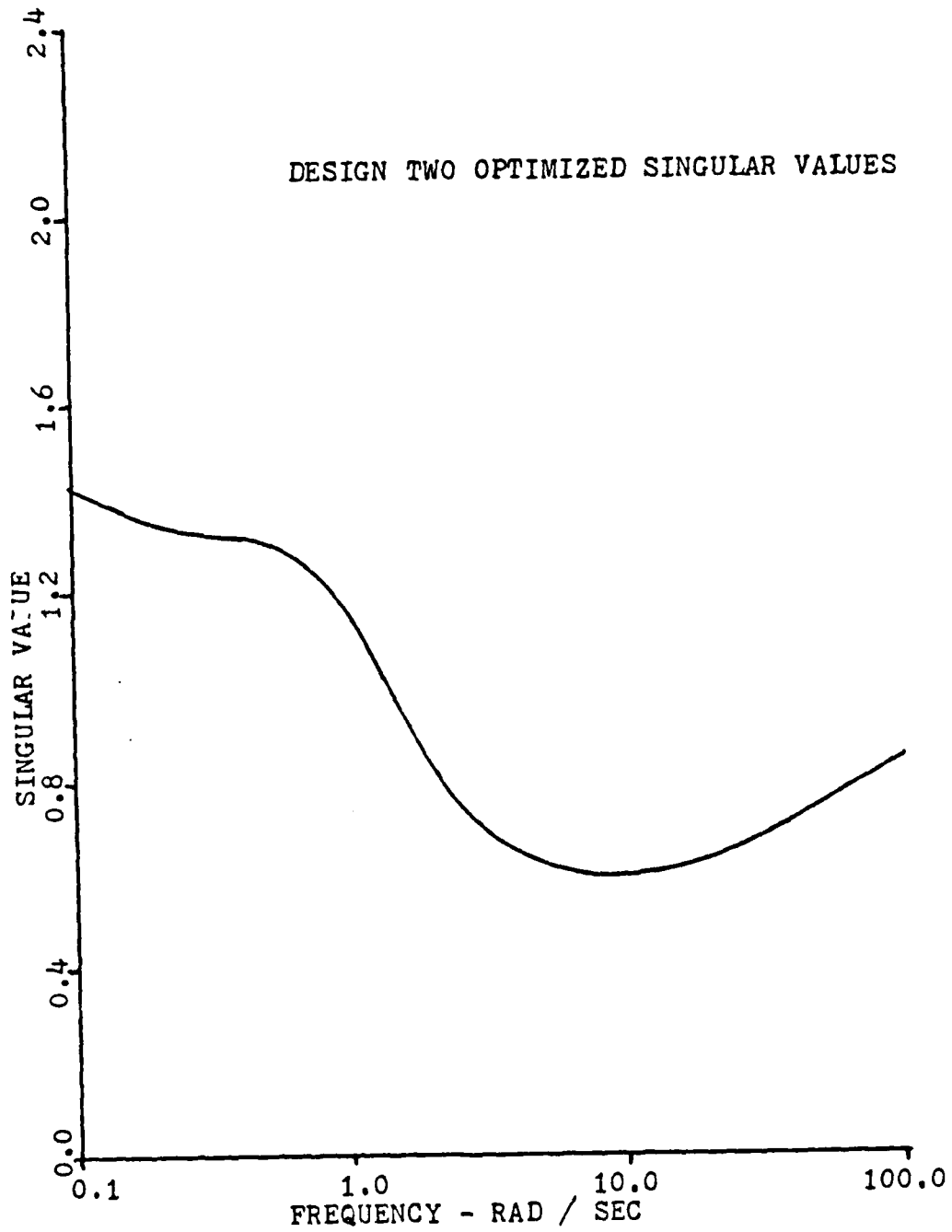


Figure 7.20 Singular Value Plot Design Two.

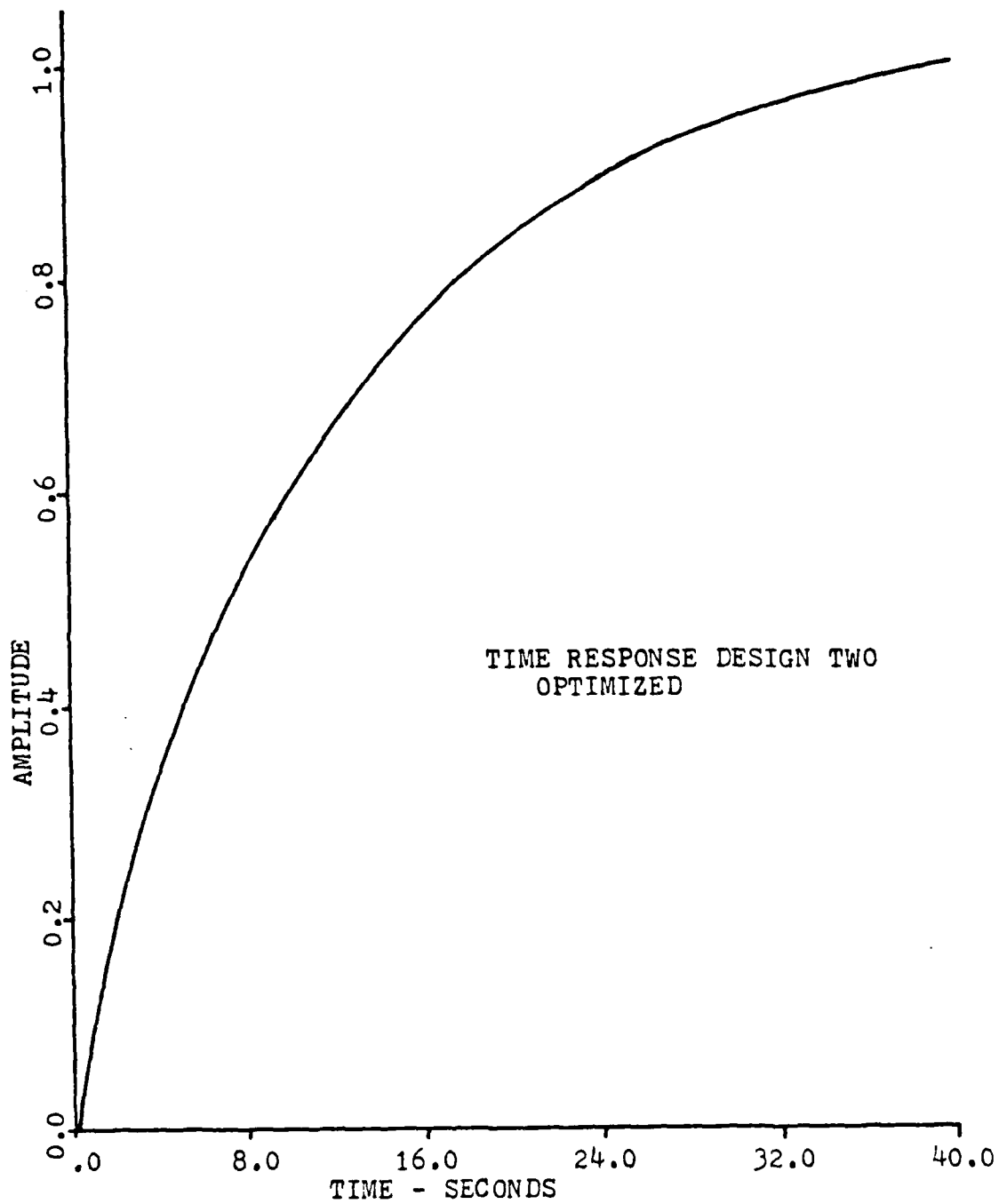


Figure 7.21 Time Response Design Two.

and have been shown to be an alternative indicator of channels that may be affected by cross-feed perturbations. The pole-zero diagrams of the closed-loop transfer functions of the transfer matrix further indicate that zero movement is in a direction that equalizes the gain level of the frequency response curves in the vicinity of the lowest singular values providing a more balanced system response.

VIII. SIMPLE OBSERVER

The pole placement and robustness design procedure can also be used for robustness recovery in observer design.

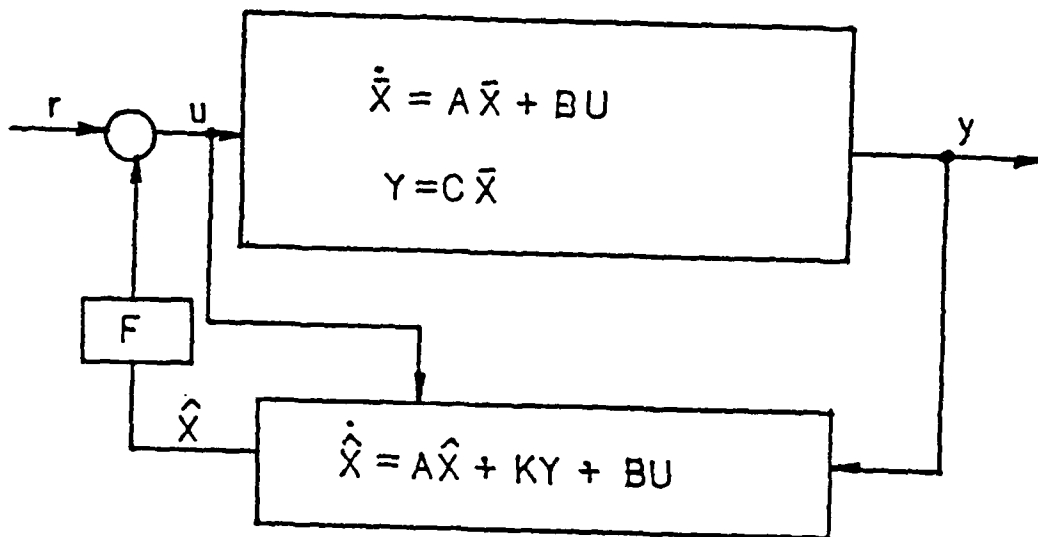


Figure 8.1 Simple Observer.

Given an observer as represented in figure 8.1 it has been shown that the system differential equation may be written as equation 8.1

$$\begin{bmatrix} \dot{\bar{x}} \\ \dot{\hat{x}} \end{bmatrix} = \begin{bmatrix} A & -BF \\ KC & A_c - BF \end{bmatrix} \begin{bmatrix} \bar{x} \\ \hat{x} \end{bmatrix} + \begin{bmatrix} B \\ B \end{bmatrix} r \quad (8.1)$$

$$A_c = A - KC$$

where \bar{x} is the state and \hat{x} is the observer variable, and the solution may be separated to independent solutions for the feedback gains and the observer gains. This separation allows the use of the feedback gains to set the pole

locations and then a second optimization run with set feedback gains so that the observer gains may be computed to adjust the system robustness level. The observer pole location could also be placed using the observer gains, K . In the currently implementation of the pole placement and robustness design routine the observer poles are simply restricted to areas of the left half plane.

In this chapter a simple stable observer system will be analyzed based on [Ref. 17]. Given the system, equation 8.2,

$$\begin{aligned} \dot{\underline{x}} &= \begin{bmatrix} 0 & 1 \\ -3 & -4 \end{bmatrix} \underline{x} + \begin{bmatrix} 0 \\ 1 \end{bmatrix} u + \begin{bmatrix} 35 \\ -61 \end{bmatrix} \underline{v} \\ y &= \begin{bmatrix} 2 & 1 \end{bmatrix} \underline{x} + \eta \end{aligned} \quad (8.2)$$

where $E(\underline{v}) = E(\eta) = 0$ and $E(\underline{v}(t)\underline{v}(\tau)) = E(\eta(t)\eta(\tau)) = \delta(t-\tau)$ with the feedback law of equation 8.3

$$u = -(50 \ 10) \underline{x} + 50r \quad (8.3)$$

An analysis has been done to compare results of the numerical optimization procedure with results presented in [Ref. 17]. The results for an optimal regulator design using quadratic cost criteria as stated in equation 8.4 are given in table 5

$$J = \int (x^T H^T H x + u^2) dt \quad (8.4)$$

with $H = 4\sqrt{5} \ (\sqrt{35} \ 1)$

Figure 8.2 shows a Nyquist plot of the full state regulator, the optimal filter and a fast filter. The full state design had poles at $s = -7.0 \pm j 2.0$ and feedback gains of 50 and 10. The optimal filter as shown in table 5 had poles of $-7.0 \pm j 2.0$ with gain and phase margins of -6.75 db and ± 15 degrees. The optimum filter gains were 30 and -50. Using a faster

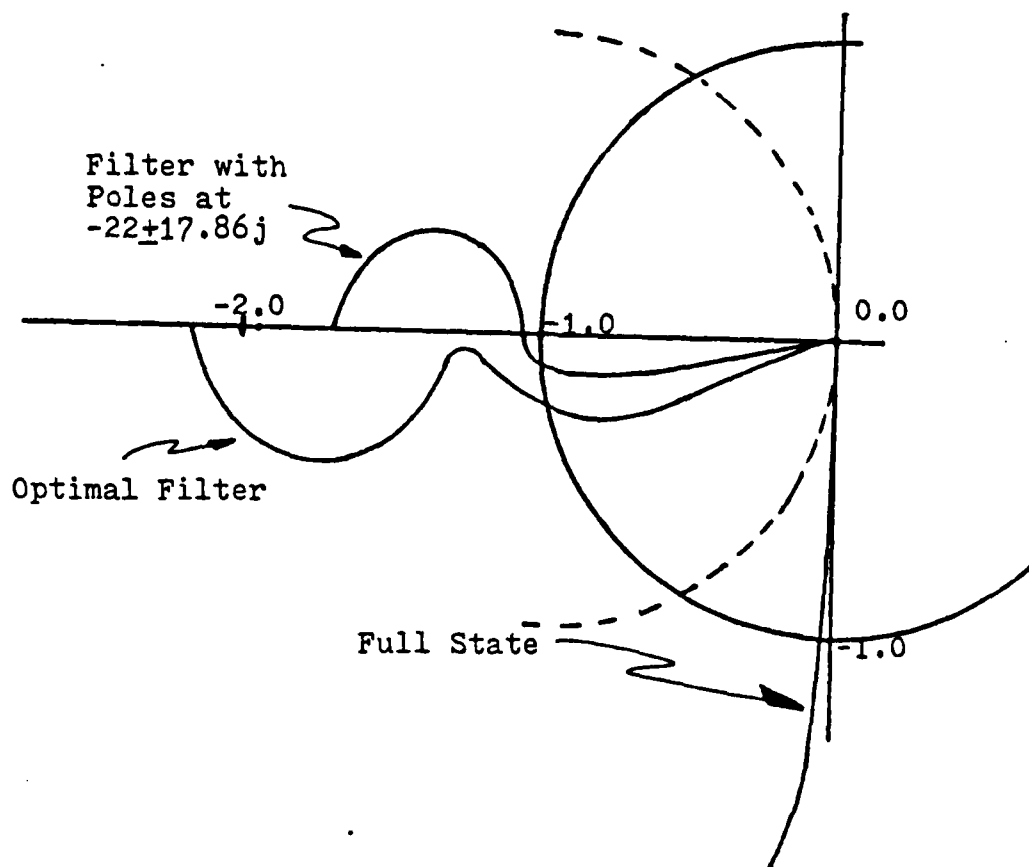


Figure 8.2 Nyquist Plot.

filter also gives poor gain and phase margins. The gain margins are on the order of -0.98 while the phase margin is less than 10 degrees. The bandwidth also increased from 12 to 40 rad/sec. A recovery procedure based on a modification to the process noise matrix [Ref. 17] may be applied to the problem. This procedure can recover a large amount of the robustness that was lost with the observer addition. Figure 8.3 shows data obtained for several trials of the fictitious noise procedure. The gain, phase margin and other parameters may be found in table 5.

TABLE 5
Observer Parameter Data

	FILTER POLES	GAIN MARGIN db	PHASE MARGIN deg	ERROR COVARIANCE $E\{(x-\hat{x})(x-\hat{x})^T\}$		STATE COVARIANCE $E\{xx^T\}$		FILTER GAIN
Optimal LQG Design	-7±2j	- 6.75	15	97	-163	221	-613	30
				-163	277	-613	2070	-60
Fast Filter Adjust- ment Procedure	-22±17.9j	- .98	10	6280	-12200	130	-613	720
				-12200	23800	-613	8520	-1400
Fictitious Noise Adjustment Procedure $q^2 = 100$	-4.3	- 7.73	19	107	-184	236	-613	26.8
	-13.1			-184	319	-613	1810	-40.2
$q^2 = 500$	-2.9	-10.9	33	163	-301	268	-613	20.4
	-24			-301	664	-613	1500	-17.7
$q^2 = 10^3$	-2.5	-13.9	42	204	-385	285	-613	16.7
	-33			-385	743	-613	1360	-1.9
$q^2 = 10^6$	-2.1	-37	74	290	-570	317	-613	6.9
	-100			-570	1170	-613	1200	84.6

POPLAR CASE I 1.00018 GM=-5.5 dB
 -2.02742 PM=117 deg

POPLAR CASE II 18.22148 GM=-19 dB
 32.59476 PM=58 deg

The singular values of the state feedback and optimal observer systems were computed for comparison with results produced using the pole placement and robustness design recovery procedure. Figure 8.4 indicates a loss in robustness represented by the observer singular values. Lower singular values are less robust. For this single-input single-output observer the Nyquist diagram will be used to define gain and phase margins. Since a singular value of 1.0 is indicative of a linear quadratic level of gain and phase margin, i.e. GM=-6 db, and PM=±60 degrees, this was chosen

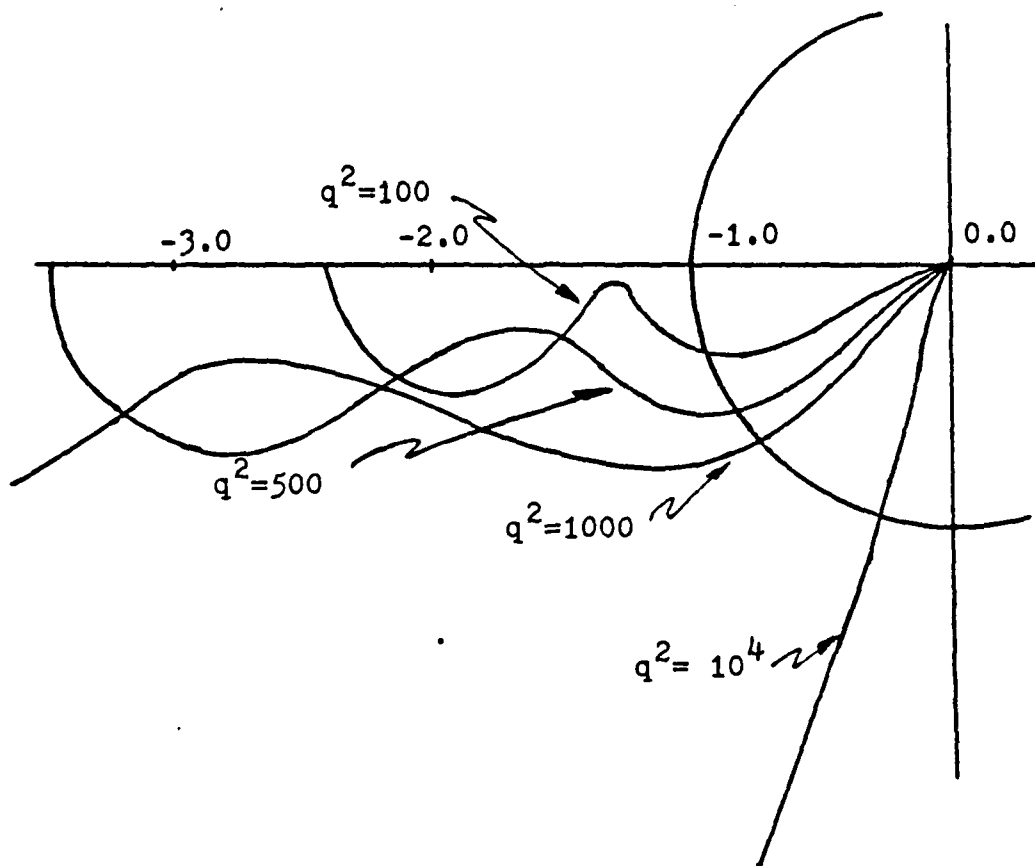


Figure 8.3 Nyquist Plot for Robustness Recovery.

as the design level. The pole placement and robustness routine was used to recover robustness while setting the pole placement at the state feedback pole locations of $-7 \pm j2$. The minimum input singular value level was set at 1.0. The pole placement and robustness routine was also set to place the observer poles anywhere between -100 and -2 that would provide robust design. The plant poles were placed at $-7.05 \pm j 1.82$. The feedback gains for this run

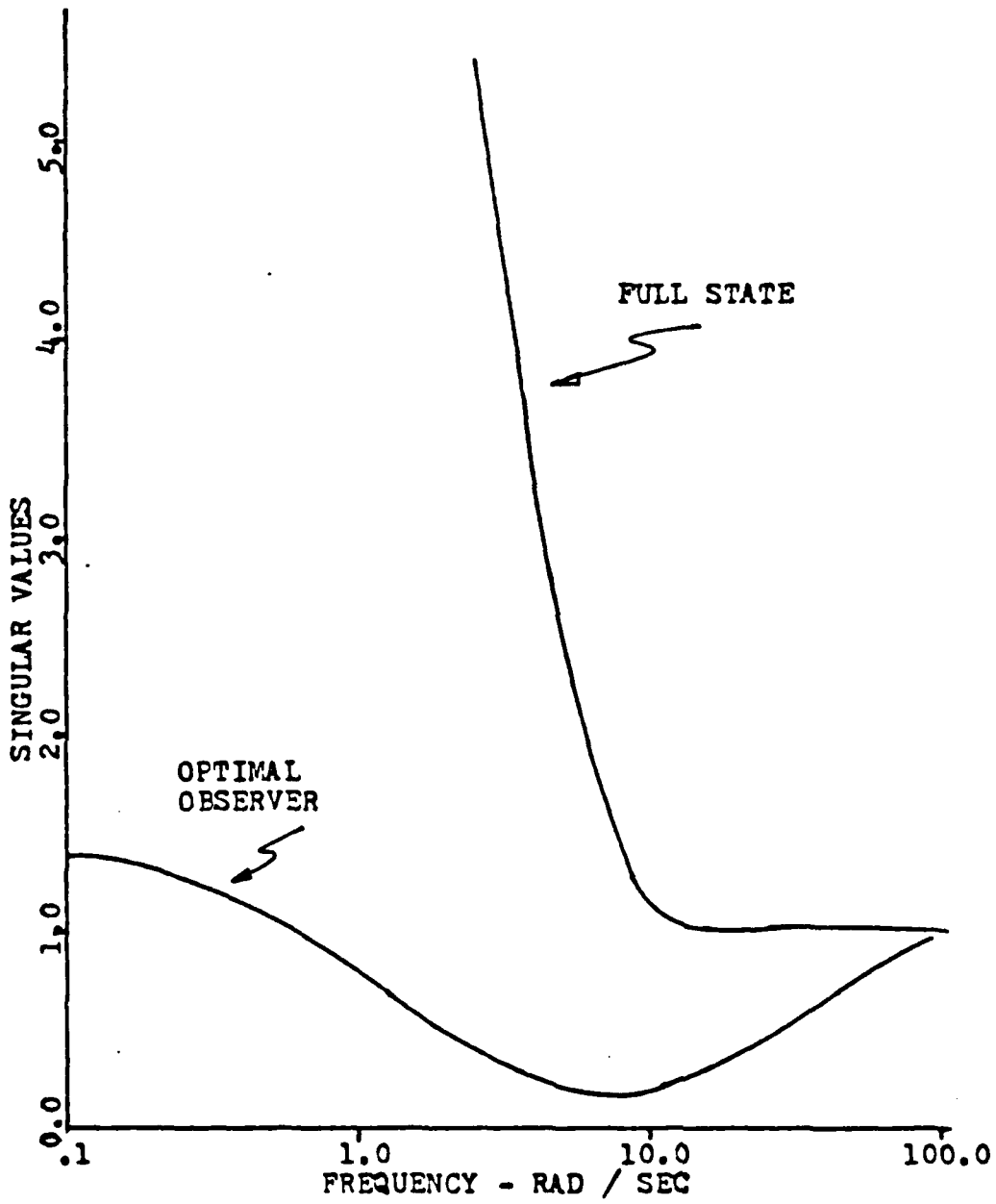


Figure 8.4 Singular Values of Observer System.

were 50 and 10.09. The optimizer output produced a filter with a gains of 1.00018 and -2.02742. The observer pole locations were $-1.99 \pm j .001$, very near the plant zero location. A significant change was produced in singular values. Figure 8.5 shows all singular value curves plotted together. The optimizer solution for this problem is well above the optimal filter curve at low frequency. Figure 8.6 shows the Nyquist plot of the optimizer developed design. The system has a gain margin of -6 db and a phase margin of 117 degrees. The most significant differences between the two designs being that the observer poles are close to the plant zero locations and the filter gains are much lower for the optimizer solution.

Using the OPTSYS program with the pole placement and robustness routine computed gains as the design parameters the data for the observer filter was computed. The error covariance matrix was found to be

$$\begin{array}{cc} 306.5 & -456.5 \\ -456.5 & 700.1 \end{array}$$

These values compare favorably with the trends established in table 5. The last comparison of the pole placement and robustness design recovery procedure was an analysis of the time response curves. Figure 8.7 shows the comparison plot. The design obtained using the pole placement and robustness routine did not degrade system performance.

One additional analysis was conducted that set the desired design parameters slightly differently. In this run the pole placement and robustness routine was set to place the observer poles between -10 and -100. The pole placement and robustness routine was unable to totally satisfy this requirement. It violated one of the constraints and moved the larger observer pole to -2.25 which is near the optimum pole location and also the high q^2 values of the fictitious noise procedure. The smaller pole was moved out to -70.8

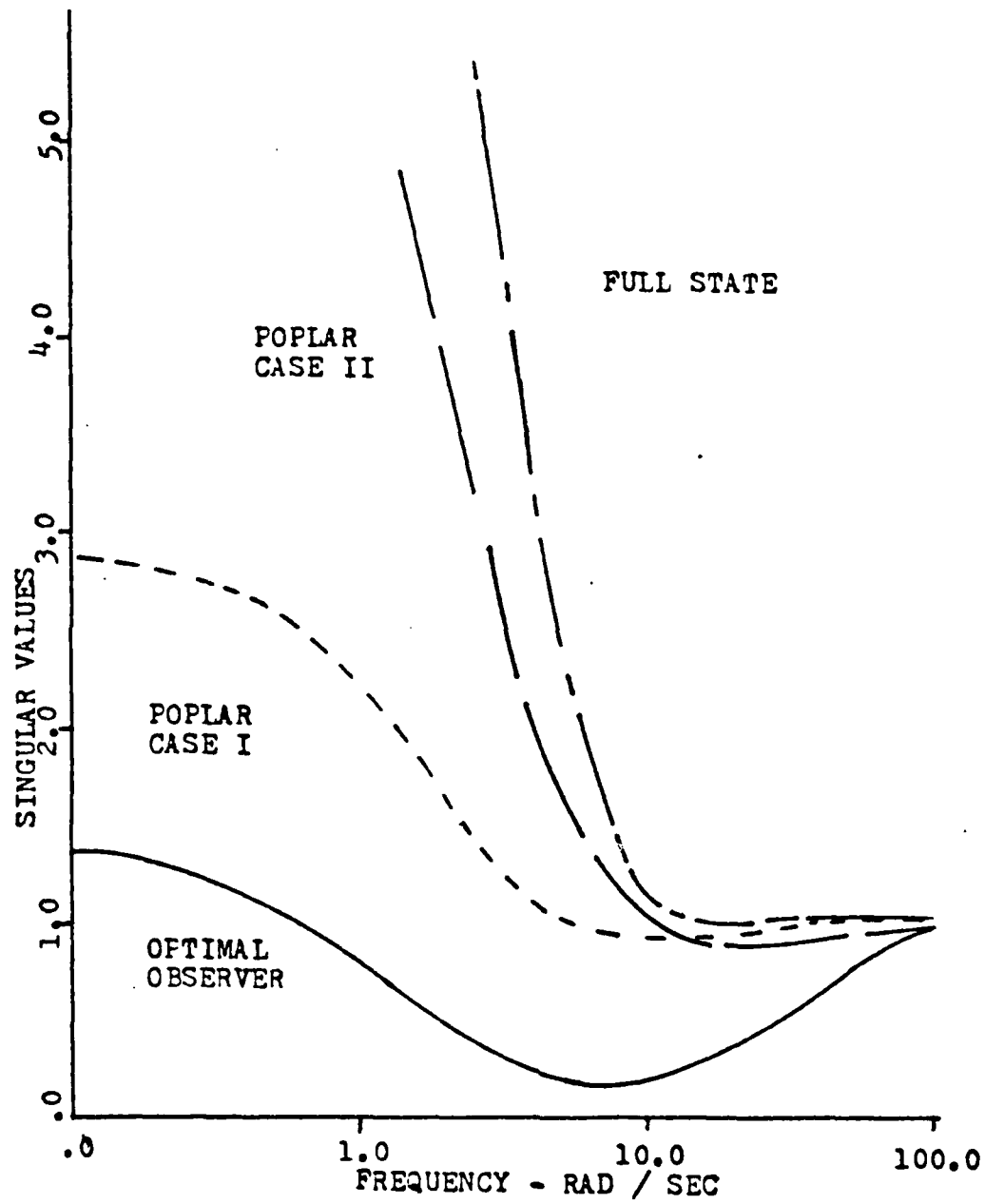


Figure 8.5 Singular Value Comparison Plot.

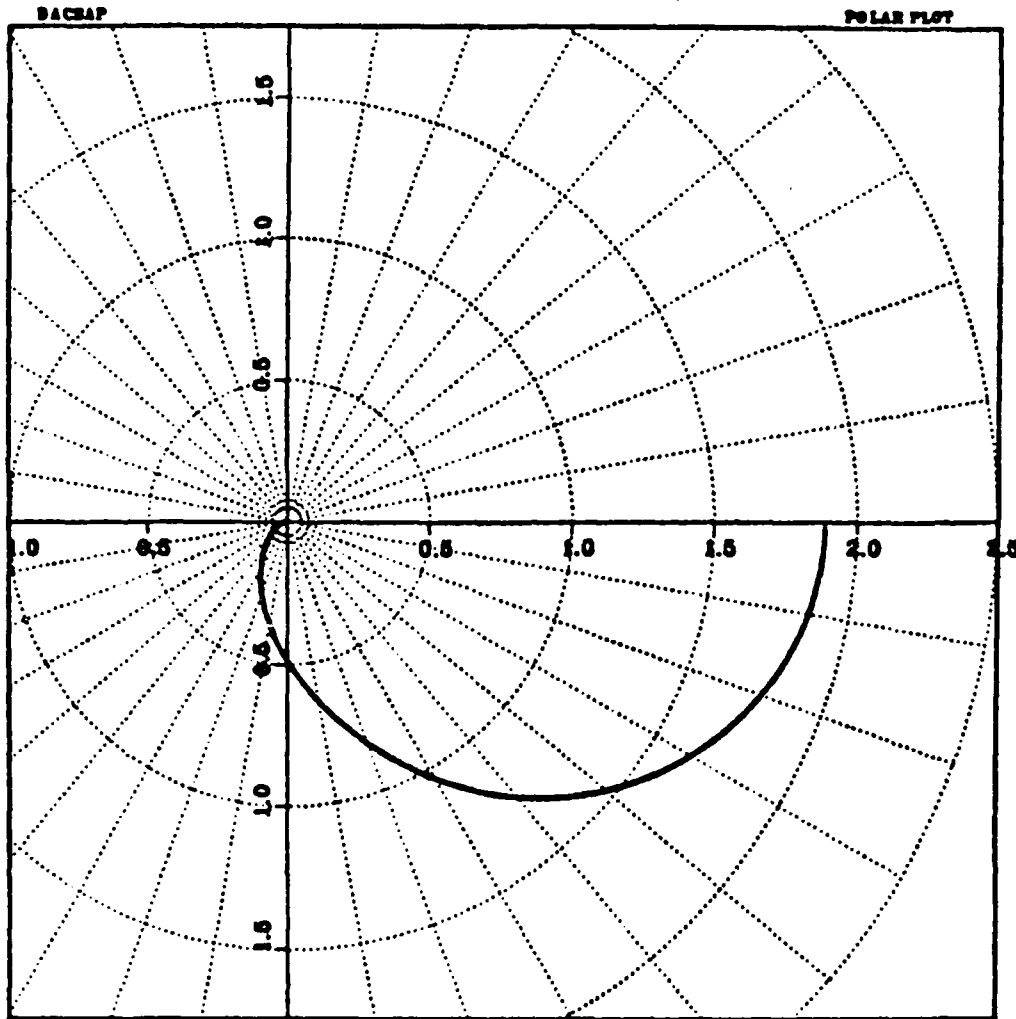


Figure 8.6 Nyquist for Computed Robustness Recovery.

which corresponds to the same level of pole movement found when g^2 becomes large. The singular value levels were raised significantly as shown in figure 8.5. The state and error covariance matrices were of the same order as the matrices found in table 5. This design has a phase margin of 58 degrees. The gain margin was about -19 db. Even though some of the constraint conditions on the design were not met the design demonstrates excellent robustness recovery.

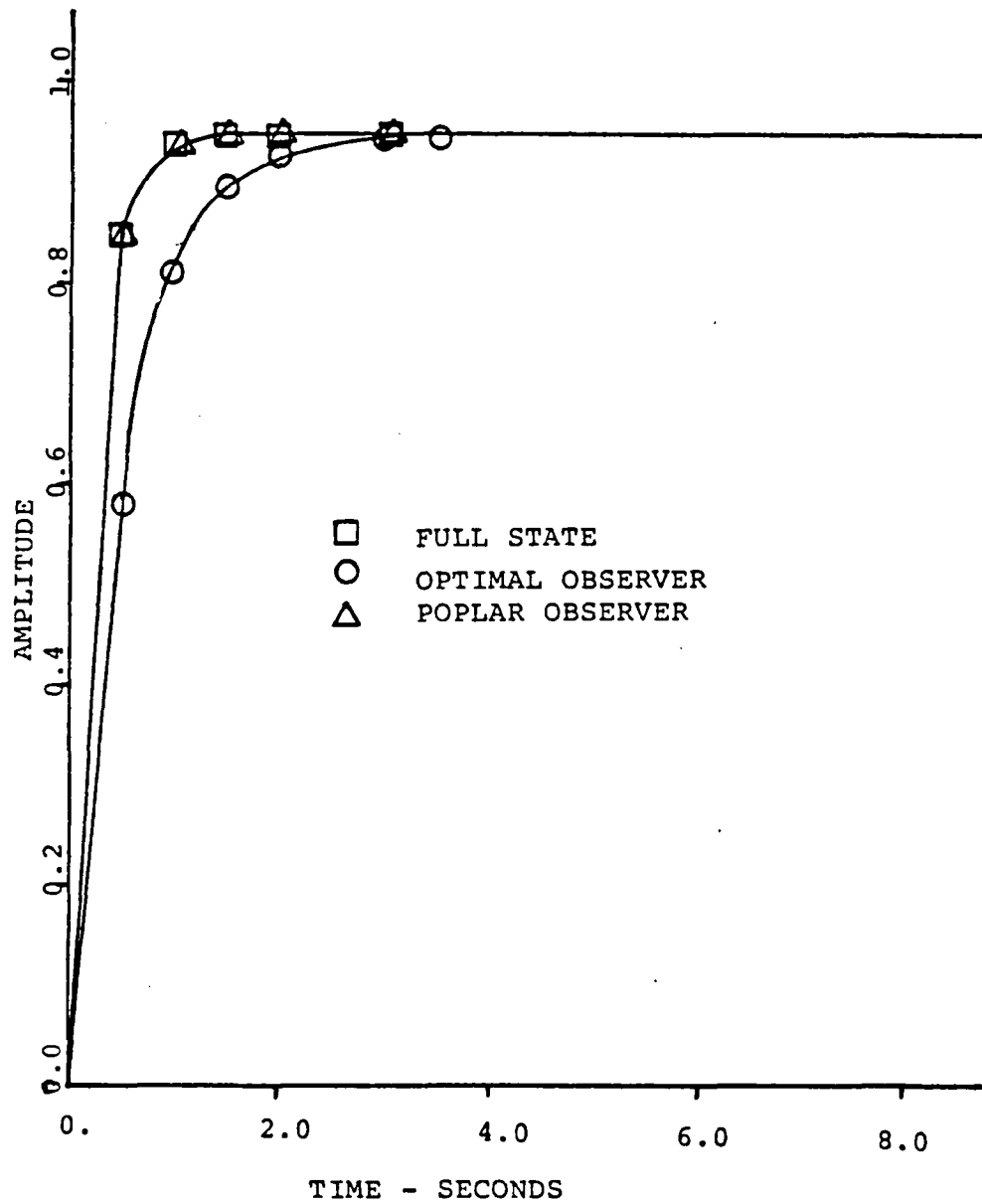


Figure 8.7 Time Response Plot for Simple Observer.

The pole placement and robustness design routine has produced a robust design for this observer based system. This design is obtained by using a numerical optimization to directly manipulate the feedback and filter gains. Modification of the IQ functional equation as done in the fictitious noise procedure is not required. The pole placement and robustness routine solution for this problem has lower gains than those found using the fictitious noise adjustment. The routine provides a good, direct methodology for selecting the feedback and filter gains for a robust observer design with excellent performance.

IX. ROBUST OBSERVER DESIGN

This chapter will be devoted to a short discussion of the robustness recovery of a fourth order observer based controller. The problem is a helicopter problem, [Ref. 6]. In this case the helicopter model is that of the longitudinal control loop of a CH-47. The nominal model is taken to be the system of equations 9.1 and 9.2 for an aircraft speed of forty knots.

$$\dot{\underline{x}} = \begin{bmatrix} -0.02 & 0.005 & 2.4 & -32. \\ -0.14 & 0.44 & -1.3 & -30. \\ 0. & 0.018 & -1.6 & 1.2 \\ 0. & 0. & 1. & 0. \end{bmatrix} \underline{x} + \begin{bmatrix} 0.14 & -.12 \\ .36 & -8.6 \\ .35 & .009 \\ 0. & 0. \end{bmatrix} \underline{u} \quad (9.1)$$

$$\underline{y} = \begin{bmatrix} 0 & 1 & 0 & 0 \\ 0 & 0 & 0 & 57.3 \end{bmatrix} \underline{x} \quad (9.2)$$

In this problem the controller is formulated as in figure 9.1 which leads to an open-loop transfer function of the form of equation 9.3

$$K(s)G(s) = F(sI - A + BF + KC)^{-1} KC(sI - A)^{-1} B \quad (9.3)$$

The pole placement and robustness recovery procedure was applied to this problem.

First, the standard full state feedback design was carried out using the Naval Postgraduate version of OPTSYS. This design produced excellent singular value output for the return difference as shown in figure 9.2. The lowest singular value being essentially 1, corresponding to a LQ design with -6 db to ∞ gain margin and 60 degrees of phase margin. The time response of the system was good as shown in

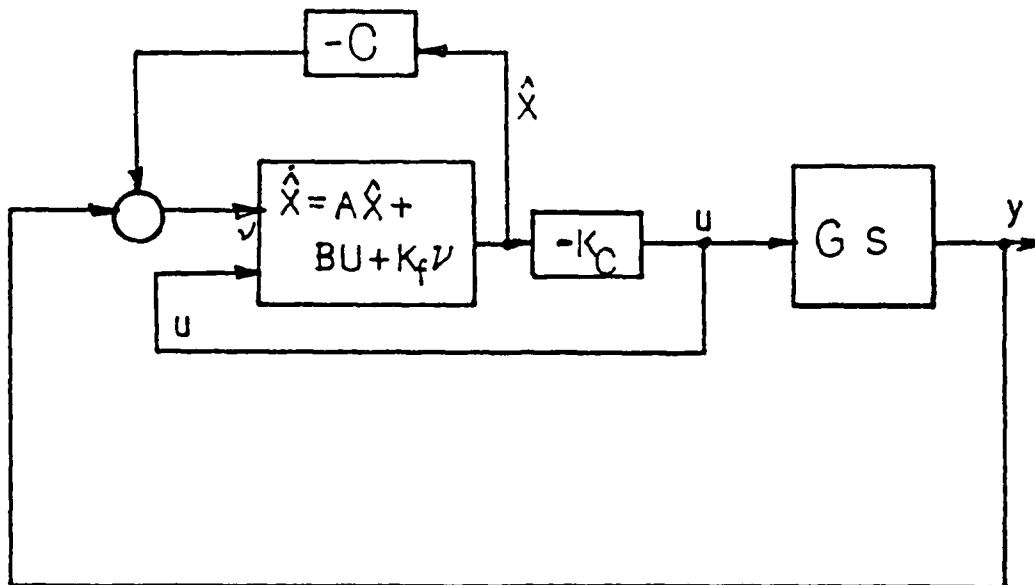


Figure 9.1 Observer Based Controller.

figure 9.3, reaching steady-state in about four seconds with only a slight overshoot. Since the characteristics for this system are acceptable no further design iteration was carried out. The full state feedback became the baseline design. Assuming that full state feedback was not available and only two measurements could be produced an observer was developed to control the two measured outputs, vertical velocity and pitch attitude. Using the measurement matrix of equation 9.2, OPTSYS was used to develop an optimal observer system for this problem. The singular values of the return difference matrix and the time response were plotted for comparison to the full state design. These are shown in figures 9.2 and 9.3 respectively. Note that the singular value of the return difference matrix is as low as 0.16 at 4 rad/sec. This equates to a gain margin of -1 db to 1 db and less than 10 degrees phase margin. The time response is

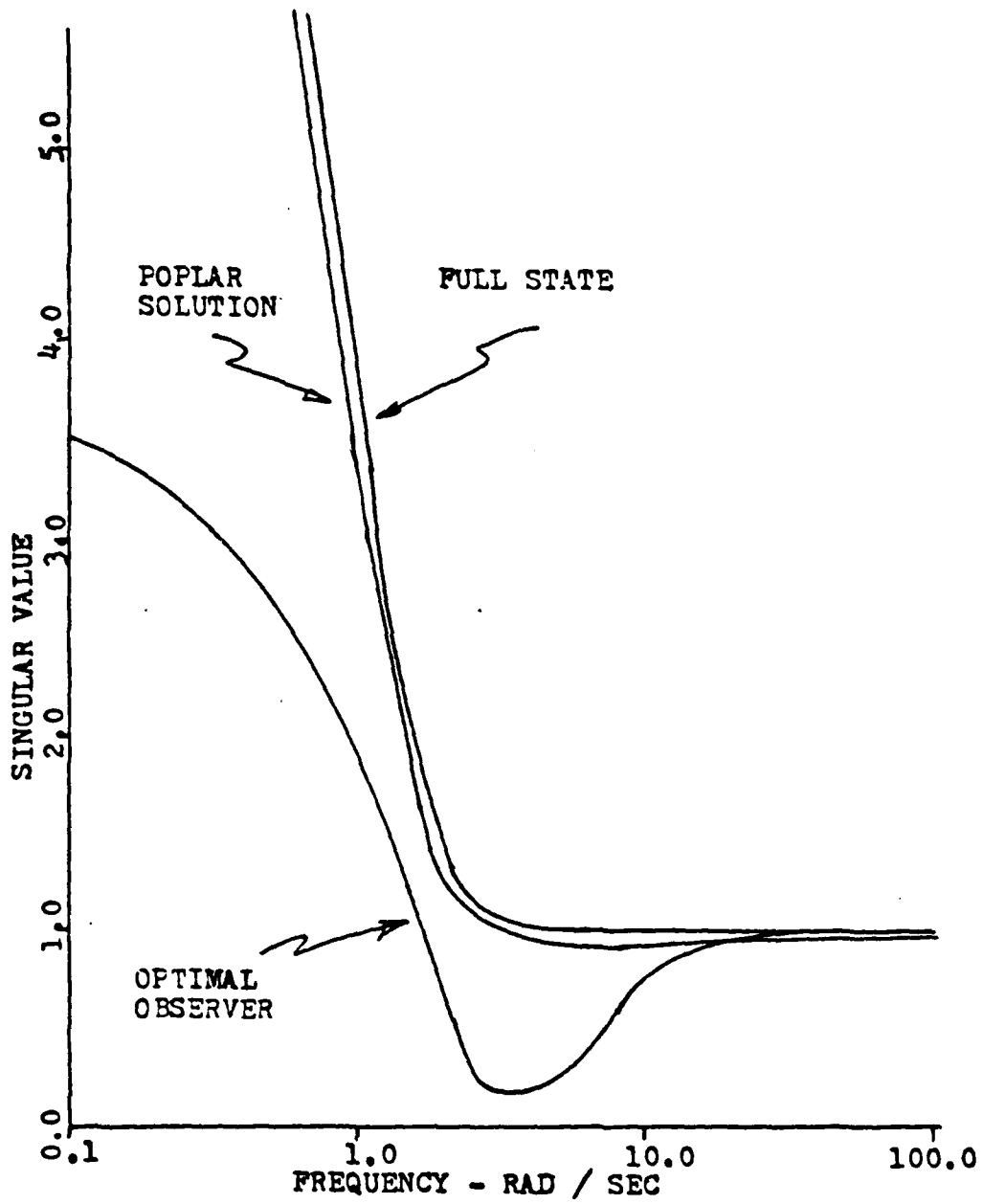


Figure 9.2 Singular Value Plot of Observer Results.

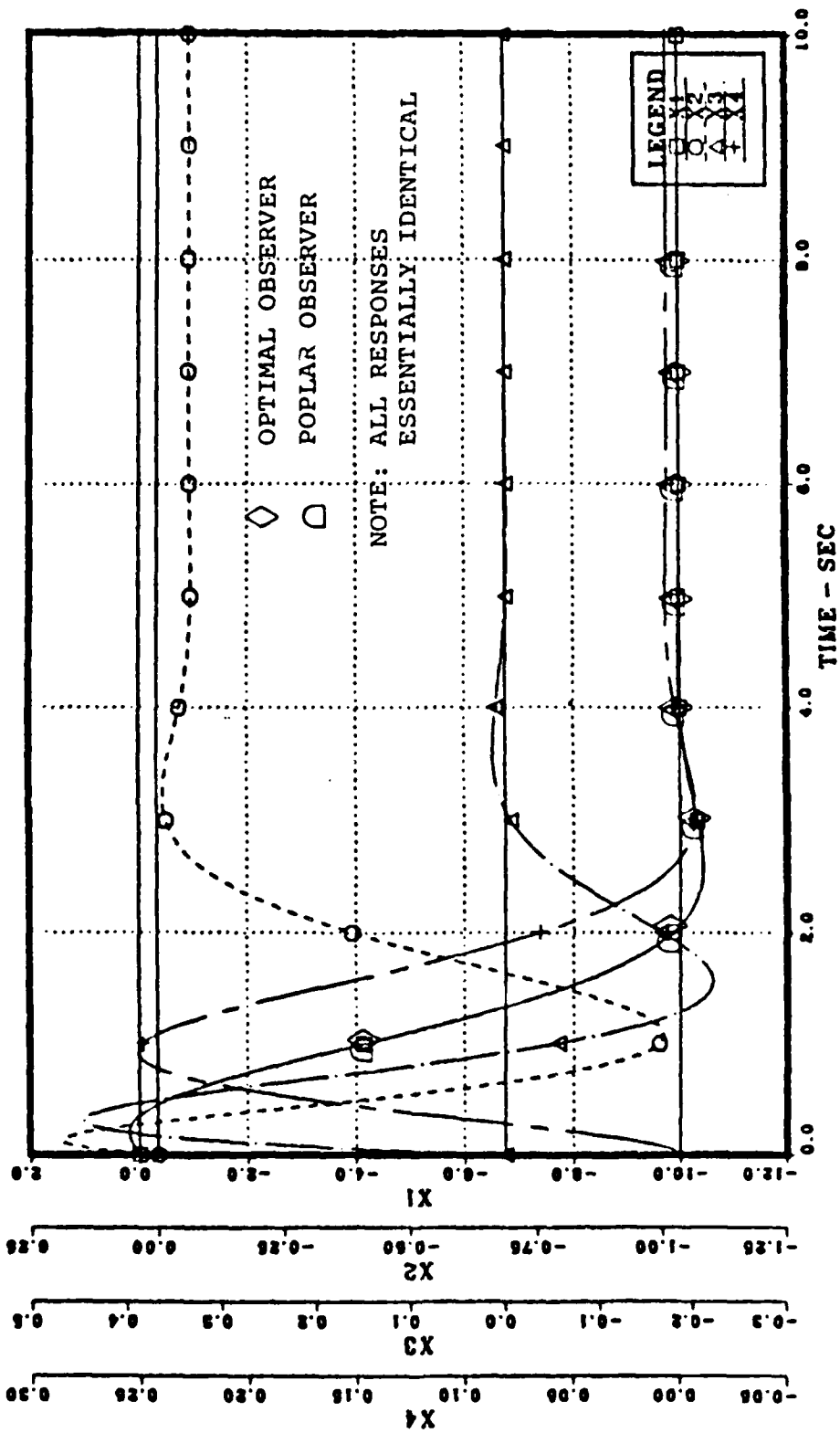


Figure 9.3 Time Response for Observer System.

plotted in figure 9.3. The steady-state was reached for the velocity after a slight overshoot in about four seconds.

As the final step in the analysis the pole placement and robustness routine was employed to recover robustness of the observer based system. The pole placement and robustness routine was first used to set the poles at approximately the same location as the poles of the LQ regulator. These were assumed to be the desired pole locations. The pole placement and robustness routine was then used to vary the filter gains, K , until the desired level of robustness was reached. The desired singular value level chosen was 1.0 which corresponds to -6 db to ∞ db gain margin and 60 degrees of phase margin. Figure 9.2 shows that the pole placement and robustness procedure failed to totally recover the robustness level to 1.0. The minimum singular value reached was only 0.936. This singular value equates to a gain margin of -5.0 db to ∞ and a phase margin of 55 degrees. While this is slightly less than the design objective, it is far superior to the optimal observer design discussed in the previous paragraphs. This recovery was made by making an optimization run, finding the filter gains with near zero values and freezing these values at zero. This reduced the number of design variables the pole placement and robustness routine was required to manipulate in a second optimization run and gave a higher robustness solution.

This analysis and the second order observer analysis presented earlier clearly indicate that it is possible to use the pole placement and robustness procedure and separation principle to develop a robustness recovery procedure. The pole placement and robustness routine provides robustness recovery by direct modification of the feedback and filter gains. This procedure requires no modification to LQ cost functionals or other parameters as done in the fictitious noise adjustment method commonly used for robustness

recovery. By providing direct gain adjustment the pole placement and robustness procedure results in a practical design with relatively low observer gains and good performance. The procedure is simple and straight forward with the only difficulty being a requirement to sometimes modify initial starting values or optimizer codes to force the solution toward the desired point.

X. CONCLUSIONS

An effective method of robustness multivariable control design utilizing a numerical optimization based algorithm has been developed. The pole placement and robustness design routine coupled with the Automated Design Synthesis program provides the designer an excellent tool with which to attack the robust design problem.

The pole placement and robustness design routine has demonstrated the capability of providing designs that solve the problems caused by cross-coupling perturbations which reduce robustness in multivariable systems. This design improvement is accomplished by modifying the system feedback gains in such a manner that the gain in channels that are affected by cross-coupling perturbations is equalized with other system gains to reduce this cross-coupling effect. The gain changes are accompanied by zero shifts which also influence the gain distribution and frequency response of the system.

Perturbation problems in multivariable systems have been shown to be detectable by singular value analysis and by using the Bode magnitude diagram of the open-loop transfer functions of the system. In the open loop transfer function large differentials in Bode gains and bandwidths are indicative of problem areas for cross-coupling perturbations. Robustness is obtained by the pole placement and robustness design program by modifying those gains and bandwidths associated with the cross-coupling perturbations thus reducing the amount of energy coupled from the perturbation into other channels. An associated zero shift has been observed when these gain modifications take place. This zero shift is in the direction of poles that are located in the vicinity

of the frequency of the minimum singular value and tends to equalize the frequency response curve gains in this region.

The use of numerical optimization to recover robustness in observer based designs was demonstrated. The pole placement and robustness routine was applied to problems previously solved using the fictitious noise procedure for robustness recovery. The direct manipulation of feedback and filter gains by the pole placement and robustness routine provided a highly robust design with relatively low filter gains. The problem of robustness recovery in filter-observer designs has been solved in a straight forward and highly practical manner.


```

C      READ (1,760) IGRAD,NDV,NCON,ISTRAT,IOPT,IONED,IPRINT,INFO
C      INPUT THE PARAMETER VALUES AND THE MATRICES A,B,C,F
C      READ (1,770) NROWA,NCCLA,NROWB,NCOLE,NROWC,NCOLC,NROWF,NCOLF,NMU
C      CALL READ (A,NROWA,NCOLA)
C      CALL READ (E,NROWB,NCOLB)
C      CALL READ (C,NROWC,NCOLC)
C      CALL READ (F,NROWF,NCOLF)
C      SPECIFY THE DESIGN VARIABLES WITHIN THE F MATRIX
C      DO 10 J=1,NROWF
C      READ (1,780) (IF(J,K),K=1,NCOLF)
C      SET THE DESIGN VARIABLE BOUNDS
C      DO 20 J=1,NCV
C      READ (1,790) VLB(J),VUB(J)
C      FORMULATE THE DESIGN VARIABLE X FROM THE INPUT GUESS FOR F
C      DO 30 J=1,NROWF
C      DO 40 K=1,NCOLF
C      IF (IF(J,K).EQ.0) GC TC 30
C      KK=IF(J,K)
C      X(KK)=F(J,K)
C      CONTINUE
C      CONTINUE
C      CONTINUE
C      READ THE DESIRED EIGENVALUES AS REAL(X)+REAL(Y)*I
C      DO 60 I=1,NMU
C      READ (1,860) REALMU(I),IMAGMU(I)
C      DO 70 J=1,NMU
C      MU(I)=CPLX(REALMU(I),IMAGMU(I))
C      CONTINUE
C      SCRT THE INPUT EIGENVALUESUSING IMSL ROUTINE VSRTR
C      DO 80 I=1,NMU
C      IR(I)=I
C      CALL VSRTR (REALMU,NMU,IR)
C      DO 90 J=1,NMU
C      K=IR(J)
C      OMCU(J)=MU(K)
C      JJ=NMU-1

```

```

CCNO2410
CCNO2420
CCNO2430
CCNO2440
CCNO2450
CCNO2460
CCNO2470
CCNO2480
CCNO2490
CCNO2500
CCNO2510
CCNO2520
CCNO2530
CCNO2540
CCNO2550
CCNO2560
CCNO2570
CCNO2580
CCNO2590
CCNO2600
CCNO2610
CCNO2620
CCNO2630
CCNO2640
CCNO2650
CCNO2660
CCNO2670
CCNO2680
CCNO2690
CCNO2700
CCNO2710
CCNO2720
CCNO2730
CCNO2740
CCNO2750
CCNO2760
CCNO2770
CCNO2780
CCNO2790
CCNO2800
CCNO2810
CCNO2820
CCNO2830
CCNO2840
CCNO2850
CCNO2860
CCNO2870
CCNO2880

```


CLN04450
 CLN04460
 CLN04470
 CLN04480
 CLN04490
 CLN04500
 CLN04510
 CLN04520
 CLN04530
 CLN04540
 CLN04550
 CLN04560
 CLN04570
 CLN04580
 CLN04590
 CLN04009
 CLN04010
 CLN04020
 CLN04030
 CLN04040
 CLN04050
 CLN04060
 CLN04070
 CLN04080
 CLN04090
 CLN04100
 CLN04110
 CLN04120
 CLN04130
 CLN04140
 CLN04150
 CLN04160
 CLN04170
 CLN04180
 CLN04190
 CLN04200
 CLN04210
 CLN04220
 CLN04230
 CLN04240
 CLN04250
 CLN04260
 CLN04270
 CLN04280
 CLN04290
 CLN04300
 CLN04310
 CLN04320

```

210 K=KEY(J) EIG(K)
220 CEIG(J)=EIG(K)
      DO 210 KK=1,NROWA
      OZ(KK,J)=Z(KK,K)
      CONTINUE
      JJ=ACCLA-1
      DO 250 J=1,CEIG(J)
      IF (REAL(CEIG(J)),NE,REAL(CEIG(J+1))) GC TO 240
      IF (AIMAG(CEIG(J)),LT,AIMAG(CEIG(J+1))) GO TO 240
      TEMPI=CEIG(J)
      TEMPI(J+1)=TEMP1
      DO 230 KK=1,NROWA
      TEMP2=CZ(KK,J)
      OZ(KK,J+1)=TEMP2
      CONTINUE
      CONTINUE
      CONTINUE
      *****
      CALL THE PLANT TRANSFER MATRIX ROUTINE AND FORM THE SYSTEM
      RETURN *****
      *****
      DEL=DELH
      NI=NI
      NC=1
      h=h
      SMINAI=C
      SMINMI=C
      SMINAC=C
      SMINMO=C
      SMAXAI=C
      SMAXMI=C
      SMAXAO=C
      SMAXMC=C
      CALL FLANT (PLAN,AX,BX,CX,h,NRCWA,NCLLA,NROMB,NCOLB,NROWC,NCOLC)
      CALL CPATML (FX,PLAN,NROWF,NCOLF,NCCLB,FXPLT)
      CALL CPATML (PLAN,FX,NROWC,NCOLB,NCCLF,PLTFX)
      DO 280 J=1,NROWF
      DO 270 K=1,NCOLB
      XI(J,K)=C.0
      CONTINUE
      DO 290 J=1,NROWF
      XI(J,J)=1.0
      DO 310 J=1,NROWC
  
```


CCNO 4810
 CCNO 4820
 CCNO 4830
 CCNO 4840
 CCNO 4850
 CCNO 4860
 CCNO 4870
 CCNO 4880
 CCNO 4890
 CCNO 4900
 CCNO 4910
 CCNO 4920
 CCNO 4930
 CCNO 4940
 CCNO 4950
 CCNO 4960
 CCNO 4970
 CCNO 4980
 CCNO 4990
 CCNO 5000
 CCNO 5010
 CCNO 5020
 CCNO 5030
 CCNO 5040
 CCNO 5050
 CCNO 5060
 CCNO 5070
 CCNO 5080
 CCNO 5090
 CCNO 5100
 CCNO 5110
 CCNO 5120
 CCNO 5130
 CCNO 5140
 CCNO 5150
 CCNO 5160
 CCNO 5170
 CCNO 5180
 CCNO 5190
 CCNO 5200
 CCNO 5210
 CCNO 5220
 CCNO 5230
 CCNO 5240
 CCNO 5250
 CCNO 5260
 CCNO 5270
 CCNO 5280

```

SVMIX(NC)=SVM1(1)
SVMMO(NC)=SVM0(NRU*NC)
SVMXO(NC)=SVM0(1)
SIGPRC(NC)=SQR T((SIGM1(NC)*SIGM2(NC))
SMINAI=(SMINAI+(AMAX1(0.0;SVMINI-SIGM1(NC)))*2)
SMINAO=(SMINAO+(AMAX1(0.0;SVMINO-SVADM(NC)))*2)
C COMPUTE LOOP FOR ALL DESIRED FREQUENCY BANDWIDTH
C
M=H+DEL
MD=10.0*C*WII
IF (M.LI.MD) GO TO 420
DEL=10.0*DEL
WII=10.0*C*WII
420 NC=NC+1
IF (M.LE.MMAX) GO TO 260
MAXA=NC-1
C
C FROM QUANTITIES TO USE IN THE COST CRITERIA OF OPTIMIZER
SVMIN=SIGM1(1)
DO 430 I=1,PAXN
IF (SIGM1(I).GE.SVMIN) GO TO 430
SVMIN=SIGM1(I)
CONTINUE
CUSTI=0.
DO 440 I=1,MMU
COST=C C I+((REAL(OMU(J))-REAL(CEIG(J)))*2+(AIMAG(OMU(J))-AIMAG(CEIG(J)))*2)
1 CONTINUE
440
C
C THE OBJECTIVE FUNCTION IS INSERTED HERE
OBJ=WT1*COST+WT2/SVMIN
OBJ=WT1*CCSI+WT2*SPINAI+WT3*SMINAO
OBJ=WT2*SMINAI
IF (NCCA.EQ.0) GC TC 460
DO 450 I=1,MMU
IDG(I)=NIDG
R(I)=RJ
R(I)=RJ
1CEIG(I)))*2)
6(I)=SCFI((REAL(CML(J))-REAL(CEIG(J)))*2+(AIMAG(OMU(J))-AIMAG(CEIG(J)))*2)
IF (KCAIPL.GT.0) GC TC 480
GO TO 12C
CONTINUE
450
460
470
C

```

```

C THE GRADIENT COMPUTATION ROUTINE GOES HERE IF NEEDED
C GO TO 125
480 CONTINUE
C
C OLUPT THE COMPUTED FINAL EIGEN VALUES AND VECTORS FROM OPT F'S
C
CALL MULL (F,C,NROWF,NCOLF,NCOLC,FC)
CALL MULL (B,FC,NROWB,NCOLE,NCCLC,BFC)
DO 500 I=1,NROWA
  DO 490 J=1,NCOLA
    AMBFC(I,J)=A(I,J)-BFC(I,J)
  CONTINUE
  IF (KCNTRL.EQ.0) GC TC 510
  WRITE (6,62C)
GO TO 520
  WRITE (6,63C)
CALL EIGRF (AMBFC,NROWA,10,2,EIG,Z,10,MK,IEF)
  WRITE (6,670)
CALL CVECTOR (OEIG,NCOLA)
DO 530 I=1,MAXN
  WRITE (6,64C) OEIG(I)
  WRITE (6,68C)
CALL CWRITE (OZ,NRCWA,NCOLA)
  WRITE (6,690)
CALL WRITE (F,NROWF,NCOLF)
  WRITE (6,650) OBJ
C
C OUTPUT THE OPTIMIZED SINGULAR VALUE DATA
C
  WRITE (6,73C)
  WRITE (6,66C) MAXN
DO 540 I=1,MAXN
  WRITE (6,67C) OMEGA(I),SIGNM1(J),SIGNM2(J),SIGNMX(J),SIGPRG(J)
  WRITE (6,74C) OMEGA(J),SIGNM1(J),SIGNM2(J),SIGNMX(J),SIGPRG(J)
DO 550 I=1,MAXN
  WRITE (6,69C) SVADPC(J),SVADX(J),SVMIP(J),SVMIX(J),SVMMD(J),SVMXD
  1(J)
550 WRITE (6,70C) OMEGA(J),SVADMO(J),SVADXC(J),SVMIM(J),SVMIX(J),SVMMD
  1(J),SVMXD(J)
  IF (KCNTRL.EQ.0.OR.KONTRL.GT.1) GO TO 560
  GO TO 12C
560 STCP
C *****
C FORMAT STATEMENTS
C *****
570 FORMAT (3F10.0)

```

```

CCNO 5290
CCNO 5300
CCNO 5310
CCNO 5320
CCNO 5330
CCNO 5340
CCNO 5350
CCNO 5360
CCNO 5370
CCNO 5380
CCNO 5390
CCNO 5400
CCNO 5410
CCNO 5420
CCNO 5430
CCNO 5440
CCNO 5450
CCNO 5460
CCNO 5470
CCNO 5480
CCNO 5490
CCNO 5500
CCNO 5510
CCNO 5520
CCNO 5530
CCNO 5540
CCNO 5550
CCNO 5560
CCNO 5570
CCNO 5580
CCNO 5590
CCNO 5600
CCNO 5610
CCNO 5620
CCNO 5630
CCNO 5640
CCNO 5650
CCNO 5660
CCNO 5670
CCNO 5680
CCNO 5690
CCNO 5700
CCNO 5710
CCNO 5720
CCNO 5730
CCNO 5740
CCNO 5750
CCNO 5760

```


CWR0C490
 CWR0C500
 CWR0C510
 CWR0C520
 CWR0C530
 CWR0C540
 CWR0C550
 CWR0C560
 CWR0C570
 CWR0C580
 CWR0C590
 CWR0C600
 CWR0C610
 CWR0C620
 CWR0C630
 CWR0C640
 CWR0C650
 CWR0C660
 CWR0C670
 CWR0C680
 CWR0C690
 CWR0C700
 CWR0C710
 CWR0C720
 CWR0C730
 CWR0C740
 CWR0C750
 CWR0C760
 CWR0C770
 CWR0C780
 CWR0C790
 CWR0C800
 CWR0C810
 CWR0C820
 CWR0C830
 CWR0C840
 CWR0C850
 CWR0C860
 CWR0C870
 CWR0C880
 CWR0C890
 CWR0C900
 CWR0C910
 CWR0C920
 CWR0C930
 CWR0C940
 CWR0C950
 CWR0C960

```

10 CONTINUE
20 CUNTINUE
30 CONTINUE
    RETURN
ENL
C ***
C *** REAL MATRIX MULTIPLICATION ROUTINE
C ***
C *** SUBROUTINE MMUL (R,I,M,LL,N,U)
    REAL*4 F(10,10),T(10,10),U(10,10)
    INTEGER M,LL,N
    DO 20 I=1,M
    DO 20 J=1,N
    U(I,J)=0.0
    DU(I,J)=U(I,J)+R(I,INDEX)*T(INDEX,J)
    CONTINUE
    CONTINUE
    RETURN
ENL
C ***
C *** CSVD ALGORITHM FOR COMPLEX MATRICES; ANY OF THE ROUTINES OF IMSL
C *** CR L INPACK COULD ALSO BE USED WITH PROPER CAUTIONS
C ***
C *** SUBROUTINE CSVD (A,M,N,MMAX,M,N,P,NU,NV,S,L,V)
    COMPLEX A(MMAX,1),L(MMAX,1),V(MMAX,1)
    INTEGER M,N,P,NU,NV
    REAL S(1)
    COMPLEX C,R
    REAL B(100),C(100),T(100)
    DATA E1A,TOL/1.5E-8,1.E-31/
    NP=N+P
    N1=N+1
C ***
C *** HCUSEHCLDEF REDUCTION
    C(1)=0.0EC
    K=1
    K1=K+1
C ***
C *** ELIMINATION OF A(I,K), I=K+1,.....,M
    DO 20 I=K,M
    Z=Z+REAL(A(I,K))**2+AIMAG(A(I,K))**2
    B(K)=0.0EC
    IF (Z.LE.TOL) GC TC 70
    Z=SQRT(Z)
    B(K)=Z
  
```


C TOLERANCE FOR NEGLIGIBLE ELEMENTS

```

140 EPS=0.EC
    DO 150 K=1,N
      S(K)=B(K)
      T(K)=C(K)
      EPS=AMAX1(EPS,S(K)+T(K))
      EPS=EPS*ETA
C
C INITIALIZATION OF L AND V
    IF (NU.EC.O) GO TO 180
    DO 170 I=1,NU
      DO 160 J=1,M
        U(I,J)=(0.EC,0.EO)
        U(J,J)=(1.EC,0.EO)
      IF (NV.EC.O) GO TO 210
      DO 200 J=1,NV
        DO 190 I=1,N
          V(I,J)=(0.EO,0.EO)
          V(J,J)=(1.EO,0.EO)
C
C OR DIAGONALIZATION
    DO 230 KK=1,N
      K=N1-KK
C
C TEST FOR SPLIT
    DO 220 LL=1,K
      L=K+1-LL
      IF (ABS(I(L)).LE.EPS) GO TO 290
      IF (ABS(S(L-1)).LE.EPS) GO TO 240
      CONTINUE
C
C CANCELLATION OF E(L)
    CS=C.EC
    SN=1.EO
    LI=L-1
    DO 280 J=L,K
      F=SN*T(I)
      T(I)=C*S+T(I)
      IF (ABS(F).LE.EPS) GO TO 290
      H=S(I)
      W=SQRT(F*F+H*H)
      S(I)=W
      CS=H/W
      SN=-F/W
      IF (NU.EC.O) GO TO 260
      DO 250 J=1,N
        X=REAL(L(J,LI))
        Y=REAL(L(J,I))

```

CWR01450
CWR01460
CWR01470
CWR01480
CWR01490
CWR01500
CWR01510
CWR01520
CWR01530
CWR01540
CWR01550
CWR01560
CWR01570
CWR01580
CWR01590
CWR01600
CWR01610
CWR01620
CWR01630
CWR01640
CWR01650
CWR01660
CWR01670
CWR01680
CWR01690
CWR01700
CWR01710
CWR01720
CWR01730
CWR01740
CWR01750
CWR01760
CWR01770
CWR01780
CWR01790
CWR01800
CWR01810
CWR01820
CWR01830
CWR01840
CWR01850
CWR01860
CWR01870
CWR01880
CWR01890
CWR01900
CWR01910
CWR01920

CMRO1530
 CMRO1540
 CMRO1550
 CMRO1560
 CMRO1570
 CMRO1580
 CMRO1590
 CMRO2000
 CMRO2010
 CMRO2020
 CMRO2030
 CMRO2040
 CMRO2050
 CMRO2060
 CMRO2070
 CMRO2080
 CMRO2090
 CMRO2100
 CMRO2110
 CMRO2120
 CMRO2130
 CMRO2140
 CMRO2150
 CMRO2160
 CMRO2170
 CMRO2180
 CMRO2190
 CMRO2200
 CMRO2210
 CMRO2220
 CMRO2230
 CMRO2240
 CMRO2250
 CMRO2260
 CMRO2270
 CMRO2280
 CMRO2290
 CMRO2300
 CMRO2310
 CMRO2320
 CMRO2330
 CMRO2340
 CMRO2350
 CMRO2360
 CMRO2370
 CMRO2380
 CMRO2390
 CMRO2400

```

250 U(J,L1)=CMPLX(X*CS+Y*SN,0.E0)
260 U(J,I)=CMPLX(Y*CS-X*SN,0.E0)
    IF (NP.EC.N) GO TO 280
    DO 270 J=N1,NP
    C=A(L1,J)
    R=A(I,J)
    A(L1,J)=C*CS+R*SN
    A(I,J)=R*CS-Q*SN
    CONTINUE
270 TEST FOR CONVERGENCE
280 W=S(K)
    IF (L.EC.K) GO TO 360
    C
    CRIGIN SPJFT
    X=S(L)
    Y=S(K-1)
    G=T(K-1)
    H=T(K)
    F=(Y-W)*Y*(G+H)*(G+H)/(2.E0*H*Y)
    G=SQRT(F*F+1.E0)
    IF (F.L7.0.E0) G=-G
    F=((X-W)*(X+W)+(Y/(F+G)-H)*H)/X
    C
    GR STEP
    CS=1.E0
    SN=1.E0
    L1=L+1
    DO 350 I=L1,K
    W=S(I)
    Y=S(I)
    H=SN*G
    G=CS*G
    W=SQRT(F*F+F*F)
    T(I-1)=h
    CS=H/W
    SN=H/W+C*SN
    F=X*CS-X*SN
    G=Y*SN
    H=Y*CS
    IF (NV.EC.0) GO TO 310
    DO 300 J=1,N
    X=REAL(V(J,I-1))
    W=REAL(V(J,I))
    V(J,I-1)=CMPLX(X*CS+W*SN,0.E0)
    V(J,I)=CMPLX(W*CS-X*SN,0.E0)
    W=SQRT(H*H+F*F)
300
310
  
```

CWR02410
 CWR02420
 CWR02430
 CWR02440
 CWR02450
 CWR02460
 CWR02470
 CWR02480
 CWR02490
 CWR02500
 CWR02510
 CWR02520
 CWR02530
 CWR02540
 CWR02550
 CWR02560
 CWR02570
 CWR02580
 CWR02590
 CWR02600
 CWR02610
 CWR02620
 CWR02630
 CWR02640
 CWR02650
 CWR02660
 CWR02670
 CWR02680
 CWR02690
 CWR02700
 CWR02710
 CWR02720
 CWR02730
 CWR02740
 CWR02750
 CWR02760
 CWR02770
 CWR02780
 CWR02790
 CWR02800
 CWR02810
 CWR02820
 CWR02830
 CWR02840
 CWR02850
 CWR02860
 CWR02870
 CWR02880

```

S(I-1,J)=W
CS=F/W
SN=H/W
X=CS*G+SN*Y
IF (INV.EC.O) GO TO 330
DO 320 I=1,N
Y=REAL(U(I,J,I-1))
U(I,J,I)=CMPLX(W*CS+Y*SN,O.EO)
U(I,J,I)=CMPLX(W*CS-Y*SN,O.EO)
IF (INV.EC.NP) GO TO 350
DO 340 I=1,NP
G=A(I-1,J)
R=A(I,J)=G*CS+R*SN
A(I-1,J)=R*CS-Q*SN
A(I,J)=R
CONTINUE
T(L)=O.EO
T(K)=F
S(K)=X
GO TO 22C

C CONVERGENCE
360 IF (W.GE.O.EO) GC TC 380
S(K)=W
IF (INV.EC.O) GO TO 380
DO 370 I=1,N
V(I,K)=-V(I,K)
CONTINUE
C SCRT SINGULAR VALUES
GO 450 F=I,N
G=-I.EC
J=K
DO 390 I=K,N
IF (S(I).LE.G) GO TC 350
G=S(I)
J=I
CONTINUE
IF (J.EC.K) GO TC 450
S(J)=S(K)
S(K)=G
IF (INV.EC.O) GO TO 410
DO 400 I=1,N
V(I,J)=V(I,J)
V(I,K)=V(I,K)
V(I,K)=C
400
  
```

CWR02E90
 CWR02S00
 CWR02S10
 CWR02S20
 CWR02S30
 CWR02S40
 CWR02S50
 CWR02S60
 CWR02S70
 CWR02S80
 CWR02S90
 CWR03000
 CWR03010
 CWR03020
 CWR03030
 CWR03040
 CWR03050
 CWR03060
 CWR03070
 CWR03080
 CWR03090
 CWR03100
 CWR03110
 CWR03120
 CWR03130
 CWR03140
 CWR03150
 CWR03160
 CWR03170
 CWR03180
 CWR03190
 CWR03200
 CWR03210
 CWR03220
 CWR03230
 CWR03240
 CWR03250
 CWR03260
 CWR03270
 CWR03280
 CWR03290
 CWR03300
 CWR03310
 CWR03320
 CWR03330
 CWR03340
 CWR03350
 CWR03360

```

410 IF (NL-EC.O) GO TO 430
    DO 420 I=1,N
    C=L(I,J)
    U(I,J)=L(I,K)
420 U(I,K)=C
430 IF (NL-EC.NP) GO TO 450
    DO 440 I=N1,NP
    C=A(I,I)
440 A(I,I)=A(K,I)
450 CONTINUE
C BACK TRANSFORMATION
    IF (NL-EC.O) GO TO 510
    DO 500 KK=1,N
    K=N1-KK
    IF (B(K),EQ,O.EO) GC TC 500
    Q=-A(K,K)/ABS(A(K,K))
460 DO 460 I=1,NU
    U(K,J)=C*L(K,J)
    DO 490 I=K,M
    Q=(C.EC I=C.EC)
470 C=C-CCAJ(A(I,K))*U(I,J)
    Q=C/CCABS(A(K,K))*B(K)
    DO 480 I=K,M
    U(I,J)=L(I,J)-Q*A(I,K)
480 CONTINUE
490 CONTINUE
500 IF (NL-EC.O) GO TO 570
510 IF (NL-EC.2) GO TO 570
    DO 560 KK=2,N
    K=N1-KK
    KI=K+1
    IF (C(KI),EQ,O.EO) GO TO 560
    Q=-CONJG(A(K,KI))/ABS(A(K,KI))
520 DO 520 I=1,NV
    V(KI,J)=L+V(KI,J)
    DO 550 J=1,NV
    C=(O.EO J=1,EO)
530 DO 530 I=K1,N
    Q=C+A(KI,I)*V(I,J)
    C=C/CCABS(A(K,KI))*C(KI,J)
540 DO 540 I=K1,N
    V(I,J)=V(I,J)-Q*CONJG(A(K,I))
550 CONTINUE
560 CONTINUE
570 RETURN
  
```


CWRO 3550
 CWRO 3560
 CWRO 3570
 CWRO 3580
 CWRO 3590
 CWRO 3600
 CWRO 3610
 CWRO 3620
 CWRO 3630
 CWRO 3640
 CWRO 3650
 CWRO 3660
 CWRO 3670
 CWRO 3680
 CWRO 3690
 CWRO 3700
 CWRO 3710
 CWRO 3720
 CWRO 3730
 CWRO 3740
 CWRO 3750
 CWRO 3760
 CWRO 3770
 CWRO 3780
 CWRO 3790
 CWRO 3800
 CWRO 3810
 CWRO 3820
 CWRO 3830
 CWRO 3840
 CWRO 3850
 CWRO 3860
 CWRO 3870
 CWRO 3880
 CWRO 3890
 CWRO 3900
 CWRO 3910
 CWRO 3920
 CWRO 3930
 CWRO 3940
 CWRO 3950
 CWRO 3960
 CWRO 3970
 CWRO 3980
 CWRO 3990
 CWRO 4000
 CWRO 4010
 CWRO 4020
 CWRO 4030
 CWRO 4040
 CWRO 4050
 CWRO 4060
 CWRO 4070
 CWRO 4080
 CWRO 4090
 CWRO 4100
 CWRO 4110
 CWRO 4120
 CWRO 4130
 CWRO 4140
 CWRO 4150
 CWRO 4160
 CWRO 4170
 CWRO 4180
 CWRO 4190
 CWRO 4200
 CWRO 4210
 CWRO 4220
 CWRO 4230
 CWRO 4240
 CWRO 4250
 CWRO 4260
 CWRO 4270
 CWRO 4280
 CWRO 4290
 CWRO 4300
 CWRO 4310
 CWRO 4320

```

REAL*4 WA(100)
S=CMPLX(C.0,W)
DO 20 J=1,NRA
DO 10 K=1,NCA
SI(J,K)=C.0
CONTINUE
DO 30 J=1,NCA
I(J,J)=1.0
SI(J,J)=SI(J,J)
DO 40 K=1,NCA
SIA(J,K)=SI(J,K)-AX(J,K)
CONTINUE
CALL LEGTIC (SIA,NCA,10,I,NCA,10,0,WA,IER)
CALL CPAIHL (I,BX,NCA,NCA,NCB,SIAIB)
CALL CPAIHL (CX,SIAIB,ARC,NCC,NCB,GP)
ENCL
C ***** THIS ROUTINE IS INPUT FOR DE SOLVER *****
C ***** THIS ROUTINE IS ADDED DIRECTLY TO CONXSV *****
C ***** SUBROUTINE FCN (N,I,X,XDDI) *****
C ***** REAL*4 I,X(N),XDDI(N),AMBFC(10,10),A(10,10),B(10,10),C(10,10), *****
1FC(10,10),BPHI(10),BFC(10,10),FC(10,10),AMBFCX(10),BPHI(10), *****
COMMON AMBFC,A,B,F,C,PHI,AMBFCX,BPHI,NCCLB *****
WRITE(6,15) *****
FORMAT(2,15) *****
WRITE(6,25) *****
FORMAT(2,15) *****
CALL WRITEE(AMBFC,N,N) *****
DO 10 J=1,N *****
BPHI(J)=BPHI(J)+B(J,K)*PHI(K) *****
CONTINUE *****
WRITE(6,5500) (BPHI(J),J=1,N) *****
FORMAT(6,5500) *****
DO 20 J=1,N *****
AMEFCX(J)=0.0 *****
DO 40 K=1,N *****
AMEFCX(K)=AMBFCX(J)+AMBFC(J,K)*X(K) *****
CONTINUE *****
WRITE(6,5501) (AMBFCX(J),J=1,N) *****
FORMAT(6,5501) *****
DO 50 J=1,N *****

```

CWR04430
 CWR04440
 CWR04450
 CWR04460
 CWR04470
 CWR04480
 CWR04490
 CWR04500
 CWR04510
 CWR04520
 CWR04530
 CWR04540
 CWR04550
 CWR04560
 CWR04570
 CWR04580
 CWR04590
 CWR04600
 CWR04610
 CWR04620
 CWR04630
 CWR04640
 CWR04650
 CWR04660
 CWR04670
 CWR04680
 CWR04690
 CWR04700
 CWR04710
 CWR04720
 CWR04730
 CWR04740
 CWR04750
 CWR04760
 CWR04770
 CWR04780
 CWR04790
 CWR04800

```

5C XDCT(J)=AMBFCX(J)+BPHI(J)
C WRITE(6,5502)(XDCT(J),J=1,N)
C5502 FORMAT(2F10.5)
END
C THIS SUBROUTINE COMPUTES THE CONTROLLER TRANSFER FUNCTION
C FOR THE CBSERVER ROBUSTNESS PROBLEM
C
SUBROUTINE CONTRL(H,AX,FX,FKX,FKC,BX,NRA,NCA,NRF,NCF,NRK,NCK,M,
1NRE)
C COMPLEX*8 H(10,10),AX(10,10),FX(10,10),FKX(10,10),FKC(10,10),
*BX(10,10),SI(10,10),I(10,10),SIA(10,10),AALG(10,10),AALK(10,10)
1BFX(10,10),WA(100),FKC(10,10),BF(10,10)
C COMPLEX*8 S
S=CMPLX(0,Q,M)
C CALL CWRITE(AX,NRA,NCA)
C CALL CWRITE(FX,NRF,NCF)
C CALL CWRITE(FKX,NRK,NCK)
DO 20 J=1,NRA
DO 10 K=1,NCA
SI(J,K)=C
1C CONTINUE=1,NRA
2C DO 12 K=1,NCA
11 I(J,K)=C.0
12 CONTINUE
3C DO 30 J=1,NCA
I(J,J)=1.0
DO 31 J=1,NRA
DO 32 K=1,NCA
SI(J,J)=S*I(J,J)
31 CONTINUE(SI,NRA,NCA)
C CALL CWRITE(SI,NRA,NCA)
DO 50 K=1,NRA
DO 40 J=1,NCA
SIA(J,K)=SI(J,K)-AX(J,K)
5C CONTINUE(SIA,NRA,NCA)
C CALL CFXCV(FKX,NRF,NCF)
C CALL CFXML(BFX,NRF,NCF)
DO 60 J=1,NRA
DO 70 K=1,NCA
AALG(J,K)=FKCX(J,K)+BFX(J,K)
7C AALK(J,K)=AAUG,NRA,NCA)
C CALL CWRITE(AAUG,NRA,NCA)
6C CONTINUE
CALL LECTIC(AAUG,NCA,10,1,NCA,10,0,NA,IER)

```

CWR04810
CWR04820
CWR04830
CWR04840
CWR04850

CALL CAJML (J, FKX, NRA, NCA, NCK, AAUK)
CALL CMATML (FX, AAUK, NRF, NCF, NCK, H)
CALL CMFITE (H, NRF, NCK)
RETURN
ENC

C


```

CCNO2E90
CCNO2S00
CCNO2S10
CCNO2S20
CCNO2S30
CCNO2S40
CCNO2S50
CCNO2S60
CCNO2S70
CCNO2S80
CCNO2S90
CCNO3000
CCNO3010
CCNO3020
CCNO3030
CCNO3040
CCNO3050
CCNO3060
CCNO3070
CCNO3080
CCNO3090
CCNO3100
CCNO3110
CCNO3120
CCNO3130
CCNO3140
CCNO3150
CCNO3160
CCNO3170
CCNO3180
CCNO3190
CCNO3200
CCNO3210
CCNO3220
CCNO3230
CCNO3240
CCNO3250
CCNO3260
CCNO3270
CCNO3280
CCNO3290
CCNO3300
CCNO3310
CCNO3320
CCNO3330
CCNO3340
CCNO3350
CCNO3360

```

```

C CALL READ (C,NRNGC,NCCLC)
C CALL READ (F,NROWF,NCOLF)
C CALL READ (FK,NRCWK,NCCLK)

C SPECIFY THE DESIGN VARIABLES WITHIN THE F MATRIX
C
C DO 10 J=1,NROWF
C READ (1,1070) ((IF(J,K),K=1,NCOLF)
C DO 20 J=1,NRCWK
C READ (1,1010) ((IFK(J,K),K=1,NCOLK)
C
C SET THE DESIGN VARIABLE BOUNDS
C
C DO 30 J=1,NCV
C READ (1,1080) VLB(J),VLB(J)
C DO 60 J=1,NROWF
C DO 50 K=1,NCOLF
C IF (IF(J,K).EQ.0) GO TO 40
C KK=IF(J,K)
C X(KK)=F(J,K)
C CONTINUE
C CONTINUE
C CONTINUE
C
C SPEC DESIGN VAR WITHIN THE FK MATRIX
C
C READ THE DESIRED EIGENVALUES AS REAL(X)+REAL(Y)*I
C DO 70 I=1,NMU
C READ (1,1150) REALPL(I),IMAGMU(I)
C DO 80 I=1,NMU
C MU(I)=CPFLX(REALMU(I),IMAGMU(I))
C CONTINUE
C
C SCRT THE INPUT EIGEN VALUES
C
C DO 90 I=1,NMU
C IR(I)=1
C CALL VSFTR (REALMU,NMU,IR)
C DO 100 J=1,NMU
C K=IR(J)
C OML(J)=PL(K)
C JJ=NMU-1
C DO 120 J=1,JJ
C IF (REAL(CMU(J)),NE.REAL(CMU(J+1))) GO TO 110
C IF (AIMPL(CMU(J)).LT.AIMAG(CMU(J+1))) GO TO 110
C TEMPI=CMU(J)
C CMU(J)=CMU(J+1)

```



```

CCN0 4 330
CCN0 4 340
CCN0 4 350
CCN0 4 360
CCN0 4 370
CCN0 4 380
CCN0 4 390
CCN0 4 400
CCN0 4 410
CCN0 4 420
CCN0 4 430
CCN0 4 440
CCN0 4 450
CCN0 4 460
CCN0 4 470
CCN0 4 480
CCN0 4 490
CCN0 4 500
CCN0 4 510
CCN0 4 520
CCN0 4 530
CCN0 4 540
CCN0 4 550
CCN0 4 560
CCN0 4 570
CCN0 4 580
CCN0 4 590
CCN0 4 600
CCN0 4 610
CCN0 4 620
CCN0 4 630
CCN0 4 640
CCN0 4 650
CCN0 4 660
CCN0 4 670
CCN0 4 680
CCN0 4 690
CCN0 4 700
CCN0 4 710
CCN0 4 720
CCN0 4 730
CCN0 4 740
CCN0 4 750
CCN0 4 760
CCN0 4 770
CCN0 4 780
CCN0 4 790
CCN0 4 800

DO 270 J=1, NMU
CC ST=(REAL(OML(J))-REAL(CEIG(J)))*2+(AIMAG(OMU(J))-AIMAG(UE
1IG(J)))**2)
CONTINUE
CBJ=MTI*CGST
IF (NCCA.EQ.0) GO TO 250
DO 280 J=1, NMU
IDG(J)=AIDG
R(J)=RJ*SQRT((REAL(CMU(J))-REAL(CEIG(J)))*2+(AIMAG(OMU(J))-AIMAG(
1OEIG(J)))**2)
10EIG(J)=R(J)**2)
1G(J)=SQRT((REAL(CMU(J))-REAL(CEIG(J)))*2+(AIMAG(OMU(J))-AIMAG(CEI
1G(J)))**2)-R(J)
IF (KCATRL.GT.0) GG TO 310
GO TO 130
CONTINUE
C THE GRADIENT COMPUTATION ROUTINE GOES HERE IF NEEDED
300
310 CONTINUE (C, 1160)
WRITE (C, 1160)
CALL CVECTOR (OEIG, NCOLA)
DO 320 J=1, NMU
WRITE (C, 1170) CEIG(J), EIGK(J)
CALL CWRITE (QZ, NROWA, NCOLA)
WRITE (C, 1180)
CALL WRITE (F, NRCWF, NCCLF)
REAL (1, 1050) IGRAC, NCV, NCCN, ISTRAT, IOPT, IONED, IPR INT, INFO
DO 330 J=1, NDV
READ (1, 1080) VLBI(J), VUBI(J)

DO 360 J=1, NROWK
DO 350 K=1, NCOLK
IF (IFK(J,K).EQ.0) GO TC 340
KK=IFK(J,K)+KK
XI(KKK)=FK(J,K)
CONTINUE
CONTINUE
IF (KONTRL.GT.0) GC TO 141
INFC=-2
***
*
* CALL ADS ROUTINE TO FIND FILTER FEEDBACK GAINS FCR
* THE ROBUSTNESS RECOVERY WITH THE CBSERVER GAINS
*
* CALL ACS (INFO, ISTRAT, IOPT, IONED, IPRINT, IGRAD, NDV, NCVN, XI, VLBI, VUB
11, CBJ, C1, ICG, NGT, JG, DXA, NRA, NCA, WK1, NRWK, IMK, NR IMK)
IWK(2)=1

```

```

370 CALL ACS (INFO,ISTRAT,IOPT,IONED,IPRINT,IGRAD,NDV,NCON,X1,VLBI,VUB,CCNO,4,810
11,CBJ1,IGL,ICG,NGI,IC,DF,XA,NRA,NCA,WKI,NRWK,IWK,NRIWK)
IF (INFC.EQ.0) GC IC 700
IF (INFC.GT.1) GC IC 650
C
C 141 CONTINUE
DO 400 J=1,NROWK
DO 390 K=1,NCOLK
IF (IFK(J,K).EQ.0) GO TO 380
KKKK=IFK(J,K)
KKKK=KKK+KKK
FK(J,K)=X1(KKKK)
CONTINUE
CONTINUE
CALL MPALL (FK,C,NROWK,NCOLK,NCOLC,FKC)
DO 420 I=1,NROWA
DO 410 J=1,NCOLA
AMFKC(I,J)=A(I,J)-FKC(I,J)
CONTINUE
CALL EICRF (AMFKC,NROWA,10,2,EIGK,ZK,10,WK,IER)
C
C
C CMPLX ALL THE INPUT SYSTEM MATRICES FOR THE TRANSFER FUNCTION
CALL CPLXCV (AX,A,NRCWA,NCCLA)
CALL CPLXCV (BX,B,NROWB,NCCLB)
CALL CPLXCV (CX,C,NRCWC,NCCLC)
CALL CPLXCV (FX,F,NROWF,NCCLF)
CALL CPLXCV (FKX,FK,NROWK,NCOLK)
C
C CALL THE PLANT TRANSFER MATRIX ROUTINE AND FORM THE SYSTEM
C RETURN DIFFERENCE MATRICES AS REQUIRED
DEL=DELW
HI=HI
NC=1
H=H
SMINMI=C
SMINMI=C
SMINAG=C
SMINMO=C
SMAXMI=C
SMAXMI=C
SMAXAO=C
SMAXAO=C
CALL PLANT (PLAN,AX,BX,CX,H,NRCWA,NCCLA,NROWB,NCULB,NROWC,NCOLC)
CALL CNTRP (CONF,AX,FX,FKX,FKC,BF,NROWA,NCCLA,NROWF,NCCLF,NROWK,NCNO,5,280

```

CCNO 5290
 CCNO 5300
 CCNO 5310
 CCNO 5320
 CCNO 5330
 CCNO 5340
 CCNO 5350
 CCNO 5360
 CCNO 5370
 CCNO 5380
 CCNO 5390
 CCNO 5400
 CCNO 5410
 CCNO 5420
 CCNO 5430
 CCNO 5440
 CCNO 5450
 CCNO 5460
 CCNO 5470
 CCNO 5480
 CCNO 5490
 CCNO 5500
 CCNO 5510
 CCNO 5520
 CCNO 5530
 CCNO 5540
 CCNO 5550
 CCNO 5560
 CCNO 5570
 CCNO 5580
 CCNO 5590
 CCNO 5600
 CCNO 5610
 CCNO 5620
 CCNO 5630
 CCNO 5640
 CCNO 5650
 CCNO 5660
 CCNO 5670
 CCNO 5680
 CCNO 5690
 CCNO 5700
 CCNO 5710
 CCNO 5720
 CCNO 5730
 CCNO 5740
 CCNO 5750
 CCNO 5760

```

1 COLK, M)
CALL CMATML (CCNT, PLAN, NROWF, NCOLK, NCOLE, HG)
CALL CMATPL (PLAN, CCNT, NROWC, NCOLB, NCOLK, GH)
DO 450 K=1, NROWF
DO 440 K=1, NCOLB
  XI (J, K) = 0.0
CONTINUE
DO 460 J=1, NROWF
  XI (J, J) = 1.0
CONTINUE
DO 480 J=1, NROWC
  XX I (J, K) = 0.0
CONTINUE
DO 490 K=1, NCOLK
  XX I (J, J) = 1.0
CONTINUE
DO 510 K=1, NROWF
  XX I (J, K) = HG (J, K)
CONTINUE
DO 500 K=1, NCOLB
  XIPHG (J, K) = XI (J, K) + HG (J, K)
CONTINUE
DO 530 K=1, NROWC
  XIPHG (J, K) = XI (J, K) + GH (J, K)
CONTINUE
DO 550 J=1, NROWF
  HG I (J, K) = 0.0
CONTINUE
DO 570 K=1, NROWC
  GH I (J, J) = 1.0
CONTINUE
CALL ELECTIC (HG, NROWF, 10, HG I, NROWF, 10, 0, MA, IER)
CALL LECTIC (GH, NROWC, 10, GH I, NROWC, 10, 0, MA, IER)
DO 590 K=1, NROWF
  XIPHG (J, K) = XI (J, K) + HG I (J, K)
CONTINUE
DO 610 J=1, NROWC
  XIPHG (J, K) = XI (J, K) + GH I (J, K)
CONTINUE

```



```

CCNO 6250
CCNO 6260
CCNO 6270
CCNO 6280
CCNO 6290
CCNO 6300
CCNO 6310
CCNO 6320
CCNO 6330
CCNO 6340
CCNO 6350
CCNO 6360
CCNO 6370
CCNO 6380
CCNO 6390
CCNO 6400
CCNO 6410
CCNO 6420
CCNO 6430
CCNO 6440
CCNO 6450
CCNO 6460
CCNO 6470
CCNO 6480
CCNO 6490
CCNO 6500
CCNO 6510
CCNO 6520
CCNO 6530
CCNO 6540
CCNO 6550
CCNO 6560
CCNO 6570
CCNO 6580
CCNO 6590
CCNO 6600
CCNO 6610
CCNO 6620
CCNO 6630
CCNO 6640
CCNO 6650
CCNO 6660
CCNO 6670
CCNO 6680
CCNO 6690
CCNO 6700
CCNO 6710
CCNO 6720

```

```

C      640      OB JJ=NT2*SMJNAI+NT3*SMINAD
C      640      UB J=WT2*SMINAI
C      640      IF (NCCA.EQ.0) GC TC 680
C      640      DO 640 J=1,NCON
C      640      IDG(J)=NICG
C      640      SUM1=0.C
C      640      DO 650 J=1,MMU
C      640      JJ=J+AMPL
C      640      GI(JJJ)=SUM1+(AMAX1(0.0,REAL(EIGK(JJJ)-EIGX)))*2
C      640      CONTINUE
C      640      SUM2=0.
C      640      DO 660 J=1,MMU
C      640      JJ=J+2*AMPL
C      640      JJ=J+AMPL
C      640      JJ=J+AMPL
C      640      GI(JJJ)=SUM2+(AMAX1(0.0,EIGM-REAL(EIGK(JJJ)))*2
C      640      CONTINUE
C      640      SUM3=0.
C      640      DO 670 J=1,MMU
C      640      JJ=J+3*AMPL
C      640      JJ=J+2*AMPL
C      640      JJ=J+AMPL
C      640      GI(JJJ)=SUM3+(AMAX1(0.0,(AIMAG(EIGK(JJJ)/REAL(EIGK(JJJ))-EIRT)))*2
C      640      CONTINUE
C      640      GO TO 700
C      690      IF (KCNTRL.GT.0) GC TC 700
C      690      CONTINUE
C      700      THE GRADIENT COMPUTATION ROUTINE GOES HERE IF NEEDED
C      700      CONTINUE
C      710      C O L U P T T H E   C O M P U T E D   F I N A L   E I G E N   V A L U E S   A N D   V E C T O R S   F R O M   U P T   F * S
C      710      IF (KCNTRL.EQ.0) GC TC 710
C      710      W R I T E   ( 6 , 5 7 0 )
C      710      G O   T O   7 2 0
C      710      W R I T E   ( 6 , 5 8 0 )
C      710      W R I T E   ( 6 , 5 9 0 )
C      710      C A L L   C V E C H R   ( E I G K , A C G L A )
C      710      W R I T E   ( 6 , 5 0 0 )
C      710      C A L L   C H F I T E   ( Z K , N R C W A , N C O L A )
C      710      W R I T E   ( 6 , 1 1 6 0 )
C      710      C A L L   C V E C H R   ( O E I G , N C O L A )
C      710      D O 730 J=1,MMU
C      710      W R I T E   ( 6 , 5 1 0 ) O E I G ( J ) , E I G K ( J )
C      710      W R I T E   ( 6 , 1 1 7 0 )
C      710      C A L L   C H F I T E   ( O Z , N R C W A , N C O L A )
C      710      W R I T E   ( 6 , 1 1 8 0 )
C      710      C A L L   W F I T E   ( F , N R C W F , N C C L F )
C      710      W R I T E   ( 6 , 5 2 0 )

```


LIST OF REFERENCES

1. Rosenbrock, H. H., Computer-Aided Control Systems Design, Academic Press, 1974.
2. Sandell, N. R., Jr., Recent Developments in the Robustness Theory of Multivariable Systems, Office of Naval Research Report CR-275-277-1F, 1979.
3. Kalman, R. E., "When Is A Linear Control System Optimal?", ASME J. Basic Engr., pp51-60, March 1964.
4. Anderson, B. D. C. and Moore, J. B., Linear Optimal Control, Prentice Hall, Inc., 1971.
5. Rosenbrock, H. E., "Design of Multivariable Control Systems Using the Inverse Nyquist Array", Proc. of IEE, Vol 116, pp 1929-1936, Nov 1969.
6. Doyle, J. C. and Stein, G., "Multivariable Feedback Design: Concepts for a Classical/Modern Synthesis", IEEE Trans. Auto. Control, Vol AC-26, No. 1, pp4-16, Feb 1981.
7. Safanov, M. G. and Athans, M., "Gain and Phase Margin of Multiloop LQG Regulators", IEEE Trans. Auto. Control, April 1977.
8. Sandell, N. S., Jr., Lehtomaki, N. A., and Athans, M., "Robustness Results in Linear Quadratic Gaussian Based Multivariable Control Designs", IEEE Trans. Auto. Control, Vol 26, No. 1, pp75-92, Feb. 1981.
9. Lehtomaki, N. A., Practical Robustness Measures in Multivariable Control System Analysis, Ph.D. Thesis, Massachusetts Institute of Technology, May 1981.
10. Vanderplaats, G. N., ADS - A Fortran Program for Automated Design Synthesis, version 1.0, Naval Postgraduate School, Monterey, Ca., May 1984.
11. Vanderplaats, G. N., Numerical Optimization Techniques for Engineering Design: With Applications, McGraw-Hill, 1984.
12. Vanderplaats, G. N., CONMIN-A Fortran Program for Constrained Function Minimization - User Manual, NASA TN X-622282, AUG 1973.

13. Shapiro, E. Y., et. al., " Pole Placement with Output Feedback", AIAA J. of Guidance and Control, Vol 4, No 4, pp 441-443, July-Aug 1981.
14. Mukhopadhyay, V. and Newsom, J., Application of Matrix Singular Value Margins of Multiloop Systems, NASA TM - 84-24, July 1982.
15. Mukhopadhyay, V. and Newsom, J., " The use of Singular Value Gradients and Optimization Techniques to Design Robust Controllers for Multiloop Systems", AIAA Guidance and Control Papers, August 1983.
16. Sandell, N. R., Jr., et al, Multivariable Stability Margins for Vehicle Flight Control Systems, TR -121, Alphatech Inc., Dec. 1981.
17. Doyle, J. C. and Stein, G., " Robustness with Observers", IEEE Trans. Auto. Control, Vol AC-24, pp 607-611, Aug. 1979.

6

INITIAL DISTRIBUTION LIST

	No. Copies
1. Defense Technical Information Center Cameron Station Alexandria, Virginia 22314	2
2. Professor D. J. Collins, Code 67Co Department of Aeronautics Naval Postgraduate School Monterey, California 93943	5
3. Library, Code 0142 Naval Postgraduate School Monterey, California 93943	2
4. Department Chairman, Code 67 Department of Aeronautics Naval Postgraduate School Monterey, California 93943	1
5. Prof M. F. Platzer, Code 67P1 Department of Aeronautics Naval Postgraduate School Monterey, California 93943	1
6. Prof T. H. Gawain, Code 67Gn Department of Aeronautics Naval Postgraduate School Monterey, California 93943	1
7. Prof R. D. Strum, Code 62St Department of Electrical Engineering Naval Postgraduate School Monterey, California 93943	1
8. Prof G. E. Latta, Code 54Lz Department of Mathematics Naval Postgraduate School Monterey, California 93943	1
9. Prof G. N. Vanderplats Department of Mechanical and Environmental Engineering University of California Santa Barbara, California 93106	1
9. Commander Vernon C. Gordon, USN 315 Alameda Blvd. Coronado, California 92118	3

END

FILMED

1-85

DTIC